Global analysis of histone variant H2A.Z acetylation in *Saccharomyces cerevisiae*

A thesis submitted to The University of Manchester for the degree of Doctor of Philosophy in the Faculty of Life Sciences

2013

Yanin Naiyachit

Contents

Word count: 39,878

List of Figures

List of Tables

The University of Manchester

Yanin Naiyachit

Doctor of Philosophy

Global analysis of histone variant H2A.Z acetylation in *Saccharomyces cerevisiae*

2013

Abstract

The histone variant H2A.Z is an evolutionarily conserved variant which is an essential chromatin component for many organisms. H2A.Z plays a pivotal role in a diverse array of chromatin-based processes such as gene transcription and chromosome segregation. In yeast, H2A.Z is acetylated at four N-terminal lysine residues (K3, K8, K10 and K14). Previous studies have shown that these acetylation sites are critical for H2A.Z function. My research aim was to examine how these four acetylatable lysines act to regulate the function of H2A.Z. Genome mapping of the acetylated K8, K10, K14 isoforms revealed that these acetyl marks are co-localised across the budding yeast genome, indicating that acetylation is a common feature of H2A.Z. Examinations of individual acetylation sites using mutational and phenotypical analyses did not reveal any distinct phenotypes between individual lysine residues. These findings indicated that individual acetylation sites are functionally redundant. Intriguingly, H2A.Z is mis-regulated when all four lysine were mutated to arginine (H2A.Z K3, 8, 10, 14 R) by showing sensitivity to a variety of agents. The global distribution profiles of H2A.Z, however, were unaffected by N-terminal lysine mutations. In fact, unacetylatable H2A.Z alleles perturbed H2A.Z chromatin abundance. Biochemical evidence showed that the altered chromatin level was severely defective when combined unacetylatable allele with mutations of SWR-C components. Together, the data presented here suggested that the N-terminal acetylation of H2A.Z regulates its genome abundance independent of its deposition pathway by SWR-C complex.

DECLARATION

No portion of the work referred to in the thesis has been submitted in support of an application for another degree or qualification of this or any other university or other institute of learning.

COPYRIGHT STATEMENT

Acknowledgements

First and foremost, I would like to express my sincere thank to my supervisor, Dr Catherine Millar for giving me the opportunity to work and pursue my postgraduate study in her lab. I am grateful for her encouragement, advice, and continuous support she has given me throughout my research career. I also want to thank her for giving me that red chilli plant when I had a tough time during my PhD.

I would like to thank my advisor, Dr Paul Shore for his helpful guidance.

Many special thanks go to Tom Wood and Dr Daniel Wratting for being incredible co-workers and best friends all along. I would like to thank Angela Thistlewaite for her kind advice and technical support and also Muxin Gu for his contribution towards genome-wide data analysis and for teaching me some bioinformatics lessons.
In addition, I would like to thank Dr Xi Chen, for his kind helps. His willingness to discuss about sciences and general life is much appreciated.
I thank Poulin's lab members for being fantastic lab neighbours.

Special thanks go to my aunt who provided me the opportunity to come to study in the UK. Finally, I would especially like to thank my beloved mother and my grandmother who always believe in me and for their love and support.

CHAPTER 1: INTRODUCTION

Chromatin, a nucleoprotein complex, is a central template for virtually all DNA-based processes. Understanding the aspects of chromatin biology such as structure, dynamics and regulation is essential to gain insights into diverse cellular mechanisms. Changes in chromatin status impose profound effects that allow enzymes and protein complexes to perform their activities on DNA sequences; for example transcription and repair. Chromatin states can be altered by multiple ways. Histone modifications and incorporation of histone variants have emerged as key means to influence chromatin regulation.

The histone variant H2A.Z is a highly evolutionarily conserved variant of histone H2A. H2A.Z is essential for viability in many organisms. It is regarded as a unique, multifunctional protein because of its roles in a wide variety of cellular processes ranging from gene activation, boundary protection, chromosome segregation, DNA repair, suppression of antisense RNAs, and embryonic stem cell differentiation. Dysregulation of H2A.Z has been reported in diseases such as cancers (Hua *et al*., 2008; Rhodes *et al*., 2004; Zucchi *et al*., 2004; Gevry *et al*., 2009; Valdes-Mora *et al*., 2011; Dryhurst *et al* 2011; Svotelis *et al*., 2010). Importantly, acetylation of H2A.Z is largely responsive to the histone deacetylase inhibitor: suberoylanilide hydroxamic acid (SAHA), a clinical drug for cancer and neurodegenerative disease treatment (Choudhary *et al*., 2009). Therefore, understanding the regulation of multifaceted identity of H2A.Z and its modes of regulation may provide the links to understanding disease pathogenesis. Post-translational modifications on H2A.Z add a major variation to H2A.Z composition, therefore impacting on H2A.Z molecules as a key functional regulation. The amino (N) terminal and carboxy (C) terminal tails of H2A.Z are modified post-translationally by acetylation and ubiquitination. Less is known on how these modified species are regulated and whether they actually contribute to diverse functions in which H2A.Z is involved. My research aims to characterise the functional features of H2A.Z acetylation by unveiling its genomic landscapes and to dissect the biological functions of this modification on H2A.Z using the *Saccharomyces cerevisiae* as a model organism.

This chapter summarises the relevant literature in order to provide the background and overview of information regarding post-translational modification by acetylation and H2A.Z variant in the context of chromatin.

1.1 Nucleosome & histones; the basic building blocks of chromatin

Chromatin is organised in such an efficient way that it allows the DNA to package in a small nucleus by tightly wrapping around arrays of repeating basic subunits called "nucleosomes". Each nucleosome core particle contains two molecules of each H2A, H2B, H3 and H4 (two H2A-H2B dimers and a H3-H4 tetramer), which are assembled into an octameric complex during the S phase of the cell cycle (Figure 1.1-left) Histone H1 is associated with linker DNA connecting the adjacent nucleosomes. The nucleosomal core histones have 1.7 turns (~147 bp) of DNA wrapped around them in a flat, left-handed superhelix (Luger *et al*., 1997) and are associated with DNA in an 11-nm dimension and assemble as beads-on-a-string structure (Figure 1.1-right) and further condense to 30-nm chromatin fibres (solenoid). The N- and C- terminal tails of histones have been characterised (in solution) as unstructured regions, protruding from the nucleosome core particles.

Nucleosomal histones are indeed a key component of chromatin, serving as a dual player in regulating DNA accessibility. It appears that not only histones play a role in packaging DNA but are also involved in multiple of chromatin-based processes in eukaryotic genomes.

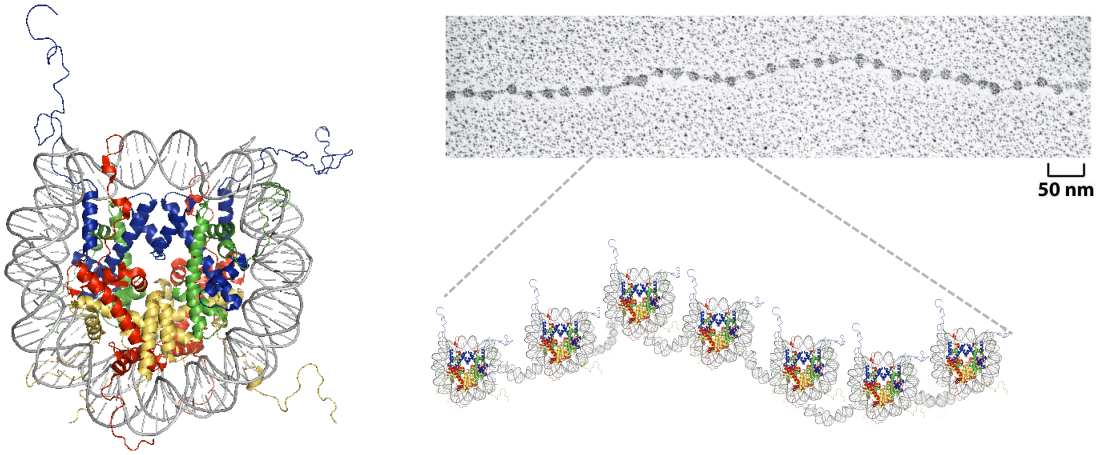

Figure 1.1: The crystal structure of the nucleosome core particle.
Left: Each histone is coloured as followed: H3 = blue; H4 =green; H2B = yellow and H2A= red, with the DNA double helix in grey. The illustration was generated by Pymol using crystal structure of nucleosome core particle from recombinant *Xenopus laevis* histones (Davey *et al*., 2002). Right: "Beads-on-a-string" structure nucleosome as seen by electron microscope (by Foe V) Illustrations taken from Molecular Biology of the Cell 5th Edition

The higher-order chromatin structure limits the accessibility of cellular machineries to DNA, therefore inhibiting DNA-related processes such as transcription, DNA replication and DNA repair. In order to regulate gene activity, changes in nucleosomal core histones and DNA interactions are required to modulate the properties of chromatin structure. Alteration of chromatin states can be achieved by various means including structural changes via ATP-dependent chromatin remodelling complexes or compositional changes via replacing canonical histones with histone variants and covalently attaching chemical groups by means of histone modifications. Several lines of evidence show that these mechanisms are interrelated to alter chromatin states (reviewed in Li *et al*., 2007; Kouzarides, 2007).

Post-translational modification (PTMs) can occur at the N- and C-terminal tails and also globular domains of histones by various manners depending on the amino acid residues on the histones. PTMs can alter the nucleosomal properties and interaction with DNA and adjacent nucleosomes, thereby regulating nucleosome dynamics and function (reviewed in Zentner and Henikoff, 2013). Distinct patterns of histone modifications are believed to form a 'histone code' that regulates chromatin-modulating factors (Strahl and Allis, 2000). A large number of PTM classes have been discovered, recent classes of histone modifications have been characterised such as lysine acetylation (Kac), lysine methylation (Kme), serine/threonine phosphorylation (Sph; Tph), ubiquitination (Kub), sumoylation, poly-ADP ribosylation, glycosylation and novel marks such as lysine crotonylation (Kcr) and tyrosine hydroxylation (Yoh) etc. (Tan *et al*., 2011; Arnaudo and Garcia, 2013; reviewed in Kouzarides, 2007). However, lysine acetylation will be mainly emphasised in this chapter.

1.2 Lysine acetylation (Kac); a key ubiquitous modification

Lysine acetylation has long been extensively studied and shown to play a multiple roles in cellular regulations. Lysine acetylation was the first discovered on histones and was associated with active transcription (Phillips, 1963; Allfrey *et al*., 1964). Other than histones, evidence from proteomic studies have demonstrated that acetylation of lysine residues is observed in a large number of transcription factors, nuclear regulators, mitochondrial and metabolic enzymes and various cytoplasmic proteins in mammalian cells (Glozak *et al*., 2005; Choudhary *et al*., 2009; Zhao *et al*., 2010). For instance, acetylation of a tumor suppressor protein p53 was shown to regulate its stability via the cross-regulation with ubiquitination and interaction with TAF1 (reviewed in Yang and

Seto, 2008). In accordance with mammalian studies, a growing number of acetylation on non-histone substrates are being documented in yeast; for example cohesin subunit Smc3 (Beckouët *et al*., 2010; Borges *et al*., 2010), subunit of histone acetyltransferase Yng2 (Lin *et al*., 2008), gluconeogenic enzyme Pck1 (Lin *et al*., 2009), cytokinesis septin proteins (Mitchell *et al*., 2011), yeast AMP-activated protein kinase Sip2 (Lu *et al*., 2011) and cell-cycle transcription factor Swi4 (Kaluarachchi Duffy *et al*., 2012). Accordingly, acetylation of lysine is involved in broad arrays of cellular pathways ranging from transcription, chromatin remodelling, cell cycle, gene splicing, nuclear transport, cytoskeleton dynamics, energy metabolism, autophagy to signalling (reviewed in Yang and Seto, 2008).

Acetylation of lysine is a reversible reaction that is involved in the process of introducing acetyl moiety from acetyl-coenzyme A (acetyl-CoA) to ε-NH_2 groups of lysine residues. The kinetic balance of acetylation and deacetylation is mediated by the actions of histone lysine acetyltransferase (KAT) and histone deacetylase (KDAC) activities. KATs are classified into three mains families: Gcn5-related N-acetyltransferases (GNATs), E1A-associated protein of 300 kDa (p300)/ CREB-binding protein (CBP) and MOZ, YBF2/SAS3, SAS2, Tip60 (MYST) (reviewed in Lee and Workman, 2007; Allis *et al*., 2007). All discovered KATs in *S. cerevisiae* and human are illustrated in Table 1.1.

KDACs in yeast are divided into three classes: Class I histone deacetylase Rpd3 Host1 and Hos2; Class II histone deacetylase Hda1 and Hos3; Class III Sir2 (silent information regulator-2) or sirtuin (Sir2-like protein) family of NAD^+-dependent deacetylases. On a genomic scale, both human KATs and KDACs occupancy are correlated with active genes, acetylated histones and RNA Polymerase II binding. It was reported that KATs and KDACs are co-localised with H3K4me3 in order to poise genes for activation (Wang *et al*., 2009).

All four-core histones have lysine rich amino terminal tails, which can be subjected to acetylation. Acetylation of histones has long been regarded as a highly dynamic modification with the half-life of a few minutes for many acetylation sites (reviewed in Barth and Imhof, 2010). However, recent studies have shown that some acetylation sites are rather stable. Zheng and colleagues (2013) used isotope labelling techniques to examine the kinetics of acetylation in human cell lines and identified 7 acetylation sites that are relatively stable (very low turnover) including H2AK13, H2AK36, H3K4, H2AK15, H3K79, H3K56 and H3K122 (Zheng *et al*., 2013). However, it has not yet been established why these sites are more stable.

Table 1.1 Summary of K-Acetyltransferases (KATs) in *S. cerevisiae* and humans (Allis *et al*., 2007)

New Name	*S. cerevisiae*	Human	Substrate Specificity	Function
KAT1	Hat1	HAT1	H4 (5, 12)	Histone deposition, DNA repair
KAT2	Gcn5		H3 (9, 14, 18, 23, 36)/H2B; yHtzl (14)	Transcription activation, DNA repair
KAT2A		hGCN5	H3 (9, 14, 18)/H2B	Transcription activation
KAT2B		PCAF	H3 (9, 14, 18)/H2B	Transcription activation
KAT3			H4 (5, 8); H3 (14, 18)	Transcription activation, DNA repair
KAT3A		CBP	H2A (5); H2B (12, 15)	Transcription activation
KAT3B		P300	H2A (5); H2B (12, 15)	Transcription activation
KAT4	Taf1	TAF1	H3 > H4	Transcription activation
KAT5	Esa1	TIP60/PLIP	H4 (5, 8, 12, 16); H2A (yeast 4, 7; chicken 5, 9, 13, 15); dH2Av/yHtzl (8,10,14)	Transcription activation, DNA repair
KAT6	Sas3		H3 (14, 23)	Transcription activation and elongation, DNA replication
KAT6A		MOZ/MYST3	H3 (14)	Transcription activation
KAT6B		MORF/MYST4	H3 (14)	Transcription activation
KAT7		HBO1/MYST2	H4 (5, 8, 12) > H3	Transcription, DNA replication
KAT8	Sas2	HMOF/MYST1	H4 (16)	Chromatin boundaries, dosage compensation, DNA repair
KAT9	Elp3	ELP3	H3	
KAT10	Hap2		H3 (14); H4	
KAT11	Rtt109		H3 (56)	Genome stability, transcription elongation
KAT12		TFIIIC90	H3 (9, 14, 18)	Pol III transcription
KAT13A		SRC1	H3/H4	Transcription activation
KAT13B		ACTR	H3/H4	Transcription activation
KAT13C		P160	H3/H4	Transcription activation
KAT13D		CLOCK	H3/H4	Transcription activation

Acetylation of lysine on histone tails is thought to be involved in neutralising the electrostatic interaction between the positive charge of lysine residues and the negatively charged DNA, thereby creating an 'open' or 'loose' chromatin conformation that permits cellular machineries such as transcription factors, replication or DNA repair complexes to access the DNA and perform their transactions. According to the charge neutralisation concept (reviewed in Grunstein, 1997), histone acetylation could result in relaxing nucleosome-DNA interactions or possibly regulating chromosome decondensaion. *In vitro* studies, using thermal shift experiment to determine the rate of nucleosome repositioning, showed that acetylation of histone H3 lysine 122 (H3K122ac) altered nucleosome mobility at nucleosome dyad (Manohar *et al*., 2009). Furthermore, acetylation of histones H4 lysine 16 (H4K16ac) has been shown to affect chromosome decompaction (Dorigo *et al*., 2004; Shogren-Knaak *et al*., 2006; Carmen *et al*., 2002; Robinson *et al*., 2008), thereby serving as a key modification to regulate higher-order chromatin structure. From the structural point of view, lysine 16 is the only residue located in the acidic patch of histone H4 that can interact with the acidic patch of H2A/H2B from adjacent nucleosomes (Dorigo *et al*., 2004). Biochemical studies have suggested that acetylation of histone H4K16ac destabilises nucleosome-nucleosome interactions and self-association of nucleosome arrays (Allahverdi *et al*., 2011; Liu *et al*., 2011). Interestingly, it was shown that the cumulative charge neutralisation modulates transcription. In yeast, mutation on lysine K16 of histone H4 affected global gene expression that was distinct from other H4 acetylation sites (K5, K8 and K12) (Dion *et al*., 2005). In addition to this, acetylation of histones also facilitates the origin firing, leading to an efficient DNA replication (Bell and Dutta, 2002; Unnikrishnan *et al*., 2010). Importantly, acetylation of histones occurs at sites of DNA breaks and is required for DNA repair process (Xu and Price, 2011; Bird *et al*., 2002). Other than acetylation at the N-terminal tails, acetylation of histone H3 lysine 56 (H3K56ac) within the globular domain, which is located at the entry-exit points of DNA wrapped around the histone octamer, is thought to destabilise nucleosome-DNA interaction (Xu *et al*., 2005). Moreover, H3K56ac has also been linked to DNA replication and repair in yeast (Driscoll *et al*., 2007; Han *et al*., 2007) and shown to be associated with transcriptional regulation and cell proliferation in higher eukaryotes (Das *et al*., 2009). Together, these data suggest that histone acetylation plays a critical role in facilitating the general ways for DNA accessibility.

Other than the roles in charge-dependent interaction with DNA, acetylation of histone N terminal tails can serve as the binding surface for regulatory proteins that interact with chromatins or protein-protein interaction. Acetylated lysine can either

positively or negatively regulate these interactions (Kurdistani and Grunstein, 2003). For instance, bromodomain-containing proteins, which are generally found in KATs, ATP-dependent chromatin remodellers and transcription factors, are known to recognise acetyl-lysine on histone H3 and H4 (Tamkun *et al*., 1992; Zeng and Zhou, 2002; Filippakopoulos *et al*., 2012). Furthermore, biochemical studies demonstrated that overexpression of histone acetyltransferase MOF, which acetylates histone H4 lysine 16, correlates with the loss of ISWI chromatin remodeller. Later, it was also shown the site-specific acetylation H4K12ac and H4K16ac antagonise the activity of chromatin remodelling ISWI complex (Corona *et al*., 2002; Shogren-Knaak *et al*., 2006). In addition to the bromodomain-containing proteins, it has been reported that a tandem plant homeodomain (PHD) finger protein, which normally recruit methylated histones, can bind acetyl-lysine of histone H3 lysine 14 (H3K14ac) (Lange *et al*., 2008; Zeng *et al*., 2010).

Lysine acetylation has emerged to play an important role in the protein stability and degradation. Mechanistic impacts of how acetylation is involved in such pathways vary from one protein to another (Glozak *et al*., 2005). Acetylation can regulate proteasome degradation by serving as a dual player to either promote or prevent poly-ubiquitination and proteosomal degradation. Several lines of evidence demonstrated that lysine acetylation could serve as a signal for ubiquitination and subsequent degradation in many proteins such as transcription factor E2F-1 (Galbiati *et al*., 2005), SV40-T antigen (Shimazu *et al*., 2006), tumor suppressor protein pRB (Leduc *et al*., 2006), cell-cycle protein cyclin A (Mateo *et al*., 2009), metabolic enzyme PEPCK1 (Jiang *et al*., 2011). Furthermore, histone acetylation is a key event for sensing of histone displacement by protamines during the process of DNA packaging in sperm cells (reviewed in Gaucher *et al*., 2010). Lately, it has been shown that bromoprotein-like proteasome protein PA200 (Blm10 in yeast) requires acetylated histones to promote ATP-independent proteasomal degradation of histones during spermatogenesis (Qian *et al*., 2013), suggesting a direct link between histone acetylation and proteasome degradation pathway. Collectively, lysine acetylation is a multifaceted modification involved in broad cellular activities. These actions include neutralising the charge, serving as acetyl-binding platform or acting as a recruiter for various regulatory proteins and signalling the degradation pathway.

1.2.1 Effects of site-specific lysine acetylation on histones

A wealth of information regarding lysine acetylation patterns is derived from genome- studies on histones. With the advent of genomic technologies such as microarray and high-throughput sequencing and the availability of acetylation-specific antibodies

(Suka *et al*., 2001), histone acetylation can be characterised and mapped across the genomes in many organisms. These technologies allow us to gain insights into site-specific histone acetylation patterns on a global scale. The consequences of histone acetylation depend on which lysine is acetylated, the location of modified nucleosomes and the enrichment levels. Individual or combinations of acetylation on lysine residues may give rise to distinct acetylation states and likely dictate the downstream biological functions. Universally, histone acetylation is enriched at the promoter and 5' end of coding regions in transcriptionally active genes and these features are conserved from yeast to man.

The most prominent example of site-specific acetylation is H4K16 acetylation. Acetylation profile of H4K16ac is unique and doesn't correlate with other acetylation site on H4 tails (Kurdistani *et al*., 2004). In budding yeast, acetylation and deacetylation of H4K16ac is an important determinant of heterochomatin formation. In yeast, heterochromatic regions are characterised by a pattern of deacetylation of H4K16ac via the action of Sir2 deacetylase. Deacetylated H4K16 together with the absence of KAT8 acetyltraseferase are important for Sir3 (one of the component of SIR complexes) binding and subsequent spreading of heterochromatin (reviewed in Millar *et al*., 2004; Millar and Grunstein, 2006). Importantly, H4K16ac has other discrete functions outside heterochromatic regions such as dosage compensation in a male X chromosome in *Drosophilla* (Turner *et al*., 1992) and gene transcription (Kind *et al*., 2008). Aberrant regulation of H4K16 acetylation caused transcriptional misregulation and loss of H4K16ac is observed in human cancers (Fraga *et al*., 2005).

Different acetylation marks may co-occur at similar regions of genes or regulatory elements. Previous works by Kurdistani et al, demonstrated similar acetylation patterns on promoters and coding regions in all core histones in yeast and identified groups of genes that are functionally related (Kurdistani *et al*., 2004). Notably, acetylation marks on histones are often clustered close together; for example, H3K9ac, H3K14ac, H3K36ac are known to occupy the transcriptional start site of active genes and correlates with active transcription and 5' end of genes coding regions are enriched with H2AK7ac, H3K9ac, H3K14ac, H3K18ac, H4K5ac, H4K12ac (Pokholok *et al*., 2005; Liu *et al*., 2005; Morris *et al*., 2007). Furthermore, the distribution patterns of various histone acetylation sites have been reported in the human genome. Analogous patterns of known acetylation marks are correlated with gene expression. It was reported that H2AK9ac, H2BK5ac, H3K9ac, H3K18ac, H3K27ac, H3K36ac and H4K91ac are localised in around the Transcription Start Site (TSS) while H2BK12ac, H2BK20ac, H2BK120ac, H3K4ac, H4K5ac, H4K8ac,

H4K12ac and H4K16ac are enriched in the promoter and transcribed regions (Wang *et al*., 2008).

Outside the promoter of genes, acetylated histones are associated with many regulatory elements such as enhancers, it was reported that diacetylated histone H3 lysine 9 and 14 marks are associated with active regulatory elements in human T cells (Roh *et al*., 2005; Wang *et al*., 2008). Other studies revealed that enhancer-bound histones are occupied with p300 acetyltransferase and H2K27ac or in combination with H3K4me1 (Heintzman *et al*., 2007; Heintzman *et al*., 2009; Creyghton *et al*., 2010; Rada-Iglesias *et al*., 2010). Lately, H4K16ac has been reported to mark active genes and enhancers in mouse embryonic stem cells (ESCs). Interestingly, this work has suggested distinct enhancer regions enriched for H3K4me1, KAT8 acetyltransferase and H4K16ac but not overlapped with H3K27ac or p300 (Taylor *et al*., 2013). Taken together, these findings indicate that similar acetylation patterns can be found on functionally related genes and certain acetylation sites. Therefore, spatial differences in terms of a combination of modified and unmodified of acetylation sites at specific loci can possibly lead to distinct biological outcomes. However, why these marks are associated with certain genomic regions remained to be elucidated.

1.2.2 Crosstalk between histone acetylation and other PTMs

Histone lysine acetylation has been reported to interplay with other PTMs such as phosphorylation and methylation. The complex communication between histone modifications can occur *in cis* (on the same histones) or *in trans* (between histones) (reviewed in Latham and Dent, 2007; reviewed in Lee *et al*., 2010). As a result, the coexistence of these marks can impact on one another by either promoting or inhibiting the neighbouring marks. For example, phosphorylation can affect acetylation state (Figure 1.2). The lysine can be adjacent to or distant away from the phosphorylation site, which can be either N-terminal or C-terminal from the acetylation site (Yang and Seto, 2008)

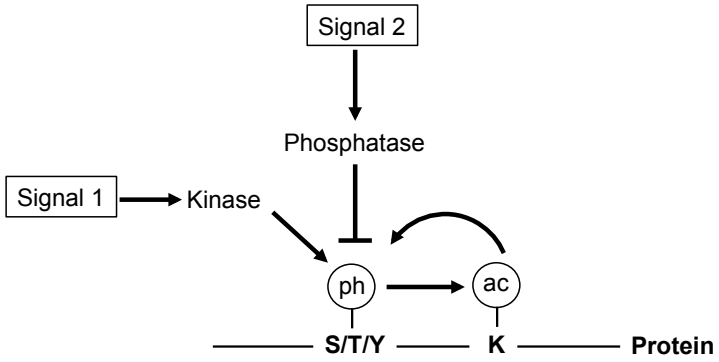

Figure 1.2. A schematic diagram demonstrates the crosstalk between phosphorylation and acetylation. Intrinsic or extrinsic cellular signals act on serine (S), threonine (T), or tyrosine (Y) phosphorylation. The phosphorylation can in turn impact on the acetylation of a neighbouring lysine residue. Conversely, acetylation could also regulate phosphorylation. (An illustration modified from Yang and Seto, 2008)

Given that lysine residues can be modified by acetylation or methylation, Acetylation at a certain lysine residue and other PTMs can be mutually exclusive. For instance, lysine acetylation blocks lysine methylation and vice versa as in the case of modifications at lysine 9 of histone H3. Importantly, H3K9ac is associated with active transcription whereas H3K9me3 is associated with repression (Nakayama *et al*., 2001).
With regard to the cross-regulation of histone acetylation and other modifications *in cis*, it was reported that phosphorylation of histone H3 (H3S10ph) enhanced the acetylation of H3K14ac and associated with open chromatin and gene activation (Cheung *et al*., 2000, Lo *et al*., 2000). In contrast, the level of H3S10 phosphorylation inhibits the adjacent H3K9 acetylation (Edmondson *et al*., 2002). Furthermore, tri-methylation of H4K20 (H4K20me3) was reported to antagonise acetylation of lysine on the H4 N-terminal tails (Kourmouli *et al*., 2004; Sarg *et al*., 2004). Interestingly, methylation of H4R3 could result

in either enhancing or preventing the acetylation on H4 in a methylase-specific manner (reviewed in Latham and Dent, 2007). In addition, serine phosphorylation can impact on acetylation states of histone H4. *In vitro* data showed that phosphorylation of H4 serine 1 (H4S1ph) inhibits N-terminal acetylation of histone H4 by NuA4. Consistent with this, the level of H4S1ph is increased upon DNA damage whilst H4 is deacetylated (Utley *et al*., 2005). A cartoon diagram of histone crosstalk is illustrated in (Figure 1.3).

Other than communication of H3-H4 tails, H2AT119 is phosphorylated during *Drosophila* mitosis. A mutation that inhibits phosphorylation at T199 caused the decrease in acetylation of H3K14ac and H4K5ac, suggesting the cross-regulation between histone marks during cell division (Ivanovska *et al*., 2005). Interestingly, histone acetylation crosstalk also functions in other cellular processes such as apoptotic cell death in yeast. Ahn et al (2006) showed that deacetylation of H2B lysine 11 (H2BK11ac) is required for yeast apoptosis induced by H2BS10ph. This study reported that the acetylation mark at H2BK11 blocks the phosphorylation of the adjacent H2BS10 by Ste20 kinase. Therefore, the deacetylation at K11 is required for the regulation of yeast apoptosis (Ahn *et al*., 2006). Zippo et al (2009) reported H3S10ph to facilitate the transcription elongation of FOSL1 gene by promoting H4K16ac. In this cascade event, phosphorylation of H3S10 creates a platform for phospho-binding protein 14-3-3. This protein then recruits KAT8 to acetylate H4K16ac (Zippo *et al*., 2009). Taken together, these findings suggest that acetylation and other PTMs histones are possibly interrelated and the complex communication between histone marks can dictate the biological functions

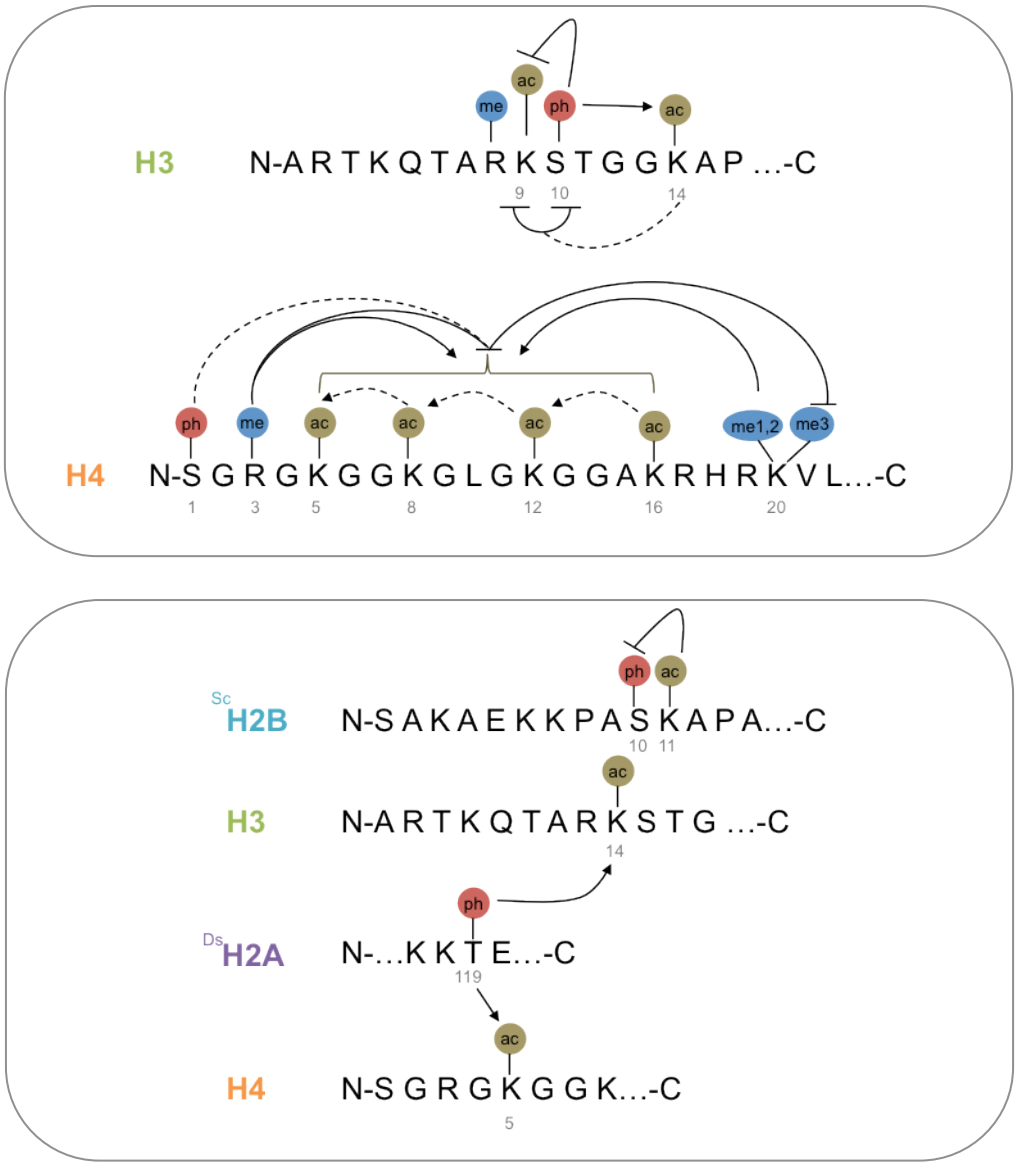

Figure 1.3 A schematic diagram illustrating cross-regulation of modifications *in cis* and *in trans*.
Ds = *Drosophila*; Sc= *S. cerevisiae*; ph = phosphorylation; ac = acetylation; black line = inhibition; black arrow = activation. Numbers indicate amino acid residues. Data modified from (Latham and Dent et al, 2007)

1.3 Histone variants and their specialised roles

Canonical core histones can be replaced by variant histones in particular nucleosomes. This event contributes to unique nucleosomal architectures that diversify the structural and functional characteristics of chromatin. Histone variants arose early in eukaryotic evolution and are universally found across eukaryotes (Malik & Henikoff, 2003). Unlike canonical histones, where synthesis and incorporation concomitantly occurs during DNA replication, non-allelic histone variants are synthesised and deposited throughout the cell cycle. Studies

have shown that variant histones have evolved for diverse cellular functions ranging from transcriptional regulation, DNA recombination and repair, chromosome segregation, sperm packaging and other processes (Talbert *et al*., 2010; reviewed in Millar, 2013)

The histones with known variants are H3 and H2A with a small number for H2B. Two major H3 variants include H3.3 and the centromere-specific CenH3 (Cse4 in budding yeast, CENP-A in mammals and CID in fly) (Malik and Henikoff, 2003). CenH3s are specifically located at centromeric regions where it confers a special role in kinetochore assembly (reviewed in Sarma and Reinberg, 2005). H3.3 variant, which only have 4 amino acids different from H3, plays a major regulatory role at the active transcribed regions, specifically in high turnover nucleosomes (Ahmad and Henikoff, 2002; Mito *et al*., 2005; Chow *et al*., 2005) and pericentric heterochromatin (Goldberg *et al*., 2010).

Of all histones, H2A variants comprise the greatest number of variants including H2A.Z, H2A.X (West and Bonner 1980), H2AvD (Van Daal et al., 1990), mH2A (macroH2A) (Pehrson and Fried, 1992), and H2A.B (H2ABbd) (Chadwick and Willard, 2001). The H2A.Z variant has emerged to be one of most studied because of its intriguing genomic localisation and multifunctional roles. The following section will summarise the relevant literatures to reconcile key information about of H2A.Z and its PTM by acetylation.

1.4 The variant histone H2A.Z

1.4.1 Overview & structural aspects

H2A.Z is an evolutionarily conserved variant, sharing ~90% protein sequence identity between species (Iouzalen *et al*., 1996; Jackson *et al*., 1996). Variant H2A.Z constitutes approximately ~5-10% of cellular H2A (Wu and Bonner 1981) but only shares ~60% sequence identity with canonical H2A (Allis *et al*., 1986). Given that H2A.Z has sequence similarity to H2A, in yeast cells these proteins cannot be substituted for each other, indicating that H2A.Z has distinct roles from H2A counterpart (Kolodrubetz *et al*., 1982; Jackson and Gorovsky, 2000).

Several lines of evidence have demonstrated that H2A.Z is essential for viability in early development in most organisms such as *Tetrahymena thermophila* (hv1) (Liu *et al*., 1996), *Drosophila melanogaster* (H2AvD) (Clarkson *et al*., 1999), *Xenopus laevis* (H2A.Zl) (Ridgway *et al*., 2004), *Mus musculus* (H2A.Z) (Faast *et al*., 2001),

Caenorhabditis. elegans (HTZ-1) (Whittle *et al*., 2008). Vertebrate H2A.Z protein is encoded by two H2A.Z genes, H2A.Z-1 and H2A.Z-2 or H2AF/Z and H2AF/V (Eirin-Lopez et al., 2007; Eirin-Lopez et al., 2009; Dryhurst *et al*., 2009; Matsuda et al., 2010). Unlike higher eukaryotes, *Saccharomyces cerevisiae* (*HTZ1*) and *Schizosaccaromyces pombe (PHT1)* cells lacking H2A.Z are viable but exhibit severe sensitivity to various cytotoxic agents. In fact, the defective growth phenotype in *htz1*Δ cells is also observed under normal condition and may be caused by cell cycle delay (Dhillion *et al*., 2006)

The overall structure of H2A.Z is largely similar to that of H2A. The crystal structure of the nucleosome core particle containing H2A.Z showed the subtle destabilisation of the interaction between the H2A.Z-H2B dimer and the H3-H4 tetramer in the 'docking domain' compared to the H2A-H2B nucleosomes (Suto *et al*., 2000). Furthermore, H2A.Z-containing nucleosomes have an extended acidic patch on the nucleosome surface compared to the H2A-containing nucleosomes. The acidic patch is the structural characteristic of nucleosomal surface that interacts with the N-terminal tail of H4 from the adjacent nucleosomes. Notably, the sequence difference between H2A.Z and H2A lies in the N- and C- termini. The main divergent regions of H2A.Z from H2A and H2A.X include L1 and L2 regions and C-terminal domains (Malik & Henikoff, 2003). The C-terminus of H2A.Z is required for its association with the chromatin (Wang *et al*., 2011; Wratting *et al*., 2012).

Importantly, H2A.Z containing nucleosomes exist in two forms: homotypic (H2A.Z-H2A.Z) and heterotypic (H2A-H2A.Z) nucleosomes in yeast (Viens *et al*., 2006) and human (Luk *et al*., 2010). In vertebrates, double variant histones containing H3.3 and H2A.Z have been observed. The combination of these variants results in rather labile nucleosome core particles (Jin *et al*., 2007; Jin *et al*., 2009). With regard to the stability, several studies examined the stability of H2A.Z-containing nucleosomes (Abbott *et al*., 2001; Fan *et al*., 2002; Park *et al*., 2004; Zhang *et al*., 2005; Thambirajah *et al*., 2006; Jin *et al*., 2007; Hoch *et al*., 2007; Ishibashi *et al*., 2009) however; the resulting profiles whether H2A.Z stabilise or destabilise nucleosomes, are still controversial. The different outcomes may be due to the methods used and the sources of reconstituted nucleosomes (recombinant versus *in vivo* sources)

In summary, the extended acidic-patch feature of H2A.Z-containing nucleosomes and the distinct N- and C- terminal regions may contribute to its specialised nucleosome properties in the chromatin.

1.4.2 H2A.Z-specific chromatin deposition and eviction complexes

The patterns of H2A.Z occupancy in the chromatin are regulated through the action of multiple protein interactors. SWR complex (SWR-C) is an ATP-dependent remodelling enzyme that performs the exchange of nucleosomal H2A-H2B for H2A.Z-H2B in a step-wise manner (Mizuguchi *et al*., 2004; Krogan *et al*., 2003; Kobor *et al*., 2004; Luk *et al*., 2010). This pathway is conserved across species (reviewed in Lu *et al*., 2009). In yeast, the SWR-C consists of 13 protein subunits; in which Swr1 is the catalytic activity (Mizuguchi *et al*., 2004) (Table 2). The C-terminal alpha helix of H2A.Z M6 region (Clarkson *et al*., 1999)) is important for its recognition by the SWR-C via the interaction of Swc2 subunit (Wu *et al*., 2005). Deleting *SWR1* in yeast led to the global loss of chromatin-associated H2A.Z levels (Li *et al*., 2005; Mizuguchi *et al*., 2004). In mammals, related SWR-C orthologues, SRCAP (SWI/SNF-2-related CBP activator protein) and p400 complexes, catalyse the incorporation of H2A.Z into chromatin (Ruhl *et al*., 2006; Wong *et al*., 2007). Inactivation of arp6 subunit of SRCAP led to approximately 70% reduction of H2A.Z in the chromatin (Matsuda *et al*., 2010). Consistently, inactivation of p400 caused H2A.Z deposition defects in human cells (Gévry *et al*., 2007; Gévry *et al*., 2009). Notably, the exchange of H2A.Z in mammalian cells can be mediated by p400 (TIP60) and SRCAP (Gévry *et al*., 2007; Martinato *et al*., 2008), suggesting these complexes perhaps share the common function in deposition of H2A.Z but they may be responsible for H2A.Z deposition in different chromosomal domains.

Unincorporated H2A.Z-H2B is observed to interact with histone chaperone Nap1 (Mizuguchi *et al*., 2004; Kobor *et al*., 2004). In yeast, an H2A.Z-specific chaperone, Chz1, has been identified. Chz1 contains conserved CHZ motifs that recognise H2A.Z and the interactions between H2A.Z-H2B and Chz1 are thought to be required for transferring them to SWR-C (Luk *et al*., 2007; Zhou *et al*., 2008). The removal of H2A.Z from nucleosomes can be mediated by two mechanisms i) general nucleosome loss during via the transit of RNA Polymerase II (Pol II) during transcription and ii) the dedicated complex(s). Intriguingly, INO80 chromatin remodelling complex is capable of performing the exchange of H2A.Z-H2B for H2A-H2B. *In vivo* genome-wide studies of G1-arrested yeast cells show that inactivation of INO80 (*ino80Δ)* led to global increase of H2A.Z. Therefore, INO80 complex has been linked for removing H2A.Z-containing nucleosome (Papamichos-Chronakis *et al*., 2011). Importantly, INO80 and SWR-C share 4 subunits including Arp4, Rvb1, Rvb2 and Act1 (Table 1.2), suggesting that SWR-C and INO80 may function co-ordinately to regulate the H2A.Z localisation in the chromatin.

In addition to SWR-C and INO80 complexes, the chromosome-remodelling enzyme Fun30 has been linked to H2A.Z localisation. It was reported that chromatin-associated H2A.Z was affected in budding yeast cells lacking Fun30 (*fun30*Δ) similar to the pattern observed in *ino80*Δ cells (Durand-Dubief *et al*., 2012). Similarly, increased H2A.Z occupancy in centromeric and sub-telomeric regions was also observed in fission yeast cells lacking Fun30 (*fft3*Δ) (Strålfors *et al*., 2011). Lately, it was demonstrated that Fun30 contains nucleosome-sliding activity in an ATP-dependent manner (Byeon *et al*., 2013). Therefore, it is possible that Fun30 is capable of removing H2A.Z like INO80.

In summary, identification of chaperones and nucleosome assembly factors involved in the pathway of H2A.Z is essential to gain further understanding of H2A.Z biology.

Subunit type	**INO80 complex**		**SWR-C and SRCAP complex**	
	S. cerevisiae	***H. sapiens***	***S. cerevisiae***	***H. sapiens***
ATPase	Ino80	INO80	Swr1	SRCAP
RuvB-like	Rvb1 and Rvb2	RUVBL1 and RUVBL2	Rvb1 and Rvb2	RUVBL1 and RUVBL2
Actin	Act1	β- Actin	Act1	β- Actin
Actin-related protein	Arp4, Arp5 and Arp8	BAF53A, ARP5 and ARP8	Arp4 and Arp6	BAF53A and ARP6
YEATS protein	Taf14	N/A	Yaf9	GAS41
Non-conserved subnit	Ies1, Ies2, Ies3, Ies5, Ies6 and Nhp10	Amida, CCDC95, FLJ20309, IES2, IES6, MCRS1, NFRKB, UCH37 and YY1	Bdf1, Swc2, Swc3, Swc5, Swc6 and Swc7	DMPA1, GAS41, tubulin, XPG, YL1 and ZnF-HIT1

Tabel 1.2. INO80 and SWR-C/SRCAP chromatin remodelling complexes
The table shows the conserved characteristics and the shared subunits (highlighted in grey); a table modified from Morrison and Shen, 2009.

1.4.3 The functional connection of KAT5 (NuA4) and SWR-C with H2A.Z

Nucleosome Acetyltransferase of histone H4 (NuA4) is an evolutionarily conserved protein complex that is responsible for histone H4 acetylation on lysine 5, 8 and 12 (Smith *et al*., 1998; Allard *et al*., 1999) and budding yeast H2A.Z (Htz1) (Millar *et al*., 2006; Barbiarz et al., 2006; Keogh *et al*., 2006; Mehta *et al*., 2010). In yeast, NuA4 complex can be divided in two forms; the large 13-subunit NuA4 and a smaller piccolo NuA4 (PicNuA4). Esa1 is the catalytic subunit that carries out acetytransferase activity and five other subunits; including Act1, Arp4, Epl1, Swc4 and Tra1 are essential genes. Eaf1, a non-essential subunit, acts as a platform, which account for the complex integrity (Auger *et al*., 2008; Mitchell *et al*., 2008). The PicNuA4 consists of 4 subunits including Esa1, Yng2, Eaf6 and Epl1 and is involved in global histone acetylation (Boudreault *et al*., 2003). A number of biochemical studies showed that four subunits are in common between SWR-C and NuA4, suggesting the functional connection between these two protein complexes (Krogan *et al*., 2003; Kobor *et al*., 2004, Mizuguchi *et al*., 2004; Zhang *et al*., 2004). These shared modules include Act1, Arp4, Swc4 and Yaf9, which are required for a proper function in both complexes and are thought to co-regulate H2A.Z. The comparison between NuA4 and SWR-C complexes and their shared subunits is shown in Table 1.3.

Evidence has suggested that that the p400 (TIP60) in higher eukaryotes is derived from the merging between NuA4 and SWR-C (Auger *et al*., 2008; reviewed in Lu *et al*., 2009). Therefore, it is possible that incorporation of H2A.Z by SWR-C and acetylation by NuA4 is functionally connected and their actions towards H2A.Z might be regulated synergistically. Understanding these two pathways may shed the light in understanding the biology of H2A.Z in mechanistic detail.

	S. cerevisiae	Tip60 *H. sapiens*	SRCAP *H. sapiens*
NuA4	Esa1	Tip60	
	Yng2	ING3	
	Elp1	EPC1	
	Tra1	TRRAP	
	Eaf1		
	Eaf3	MRG15	
	Eaf5		
	Eaf6	hEaf6	
	Eaf7	MRGBP	
	Yaf9	GAS41	GAS41
	Swc4	DAMP1	DAMP1
	Arp4	BAF53a	BAF53a
	Act1	Actin	Actin
SWR-C	Swr1	p400	SRCAP
	Bdf1	Brd8	
	Swc2	YL1	YL1
	Swc3		
	Swc5		
	Swc6		
	Swc7		
	Arp6		
	Rvb1	TIP49a	TIP49a
	Rvb2	TIP49b	TIP49b
	Htz1	H2A.Z	H2A.Z

Table1.3 The conservation of NuA4 and SWR-C in budding yeast and human.
The middle panel is coloured in grey to highlight 4-shared components between NuA4 and SWR-C complexes (modified from Lu *et al*., 2009)

1.4.4 Genome-wide distribution of H2A.Z-containing nucleosomes

The essential information of H2A.Z genomic patterns has come from global analyses in various organisms. Genome-wide localisation studies carried out in *S. cerevisiae* showed that H2A.Z (Htz1) is distributed in a non-random fashion throughout all 16 yeast chromosomes, (Guillemette *et al*., 2005; Li *et al*., 2005; Raisner *et al*., 2005 Zhang *et al*., 2005). In yeast, H2A.Z is preferentially localised in the 'hot' or ' high turnover' promoter nucleosomes (Dion *et al*., 2007) flanking nucleosome deficient regions (NDR). Also H2A.Z can occupy at the 5' end of genes in both active and inactive loci. Several lines of evidence indicate that H2A.Z is preferentially enriched at repressed/basal promoters of inactive genes or lowly expressed genes and intergenic regions (IGRs) compared with gene coding regions. H2A.Z occupancy correlated with histone acetylation but negatively correlated with transcription rate (Zhang *et al*., 2005; Guillemette *et al*., 2005; Li *et al*., 2005; Liu *et al*., 2005; Millar *et al*., 2006). In contrast to yeast, human H2A.Z occupancy

correlates with gene activity and H3K4me3 marks (Bruce *et al*., 2005; Barski *et al*., 2007; Schones *et al*., 2008; Hardy *et al*., 2009; Valdes-Mora *et al*., 2011). Furthermore, mammalian H2A.Z is also enriched in non-promoter regions such as in enhancers, insulators and in heterochromatin (Barski *et al*., 2007; Jin *et al*., 2009; Hardy *et al*., 2009; reviewed in Maston *et al*., 2012), suggesting H2A.Z may influence transcriptional regulation via its incorporation at these domains.

Notably, general profiles of H2A.Z localisations are evolutionarily conserved, although there are slight different patterns. Many studies have revealed that H2A.Z localise at the strongly positioned (+1) nucleosome downstream of TSSs and relatively depleted in the coding sequences (CDS). Budding yeast and human H2A.Z is enriched both upstream and downstream of TSS. In contrast, fly, plant, and fission yeast lack H2A.Z upstream of TSS; only at the downstream regions of the NDR were observed (Mavrich *et al*., 2008; Zilberman *et al*., 2008; Lantermann *et al*., 2010). Recent work has showed that the majority of H2A.Z-containing nucleosomes associated with active genes (downstream of TSS) are homotypic whereas the heterotypic versions were found at the intron-exon junctions (Weber *et al*., 2010). As several lines of evidence reported the preferential binding of H2A.Z at promoter, one may ask 'How does H2A.Z target to the promoter regions?' Interestingly, it was proposed that H2A.Z might function in nucleosome positioning since it resides in well-positioned nucleosomes. However, It has been demonstrated that nucleosome positioning is not dependent to H2A.Z but NDR establishment is required for H2A.Z deposition (Hartley and Madhani, 2009). It is not well established how H2A.Z is incorporated into chromatin in this specific manner; however, promoter DNA sequences and posttranslational modifications on other histones may contribute to recruit SWR-C to promoters (Raisner *et al*., 2005; Zhang *et al*., 2005).

Recent studies suggest that cell-cycle states could cause changes in H2A.Z localisation patterns. In response to cell cycle, H2A.Z-nucleosomes become heterotypic during S-phase and less stable than the homotypic version. During mitosis, H2A.Z-nucleosomes localise to centromeres and are reported to shift upstream into TSS. As a result, it diminishes the NDR region (Kelly *et al*., 2010; Nekrasov *et al*., 2012). Collectively, these findings suggest that the high conservation of H2A.Z genome-wide distribution and spatio-temporal regulation of H2A.Z by cell cycle state.

1.4.5 The role of H2A.Z in transcriptional regulation

H2A.Z has been implicated to play a role in transcriptional regulation. In *T. thermophila*, H2A.Z is associated with transcriptional-active macronucleus, implying its role in gene transcription (Allis *et al*., 1980). It was also shown in yeast that H2A.Z regulates transcription of inducible genes and that is redundant with chromatin remodelling complexes SAGA and SNF/SWI (Santisteban *et al*., 2000). Loss of yeast H2A.Z disrupts specific gene activation of *PHO5* and *GAL1* genes and affects the silencing of HMR and telomeric loci (Dhillon and Kamakaka 2000; Santisteban *et al*., 2000). Moreover, deletion of *HTZ1* affects the binding of RNA Polymerase II transcription machinery in *GAL* genes (Adam *et al*., 2001). In human cells, H2A.Z occupancy was associated with the recruitment of RNA pol II (Hardy *et al*., 2009), suggesting the conservation of its role in poising at genes prior to eviction during transcription. Lately, the relationship between H2A.Z and the transcription elongation was observed at specific loci in budding yeast. It was reported that the presence of H2A.Z-nucleosomes might facilitate the transcription elongation complexes (Santisteban *et al*., 2011). In order to achieve transcription, nucleosomes are evicted from the promoter regions to allow the transcriptional machinery to be recruited to targeted genes. Others suggested that perhaps incorporation of H2A.Z could contribute to the stability of nucleosome. Zhang et al demonstrated that H2A.Z-containing nucleosomes are less stable and this is likely to facilitate the gene activation because of its easy removal (Zhang *et al*., 2005).

If H2A.Z is responsible for transcriptional regulation, loss of H2A.Z should result in inappropriate transcription globally. Previously, the differential gene expression of wild type and *htz1*Δ from the steady-state yeast cells growing in rich media was directly compared. However, the result showed that global gene expression was only subtly altered; only genes in the Htz1-activated domains (HZADs) domains were to be affected and some of these effects could be indirect (Meneghini *et al*., 2003). In agreement with the budding yeast, deletion of *PHT1* in fission yeast results in only modest changes in the transcription of sense strand transcripts. Furthermore, this study demonstrated the link between H2A.Z and heterochromatin protein Clr4 and RNA interference component Ago1 in suppression of antisense RNAs (Zofall *et al*., 2009). Taken together, H2A.Z perhaps indirectly affects gene expression in budding and fission yeast. However, the case might be different in higher eukaryotes because H2A.Z is required during the transcriptional response in ESC self-renewal and differentiation. H2A.Z knockdown caused transcriptional misregulation in ESCs (Creyghton *et al*., 2008; Li *et al*., 2012; Hu *et al*., 2013).

Interestingly, H2A.Z plays a unique role in antagonising DNA methylation in CpG-rich promoters. In plants, the presence of H2A.Z at the promoter serves to protect genes from DNA methylation-mediated silencing (Zilberman *et al*., 2008). Importantly, the inverse relationship between H2A.Z and DNA methylation has also been reported in puffer fish (Zemach *et al*., 2010) and mouse (Conerly *et al*., 2010), suggesting the conservation of H2A.Z in antagonising the DNA methylation. Collectively, numerous studies have highlighted the intimate relationship of H2A.Z roles in transcriptional regulation, although some nuanced regulations may be species-specific.

1.4.6 H2A.Z roles in heterochromatin and in chromosome segregation

Genetic studies have identified silent regions in *S. cerevisiae* including *HMR* and *HML* silent mating type cassettes, telomeres, and the rRNA-encoding DNA (rDNA) (reviewed in Rusche *et al*., 2003). Chromatin silencing in *S. cerevisiae* is mediated by the spreading of Sir proteins together with hypoacetylated histones. In yeast, H2A.Z is enriched near telomeric regions and euchromatic regions flanking the *HMR* mating loci (Meneghini *et al*., 2003; Guillemette *et al*., 2005; reviewed in Millar and Grunstein, 2006). Deletion of *HTZ1* gene induces Sir-2 mediated heterochromatin silencing to spread into euchromatic locations flanking these regions (Meneghini *et al*., 2003). Therefore, H2A.Z acts as guardian to protect heterochromatin spreading and affect the heterochromatin indirectly in budding yeast.

In mammals, a small population of H2A.Z is associated with heterochromatin and is co-localised with H3K9me2 (Hardy *et al*., 2009). Biochemical and immunofluorescent studies showed that H2A.Z is enriched within pericentric and centric heterochromatin regions in mouse (Rangasamy *et al*., 2003) and human cells (Greaves *et al*., 2007). The presence of H2A.Z in these regions contributed to the formation of pericentromeric heterochromatin and interaction with heterochromatin protein (HP1α) (Rangasamy *et al*., 2003; Fan *et al*., 2004). An analogous pattern of H2A.Z function in the heterochromatic region exists in *Drosophila.* H2A.Z is localised at centromeric heterochromatin and required for the establishment of heterochromatin. This work also reported that the loss of H2A.Z affected HP1 recruitment to centromeric heterochromatin, suggesting that the interplay between H2A.Z and HP1 is conserved (Swaminathan *et al*., 2005). These results together suggest H2A.Z role in regulating the structural organisation of heterochromatin and perhaps chromosome stability.

Heterochromatin formation is critical for centromere function and proper centromere function is essential for the chromosome segregation process. H2A.Z has been implicated to play a major part in chromosome segregation in many organisms. In *S. cerevisiae,* H2A.Z displayed genetic interactions with kinetochore components. Mutations in H2A.Z, the SWR-C, and NuA4 cause defects in chromosome segregation (Krogan *et al*., 2004), suggesting its role in centromere organisation. Deletion of H2A.Z (*pht1*Δ) in *S. pombe* causes misregulation in the chromosome architecture, most likely due to the premature disassociation of the condensin protein complex during anaphase (Carr *et al*., 1994; Kim *et al*., 2009), indicating the requirement of H2A.Z to interact with other regulatory proteins for efficient chromosome segregation. In higher eukaryotes, it was reported that depletion of H2A.Z caused chromosome instability and defects in chromosome segregation process (Rangasamy *et al*., 2004). Together, these findings suggest that H2A.Z plays an important role in chromosome compaction and segregation, thereby contributing to the maintaining genome stability.

1.5 The emerging roles of H2A.Z acetylation

Like canonical histones, the N-terminal and C-terminal regions of H2A.Z can be modified by multiple post-translational modifications. These modifications include acetylation (Barbiarz *et al*., 2006; Keogh *et al*., 2006 Millar et al., 2006), sumoylation (Kalocsay *et al*., 2009) and ubiquitylation (Sarcinella *et al*., 2007; Ku *et al*., 2012). However, I will focus on the N-terminal acetylation of H2A.Z, as it is the most relevant to this study.

Importantly, the N-terminal lysine residues on H2A.Z are presented across the species, indicating that they are highly conserved. To date, evidence from mass-spectrometry and biochemical analyses have identified the acetylated lysine isoforms in budding and fission yeast, fly, chicken and human. Given that the conservation of lysine residues on the H2A.Z N-terminus exists, it is very likely that lysine sites present in other organisms can be modified by acetylation. Hence, it is possible that H2A.Z acetylation may have evolved to confer specialised functions for H2A.Z.

The N-terminal tail of budding yeast H2A.Z is acetylated at four lysine residues (K3, K8, K10 and K14) while acetylated H2A.Z K14 species is preferentially localised at the promoters of active genes. This data illustrated a key feature acetylated H2A.Z populations at K14 are correlated with promoter's nucleosomes (Millar *et al*., 2006). However, it is still unknown whether the genome profiles of other acetylation sites (K3, K8 and K10) overlaps with K14 profiles or possess distinct genomic patterns.

Similarly, in mammalian cells, acetylated H2A.Z isoforms are associated with promoter of active genes and enhancers (Valdes-Mora *et al*., 2011; Ku *et al*., 2012; Hu *et al*., 2013) whereas hypoacetylated H2A.Z isoforms are associated with heterochromatin (Hardy et al., 2009). In chicken cells, hyperacetylated H2A.Z isoforms (tri-acetylated lysines; K4, K7 and K11) is also found at 5' end of active genes but it is absent from inactive genes (Bruce *et al*., 2005). Furthermore, the doubly acetylated and unbiquitinated H2A.Z species is enriched at bivalent promoters but not at stably repressed promoters in mouse ESCs (Ku *et al*., 2012).

KATs that modulate the H2A.Z acetylation state have been identified. H2A.Z is acetylated by NuA4 (KAT5) and SAGA (KAT2) complexes after assembly into chromatin by SWR-C (Millar *et al*., 2006; Keogh *et al*., 2006; Barbiarz *et al*., 2006). Hda1 was identified as a KDAC responsible for H2A.Z deacetylation (Lin *et al*., 2008; Metha *et al*., 2010). Table 1.4 summarises up-to-date findings on H2A.Z acetylation across organisms.

The N-terminal lysine acetylation sites have emerged as a key functional modification on H2A.Z. In *Tetrahymena,* these acetylatable lysine residues were shown to be critical for the function of the H2A.Z because mutations of all six acetylatable lysine sites to arginine residues cause death in this organism. It was proposed that the N terminal acetylation modulates charge on the H2A.Z tail because any given mutation that reduced the charge can rescue the phenotype whether it is an acetylatable site or not (Ren and Gorovsky, 2001). Furthermore, Kim et al (2009) have shown that acetylated forms of H2A.Z in *S. pombe* play a pivotal role in chromosome stability. Unacetylable mutant cells show similar phenotypes to the null H2A.Z cells in both genetic interaction and gene expression studies (Kim *et al*., 2009). These findings strongly suggest that acetylation of H2A.Z is integral to its function.

Histone acetylation is commonly connected to transcriptional activation. While H2A.Z has been implicated in transcriptional regulation, the mechanism of how H2A.Z acetylation regulates transcription remains elusive. Several lines of evidence reported the contribution of H2A.Z acetylation in transcriptional regulation in various inducible gene systems: either the association of H2A.Z at these loci or the resulting gene expression changes upon transcriptional activation. Particularly, in yeast, these data were examined in acetylatable wild-type strains, irrespective of their site-specific acetylation patterns, and in unacetylatable lysine-to-arginine mutants, which mimic constitutive unacetylated state of H2A.Z. Several lines of evidence reported that acetylation sites on H2A.Z are required for a proper gene induction in budding yeast. Halley et al (2010) demonstrated that completely unacetylatable H2A.Z mutant strains exhibit *GAL1* induction defects, suggesting the role

of H2A.Z acetylation in *GAL1* induction (Halley *et al*., 2010). Consistent with the findings in yeast, acetylation sites at the N-terminus of H2AvD in fly are required for the activation of heat-shock activated *hsp70* gene and heat shock–induced puff formation on polytene chromosomes (Tanabe *et al*., 2008). Others reported that acetylation at lysine K14 site is required for H2A.Z localisation and proper gene expression at oleate-responsive gene promoters, such as *FOX2*, *POX1*, *CTA1* and *POT1* during the repressed state (Wan *et al*., 2009). Together, these data represent the intimate relationship between acetylation sites to be required for fully functional H2A.Z during gene activation.

The mechanistic insight into the functional relevance of H2A.Z acetylation is not well established. The phenotypes of mutant cells lacking acetylation sites were linked to their biological importance. Previous work demonstrated that unacetylatable H2A.Z mutants displayed the boundary protection defects, indicating that acetylation sites were required for the H2A.Z to protect heterochromatin spreading (Babiarz *et al*., 2006). Furthermore, yeast cell lacking the major site of acetylation (*htz1*-K14R) or harbouring completely unacetylatable allele (*htz1* K3, 8, 10, 14 R) exhibits defects in chromosome segregation by showing sensitivity to microtubule destabilising agent benomyl (Keogh *et al*., 2006; Lin *et al*., 2008; Mehta *et al*., 2010). In support of these findings, it was demonstrated that fission yeast cells expressing unacetylatable H2A.Z allele (*pht1*-4KR) exhibited defects in chromosome segregation which phenocopied the *pht1*Δ strain (Kim *et al*., 2009). Recently, it was suggested that the role of H2A.Z acetylation may be involved in regulation of sister chromatid cohesion in budding yeast (Sharma *et al*., 2013). To help integrate the functional connection of pathways involved in H2A.Z function, Figure 1.4 summarises the current findings of these pathways for H2A.Z regulation.

Seemingly, lysine acetylation sites are associated with many roles in which H2A.Z are involved. These biological observations suggest that acetylation of H2A.Z might function in regulating diverse chromatin- associated processes.

Species	Residues modified/enzymes	Genome locations	Phenotype/Biological function
S. cerevisiae (Htz1)	K3, K8, K10 and K14 (by KAT5 and KAT2)	K14 is associated with active-transcribed regions (Millar *et al*., 2006)	- Boundary protection defects (Barbiarz *et al*., 2006); synthetic lethality with *h4 K5, 8, 12 R* and *eaf1*Δ - Sensitivity to benomyl (*K14R*) and exhibit elevated chromosome loss (Keogh *et al*., 2006) - Htz1 deposition at *PHO5* (Millar *et al*., 2006) - *GAL1* induction (Halley *et al*., 2010) - Sister chromatid cohesion defects (Sharma *et al*., 2013)
S. pombe (Pht1)	K5, K7, K12 and K16 (by Mst1)	N.D.	- Chromosome segregation (Kim *et al*., 2009)
H. sapiens (H2A.FZ)	K4, K7, K11, K13 and K15	Dual Kac/Kub associated with bivalent promoters	N.D.
G. gallus (H2A.FZ)	K4, K7 and K11	Tri-acetylated (K4+K7+K11) associated with 5' end of active genes	N.D.
D. melanogaster (H2AvD)	K4, K7, K11, K13 and K15 (by dTip60 complex)	N.D.	- Prerequisite for exchange at DNA damage site (Kush *et al*., 2004)

Table 1.4. **Overview of H2A.Z acetylation sites and their functional significance across species**.
Summary of known acetylation sites in budding and fission yeast, human, chicken and fly is shown. The residues modified and functions that have been associated with acetylation are also demonstrated. The degree of enrichment at individual site in fission yeast and fly has not yet been established by mass-spectrometry analysis.

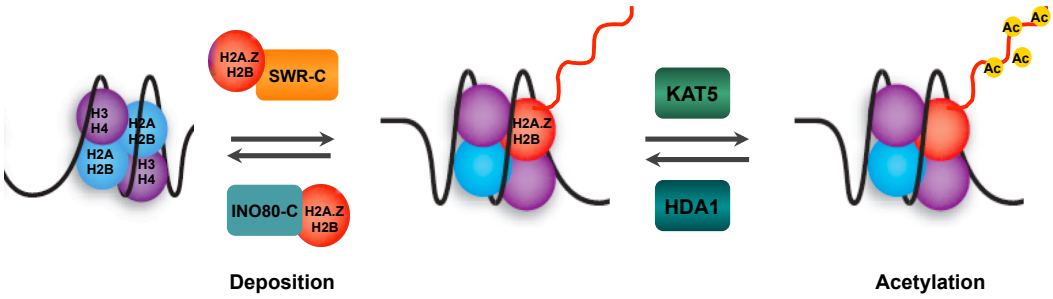

Figure 1.4 A schematic diagram illustrates pathways involved in the regulation of H2A.Z in the chromatin
H2A.Z-H2B dimer is deposited by SWR-C and removed by INO80-C. After H2A.Z is incorporated into chromatin, it is acetylated by KAT5 (NuA4). Deacetylation of H2A.Z is performed by Hda1 deacetylase enzyme. However, the interconnection between these pathways still remains to be elucidated.

1.6 Project Aims

Histone variants and their post-translational modifications contribute to the regulation of chromatin functions. H2A.Z or Htz1 is a highly conserved histone H2A variant in *S. cerevisiae* and has been extensively studied in this organism. Like other major histones, the N-terminal tail of H2A.Z is subjected to post-translational modifications. H2A.Z is acetylated at lysine K3, K8, K10 and K14 by KAT2 and KAT5 and deacetylated by Hda1. Mass-spectrometric analysis showed that the gradient abundance between individual acetylation sites, indicating that they may differ in terms of regulation (Millar *et al*., 2006).

Despite known H2A.Z acetylation sites, much less supporting evidence exist *in vivo*. The exact molecular mechanism of H2A.Z acetylation to H2A.Z functions remains unexplored. Little is known about acetylation and deacetylation of H2A.Z regulates transcription, silencing or chromosome segregation, thus raising the question of what roles acetylation at these lysine sites plays in vivo. The key information is that the most frequently acetylated H2A.ZK14ac populations are observed at promoters of active gene and H2A.Z protein seems to be misregulated in the absence of all acetylatable lysine sites. Therefore, insertion of acetylated H2A.Z isoforms at certain chromosomal domains may confer important biological implications.

The key questions that this project aims to address are: Does site-specific acetylation at each lysine residue of H2A.Z have distinct functional implications? How does acetylation regulate H2A.Z function? Can we use genome-wide information to correlate the function of individual/overall acetylation sites?

The global analyses of H2A.Z acetylation across the genome will be used to correlate its localisation with its functions by the *in vivo* mapping of acetylated and constitutive

unacetylated H2A.Z isoforms. Biochemical and genetics studies were conducted to investigate the role of individual acetylation sites and examine the functional connection of the acetylation sites of H2A.Z to uncover how they regulate H2A.Z function.

CHAPTER 2: MATERIALS AND METHODS

2.1 Materials

General laboratory chemical and reagents are purchased from Fisher Scientific, Life technologies™ (Invitrogen™), Sigma-Aldrich, if not otherwise indicated. DNA oligonucleotides for polymerase chain reaction (PCR) and cloning were custom-made by Eurofins MWG Operon. Yeast media components were obtained from Formedium™. For all buffers and solutions described, Milli-Q ultrapure water (Millipore) was used.

2.1.1 *Escherichia coli* (*E. coli)* media and buffers

LB medium/plates:	1% Yeast extract 0.5% Tryptone 1% NaCl (1.5% agar for LB solid medium) Ampicillin 100 μg/ml
SOC medium:	0.5% Yeast extract 2% Tryptone 10mM NaCl 2.5mM KCl 10mM $MgCl_2$ 10mM $MgSO_4$ 20mM Glucose

2.1.2 *S. cerevisiae* media and buffers

YPD/YPG:	69g/l YEP broth (Formedium™) (10g/l yeast extract; 20g/l peptone) 2% carbon source (glucose/galactose) 1.5% agar for plates
YPD G418/NAT plates:	After autoclaving, YEP agar+ 2% glucose was cool to 50°C. G418 (Melford) or ClonNAT (Werner Bioagent) was added to 300μg/ml or 100 μg/ml respectively

SC dropout media: 10% Yeast Nitrogen Base (YNB) without amino acids
10% Complete Synthetic Media (CSM) drop out mix
2% carbon source (glucose or galactose)

FOA plates: After autoclaving, SC agar + 2% carbon source was cool to 50°C. Uracil and 5-FOA was added to 0.025g/l and 0.1% respectively.

2.1.3 Antibodies

Table 2.1 Primary antibodies used in western blot analysis

Antibody	Description	Dilution	Condition
Anti-Htz1affinity-purified (α660)	Rabbit polyclonal	1:1000	WB: 3% milk PBS-0.1% Tween
Anti-HA clone 12CA5	Mouse monoclonal IgG2B K (Roche 11583816001)	1:5000	WB: Odyssey Licor blocking buffer+0.1%Tween
Anti-histone H2B	Rabbit polyclonal (Active Motif-39237)	1:20,000	WB: Odyssey Licor blocking buffer+0.1%Tween
Anti-histone H4	Rabbit polyclonal (Abcam Ab10158)	1:1000	WB: Odyssey Licor blocking buffer+0.1%Tween
Anti-TAT1 (tubulin)	Mouse-monoclonal (Sharrock's lab)	1:5000	WB: Odyssey Licor blocking buffer+0.1%Tween
Anti-Htz1 Lys8	Rabbit polyclonal (Millipore 07-770)	1:500	WB: Odyssey Licor blocking buffer+0.1%Tween
Anti-Htz1 Lys10	Rabbit Polyclonal (Millipore 07-771)	1:500	WB: Odyssey Licor blocking buffer+0.1%Tween
Anti-CBP	Rabbit polyclonal Millipore 07482	1:1000	WB: 3% milk PBS-0.1% Tween
Anti-G6PDH	Rabbit polyclonal (A9531, Sigma)	1:5000	WB: Odyssey Licor blocking buffer+0.1%Tween

Table 2.2 Secondary antibodies used in western blot analysis

Antibody	Description	Dilution	Condition
HRP-conjugated Anti-mouse antibody	GE Healthcare NXA931	1:3000	ECL WB: 1% milk PBS-0.05% Tween
HRP-conjugated Anti-Rabbit antibody	GE Healthcare NA934	1:3000	ECL WB: 1% milk PBS-0.05% Tween
IRDye 800 CW Anti-Mouse IgG	Goat Li-Cor 92632210	1:10000	Odyssey Li-cor blocking buffer+0.1%Tween+0.01%SDS
IRDye 800 CW Anti-Rabbit IgG	Goat Li-Cor 92632211	1:10000	Odyssey Li-cor blocking buffer+0.1%Tween+0.01%SDS
IRDye 680 LT Anti-Mouse IgG	Donkey 92668022	1:20000	Odyssey Li-cor blocking buffer+0.1%Tween+0.01%SDS
IRDye 680 LT Anti-Rabbit IgG	Donkey 92668023	1:20000	Odyssey Li-cor blocking buffer+0.1%Tween+0.01%SDS

Table 2.3 Primary antibodies used in Chromatin Immunoprecipitation

Antibody	Description
Anti-660 Htz1	1µl in 50 µl WCEs
Anti-779 Htz1K8ac	2.5 µl in 100 µl WCEs+0.5M NaCl
Anti-735 Htz1K10ac	2.5 µl in 100 µl WCEs
Anti-741 Htz1K14ac	1 µl in 100 µl WCEs

2.1.4 Oligonucleotides

Table 2.4 Oligonucleotides for RT-qPCR

Name	Sequence 5'- 3'	Target genes
Htz1p3 (F) Htz1p39(R)	CTTCTTCAGCAAGGGCTGGC TGGCAGCTTTGGATCCTACT	*HTZ1*
Act1CDS_F Act1CDS_R	GGTTATTGATAACGGTTCTGGTATG ATGATACCTTGGTGTCTTGGTCTAC	*ACT1*

Table 2.5 Oligonucleotides for ChIP-qPCR

Name	Sequence 5'- 3'	Genomic coordinates
YN_1F YN_1R	ACTTGGGAACGTTGGAAACA CCATGACTGTCGTTGTTTGTG	ChrXV: 579652+579754
YN_2F YN_2R	ACCCACAAAACGAGATGGAG GGAGACGGCTTGGACATAGA	ChrIV: 148204+148309
YN_3F YN_3R	TTGCTTCAACAACGGGATAA ATTTAGTGGCCAGCGAAGAG	ChrX: 152102+152206
YN_4F YN_4R	GGAAAGGAAAAGTGTTCGAGA CACCGTGAATACTACCTCATCAA	ChrVIII: 360542+360643
YN_5F YN_5R	GAAAGCAATACCAGCATCAACA GTCCTCTTATCACGGGCAAC	ChrXV: 611966+612078
YN_6F YN_6R	AAAACTGGCGAGGGTAAATG TCAGCCAACGATTGAAAACA	ChrXIV: 258421+258534
YN_7F YN_7R	CAACAACAGCGGCAACAG TCTAATCGTGGTGGCAAAAA	ChrIV: 126348+126450
YN_8F YN_8R	CGCTGGATACTCTTCTCTATCAA AGCATGTGGGGTGAGGATAA	ChrX: 60066+60168
YN_9F YN_9R	AGATGAGGTGCAGAGAACAACA TGAGGAAGTTCGTGGAGGAC	ChrXVI: 360149+360298
ARF317F D-F (R)	GAATAAGCGCAGGTACTCCTG GCCTACCTTCTTGAACAAGA	ChrIII: 292903+293051
GAL9A GAL9B	TGAACGCACCATAATCTCCGTACC GGGACCCATCATTCAAAATCCTTC	ChrII: 276676+276943
YCR081W_F YCR081W_R	CCCTGATTTCAAGCCTTGGGAG GTATGGTAAAAGCCCTTAGCCAC	ChrIII: 254457+254537
YBR276C_F YBR276C_R	GGGCTCATGATATTTCCTTTGGTC ACGCAAAAGCGCAGAATTGTTAGC	ChrII: 759842+759939

Genome coordinates correspond to the size of amplicon for each primer pair. The yeast chromosome number and genomic positions (UCSC genome browser) are also displayed.

Table 2.6 Oligonucleotide for plasmid constructions

Name	Sequence 5'- 3'	Application
Htz1dsR1	AATTGCAATTGATAGATGATTTTCTGGTTATAAAAA GGAACCAACAAATCGGAATTCGAGCTCGTTTAAAC	Cloning: Insert Htz1 cloned point mutants plus KAN gene downstream of SalI site
Htz1F1	CAATTTCGCACTATAGCCGCACGTAAAAATAACTTA ACATACGGATCCCCGGGTTAATTAA	Deletion of *HTZ1* gene
Htz1p4	TCCACTTTCAATAATAATGC	Sequencing
Htz1p5	CACTGCGGACTCTATTATAC	Sequencing
Htz1p7-SalI	GTAGAAAGTCGACAGTATAAC	Cloning
Htz1p36-HindIII	CGCACAAAGCTTGTGCACGAAAAC	Cloning: To generate *HTZ1* promoter truncation 200bp
Htz1p37-HindIII	CGCACAAAGCTTAACTAAAAAACACTGCGG	Cloning: To generate *HTZ1* promoter truncation 100bp

2.1.5 Yeast expression plasmids

Table 2.7 Plasmids used in this study

Plasmid Name	Description	Reference
pRM200	CEN4-ARS1-*TRP1*	Grunstein's lab
pRS416	CEN6-ARS4-*URA3*	Sikorski and Hieter, 1989
pRS418	CEN6-ARS4-NatMX	Addgene
pRS425	2 micron - *LEU2*	Pavitt's lab
pRS426	2 micron - *URA3*	Ashe's lab
pCM301	2 micron - *LEU2 HTZ1*	Dr Catherine Millar, unpublished
pCM305	CEN6-ARS4 *URA3* HA-*HTZ1*	Millar et al., 2006
pCM307	CEN4-ARS1-*TRP1* H3-H4K16Q	Dr Catherine Millar, unpublished
pCM433	CEN6-ARS4 *URA*3 *HTZ1*	Dr Catherine Millar, unpublished
pCM565	CEN6-ARS4 *URA*3 *HTZ1*-HA	Dr Catherine Millar, unpublished
pCM544	CEN6-ARS4 *URA*3 *htz1* K3, 8, 10, 14 R (4KR)	Dr Catherine Millar, unpublished
pCM566	CEN6-ARS4 *URA*3 *htz1* K3, 8, 10, 14 Q (4KQ)	Dr Catherine Millar, unpublished
pCM617	CEN6-ARS4 NatMX *HTZ1*	This study
pCM618	CEN6-ARS4 NatMX *htz1* K3R	This study
pCM619	CEN6-ARS4 NatMX *htz1* K8R	This study
pCM620	CEN6-ARS4 NatMX *htz1* K10R	This study
pCM621	CEN6-ARS4 NatMX *htz1* K14 R	This study
pCM622	CEN6-ARS4 NatMX *htz1* K3, 8, 10, 14 R (4KR)	This study
pCM624	CEN6-ARS4 NatMX *htz1* K8, 10, 14 R	This study
pCM625	CEN6-ARS4 NatMX *htz1* K3, 10, 14 R	This study
pCM626	CEN6-ARS4 NatMX *htz1* K3, 8, 14 R	This study
pCM627	CEN6-ARS4 NatMX *htz1* K3, 8, 10 R	This study
pCM672	CEN6-ARS4 *URA*3 *HTZ1*^{cp200}	This study
pCM679	CEN6-ARS4 *URA*3 *htz1*-4KR^{cp200}	This study
pCM680	CEN6-ARS4 *URA*3 *htz1*-4KR^{cp100}	This study
pCM681	CEN6-ARS4 *URA*3 *HTZ1*^{cp100}	This study
pCM690	2 micron - *LEU2 htz1* K3, 8, 10, 14 R	This study

2.1.6 *S .cerevisiae* used in this study

Table 2.8 Yeast strains

Names	Genotype	Reference
YDS2	MAT-a ade2-1, can1-100, his3-11, leu2-3, 112, trp1-1, ura3-1	Laman et al., 1995
BY4741	MAT-a his3D1 leu2D0 met15D0 ura3D0	Wu's lab
RMY102	MAT-a /ade2-101 his3-Δ200 lys2-801 trp1Δ901 ura3-52 hht1 hhf1::LEU2 hht2 hhf2::HIS3 + pRM102 (CEN/URA3 GAL10 prom -*HHT2* Gal1-prom-*HHF2*)	Grunstein'slab
CMY104	YDS2 / htz1::KanMX	Millar et al., 2006
CMY189	YDS2 / htz1::KanMX+pRS416	Millar et al., 2006
CMY190	YDS2 / htz1::KanMX+ p[HA-HTZ1] (pCM305)	Millar et al., 2006
CMY584	YDS2 / htz1::KanMX + p[HTZ1-HA] (pCM565)	This study
CMY218	RMY102 htz1::KanMX	Dr Catherine Millar, unpublished
CMY231	YDS2 /HA-Htz1WT-KAN	Millar et al., 2006
CMY272	RMY102 HA-HTZ1-KanMX+ pRM200 (HHT2-HHF2)	Dr Catherine Millar, unpublished
CMY274	RMY102 HA-HTZ1-KanMX+ pCM307 (H4K16Q)	Dr Catherine Millar, unpublished
CMY277	RMY102 HA-htz1 K3, 8, 10,14 R-KanMX + pRM200 (HHT2-HHF2)	Dr Catherine Millar, unpublished
CMY279	RMY102 HA-htz1 K3, 8, 10,14 R-KanMX + pCM307 (H4K16Q)	Dr Catherine Millar, unpublished
CMY282	RMY102 HA-htz1 K14R-KanMX+ pRM200 (HHT2-HHF2)	Dr Catherine Millar, unpublished
CMY284	RMY102 HA-htz1 K14R-KanMX+ pCM307 (H4K16Q)	Dr Catherine Millar, unpublished
CMY485	RMY102 HA-htz1 K3R-KanMX+ pRM200 (HHT2-HHF2)	This study
CMY483	RMY102 HA-htz1 K3R-KanMX+ pCM307 (H4K16Q)	This study
CMY488	RMY102 HA-htz1 K8R-KanMX+ pRM200 (HHT2-HHF2)	This study
CMY486	RMY102 HA-htz1 K8R-KanMX+ pCM307 (H4K16Q)	This study
CMY491	RMY102 HA-htz1 K10R-KanMX+ pRM200 (HHT2-HHF2)	This study
CMY489	RMY102 HA-htz1 K10R-KanMX+ pCM307 (H4K16Q)	This study
CMY697	RMY102 htz1D::KanMX + p[HTZ1-NAT] +pRM200 (HHT2-HHF2)	This study
CMY707	RMY102 htz1D::KanMX + p[HTZ1-NAT] + pCM307 (H4K16Q)	This study
CMY703	RMY102 htz1D::KanMX + p[htz1 K8,10,14R-NAT] +pRM200 (HHT2-HHF2)	This study
CMY713	RMY102 htz1D::KanMX + p[htz1 K8,10,14R-NAT] +pCM307 (H4K16Q)	This study

Names	Genotype	Reference
CMY704	RMY102 htz1D::KanMX + p[htz1 K3,10,14R-NAT] +pRM200 (HHT2-HHF2)	This study
CMY714	RMY102 htz1D::KanMX + p[htz1 K3,10,14R-NAT] +pCM307 (H4K16Q)	This study
CMY705	RMY102 htz1D::KanMX + p[htz1 K3,8,14R-NAT] +pRM200 (HHT2-HHF2)	This study
CMY715	RMY102 htz1D::KanMX + p[htz1 K3,8,14R-NAT] +pCM307 (H4K16Q)	This study
CMY706	RMY102 htz1D::KanMX + p[htz1 K3,8,10R-NAT] +pRM200 (HHT2-HHF2)	This study
CMY716	RMY102 htz1D::KanMX + p[htz1 K3,8,10R-NAT] +pCM307 (H4K16Q)	This study
CMY702	RMY102 htz1D::KanMX + p[htz1 K3,8,10,14R-NAT] +pRM200 (HHT2-HHF2)	This study
CMY712	RMY102 htz1D::KanMX + p[htz1 K3,8,10,14R-NAT] + pCM307 (H4K16Q)	This study
CMY379	YDS2 + bar1::HIS htz1::TRP	Dr Catherine Millar, unpublished
CMY394	YDS2 + bar1::HIS htz1::TRP+ p[HA-HTZ1] (pCM305)	Dr Catherine Millar, unpublished
CMY569	YDS2 + bar1::HIS htz1::TRP+ p[htz1K3, 8, 10 ,14 R] (pCM544)	Dr Catherine Millar, unpublished
CMY601	YDS2 + bar1::HIS htz1::TRP+ p[htz1K3, 8, 10 ,14 Q] (pCM566)	Dr Catherine Millar, unpublished
CMY665	YDS2 + bar1::HIS htz1::TRP+pRS416	Wood et al., 2013
CMY666	YDS2 + bar1::HIS htz1::TRP+p[HTZ1] (pCM433)	Wood et al., 2013
CMY801	YDS2 + bar1::HIS htz1::TRP+ p[HTZ1^{cp200}] (pCM672)	This study
CMY887	YDS2 + bar1::HIS htz1::TRP+ p[htz1-4KR^{cp200}] (pCM679)	This study
CMY888	YDS2 + bar1::HIS htz1::TRP+ p[HTZ1^{cp100}] (pCM681)	This study
CMY749	MATa his3D1 leu2D0 met15D0 ura3D0 KanMX-pGAL-HTZ1	Dr Catherine Millar, unpublished
CMY742	YDS2/ HTZ1-KanMX	This study
CMY743	YDS2/htz1 K3, 8. 10, 14 R-KanMX	This study
CMY744	YDS2/htz1 K3, 8, 10, 14 Q-KanMX	This study
CMY774	YDS2 + bar1::HIS htz1::TRP+pRS418	This study
CMY775	YDS2 + bar1::HIS htz1::TRP+ p[HTZ1-NAT](pCM617)	This study
CMY780	YDS2 + bar1::HIS htz1::TRP+ p[htz1 K3, 8, 10, 14 R-NAT] (pCM622)	This study
CMY981	YDS2/ HTZ1-KanMX+ p[HTZ1]-2µ-LEU (pCM301)	This study
CMY982	YDS2/ HTZ1-KanMX+ p[htz1 K3, 8, 10, 14 R]-2µ-LEU (pCM690)	This study
CMY984	YDS2/ HTZ1-KanMX+pRS425	This study
CMY985	YDS2/htz1 K3, 8. 10, 14 R-KanMX+pRS425	This study

Names	Genotype	Reference
CMY986	YDS2/htz1 K3, 8. 10, 14 R-KanMX+ p [HTZ1]-2µ-LEU (pCM301)	This study
CMY987	YDS2/htz1 K3, 8. 10, 14 R-KanMX+ p[htz1 K3, 8, 10, 14 R]-2µ-LEU (pCM690)	This study
CMY994	YDS2 + HTZ1-WT-KanMX arp8::HisMX6	This study
CMY995	YDS2 + htz1-K3, 8,10,14 R-KanMX arp8::HisMX6	This study
CMY996	YDS2 + htz1-K3, 8,10,14 Q-KanMX arp8::HisMX6	This study
CMY997	YDS2 + HTZ1-WT-KanMX swc2::HisMX6	This study
CMY998	YDS2 + htz1-K3, 8,10,14 R-KanMX swc2::HisMX6	This study
CMY999	YDS2 + htz1-K3, 8,10,14 Q-KanMX swc2::HisMX6	This study
CMY1003	YDS2 + HTZ1-WT-KanMX swc5::HisMX6	This study
CMY1004	YDS2 + htz1-K3, 8,10,14 R-KanMX swc5::HisMX6	This study
CMY1005	YDS2 + htz1-K3, 8,10,14 Q-KanMX swc5::HisMX6	This study
CMY1008	YDS2 + HTZ1-WT-KanMX swr1::HisMX6	This study
CMY1009	YDS2 + htz1-K3, 8,10,14 R-KanMX swr1::HisMX6	This study
CMY1010	YDS2 + htz1-K3, 8,10,14 Q-KanMX swr1::HisMX6	This study

2.2 Methods

Gene disruptions and epitope tagging were carried out using standard molecular biological techniques (Longtine et al., 1998). DNA and RNA concentration was measured using a NanoDrop® ND-1000 Spectrophotometer (Labtech International). DNA sequencing was performed by GATC biotech. The sequencing results were verified using laser gene software (DNASTAR) and NCBI blast.

2.2.1 Bacterial growth, transformation and storage

All *E.coli* strains were grown at 37°C in a shaking incubator. Bacteria transformed with plasmids were selected during growth in media containing 100µg/ml ampicillin.

For bacterial transformation, 10-100 ng of plasmid DNA or 5µl of a ligation reaction were added to 50-100 µl of competent XL1-Blue cells. After incubation on ice for 30 minutes, cells were heat-shocked in 42°C water bath for 45 seconds. Cells were then immediately placed back on ice for 3 minutes and 1 ml of SOC medium was added. Following this step, cells were incubated at 37°C for 1 hour and pelleted at 10,000 g for 30 seconds, resuspended in 100 µl of SOC and spread on to agar plate containing the appropriate

antibiotics. Plates were incubated overnight at 37°C. For long-term storage of bacterial cells, stationary phase cultures were stored in the presence of sterile 50%(v/v) glycerol at -80 °C.

2.2.2 Plasmid construction

Plasmid DNA was isolated from transformed XL1-blue cells. The membrane-containing columns (Qiagen) were used for isolation of plasmid DNA on a mini scale, cleaning DNA after enzymatic reaction. For purification of DNA fragments after gel electrophoresis, DNA was isolated using Qiaquick gel extraction kit (Qiagen) according to the manufacturer's instructions. 1 µg of DNA was digested using appropriate restriction enzymes and buffer according to manufacturer's instructions (New England Biolabs (NEB) and Roche). Digestion reaction was incubated at 37°C for 1.5 hours. Digested products were resolved in 0.8-1% agarose gels for examining DNA fragment and excising the band. Agarose gel was made in 0.5X TBE (45 mM Tris-borate/1 mM EDTA) containing ethidium bromide and visualised under UV transilluminator. Ligation of DNA was performed at room temperature using T4 Rapid DNA ligation kit (Roche) following the manufacturers' protocol. Ligation reactions included insert and vector DNA a molar ration of approximately 1:10 in a total volume of 20 µl. Ligation of plasmid backbone without DNA insert was also performed as a identify vector self-ligation. As necessary, prior to ligation step, linearised plasmid backbone that has been cut using the same enzyme is dephosphorylated using Calf Intestinal Phosphatase (CIP) (NEB) followed by spin-column purification before ligation step. After ligation and transformation, further diagnostic digestion experiments with different restriction enzymes were always performed to ensure the success of cloning.

2.2.3 Cultivation and manipulation of *S. cerevisiae*

Liquid cultures were inoculated from freshly streaked plates and grown overnight in a 5-ml appropriate media at 30°C on a 200-rpm shaking platform incubator. This pre-culture is used to inoculate the main culture to an OD_{600} equal to 0.15-0.2 in Erlenmeyer flasks (flask size $\geq$ 5x liquid culture volume). The yeast cultures were grown at 30°C until mid-log phase (OD_{600} = 0.6-0.8). The culture density was assessed photometrically using SmartSpec™ Plus (Bio-Rad). Yeast cells on solid agar plates are stored at 4°C up to 4

weeks. For long-term storage, stationary-phase cultures were frozen in sterile 50% (v/v) glycerol solutions at –80°C.

2.2.4 Yeast growth assays

Yeast cells were inoculated and grown overnight to saturated stationary phase in an appropriate media. Next day, the OD_{600} of each culture was measured. Cells were then diluted to a volume corresponding to 4 OD units in a sterile 1.5-ml microtube and pelleted by centrifugation at 2000g for 30 seconds. The media were removed and cells were resuspended in 1 ml of sterile dH_2O. Serial five-fold dilutions were carried out in sterile dH_2O for a total of 6 dilutions for each yeast strain. 5 µl of each cell dilution was spotted from left to right onto the control and appropriate drug-containing plates. The spotted cells were allowed to dry at room temperature. Plates were incubated at 30°C and examined every 24 hours. Plates were scanned at 72 hours.

2.2.5 Growth curve analysis

Growth curves were monitored kinetically with a SPECTROstar Nano machine (BMG LAB TECH) following the manufacturers' protocol. Overnight pre-culture of yeast cells were dilute to OD_{600} equal to 0.2 in YPD or appropriate dropout media. 120µl of cells were transferred into Costar® 96-well plate (Corning Incorporated) containing appropriate media with or without the presence of appropriate testing agents. The concentration of agents used in this study (0.008-0.01% MMS, 7.5-10mM caffeine; 200mM HU) was determined empirically. All of the samples analysed were performed in triplicate. Absorbance at 600-nm wavelength was measured every 5 minutes at 30°C for 72 hours. At least two biological replicates were performed for a given experiment. Growth curve data were analysed using MARS data analysis software.

2.2.6 Lithium acetate transformation of *S. cerevisiae*

Yeast cells were grown overnight in 5-ml culture in an appropriate media. The absorbance OD_{600} was measured and the cultures were diluted to an OD_{600} of 0.2 in 50 ml YPD or minimal selective medium. Cells were then grown to OD_{600} of 0.6 at 30°C in a 200 rpm shaking platform incubator. The culture was transferred into a pre-chilled 50ml Falcon

tube and cells were pelleted by centrifuging (Sigma 3-16K centrifuge) at 3000g for 3 minutes at 4°C. The supernatant was then discarded and cells were resuspended in 0.5-ml sterile dH_2O before transferring to a 1.5-ml microtube and cells were pelleted by centrifugation at 2000g for 30 seconds. The supernatant was then removed and the cell pellets were resuspended in 0.5-ml lithium acetate (LiAc) solution (100mM LiAc, pH 7.5, 10mM Tris, 1mM EDTA). These "competent" yeast cells can be stored at 4°C for the maximum of 1 week to maintain the transformation efficiency. For each transformation reaction, the mixture comprised 20µl of single-stranded carrier DNA (ssDNA) (2mg/ml, boiled for 5 minutes), 200-500 ng of plasmid DNA or ~1µg PCR fragments, and 100µl of competent yeast cells in lithium acetate solution. Subsequently, 700µl of polyethylene glycol (PEG) solution (40% PEG 3350, 100mM LiAc, pH 7.5, 10mM Tris, 1mM EDTA) was added to the mixtures. The transformation reaction was incubated at 30°C for 2 hours. Subsequently, cells were then heat shocked at 42°C in the water bath for 15 minutes and incubated on ice for 2 minutes. Transformant cells were centrifuged at 2000g for 30 seconds. Supernatant was removed and pelleted cells were resuspended in 100-µl sterile dH_2O or appropriate medium. For selection on dropout medium, transformant cells were spread on a dropout agar plate and incubated at 30°C. For selection on a drug–containing medium, transformant cells were resuspended in 5ml of appropriate medium minus drug and grown for ~ 6 hours at 30°C in a shaking incubator before plating.

2.2.7 Isolation of yeast genomic DNA

Yeast cell pellets were resuspended with 200µl genomic DNA lysis buffer (2% Triton-X 100, 1% SDS, 100 mM NaCl, 10 mM Tris pH 8.0, 1 mM EDTA pH 8.0) and vortexed rigorously in the presence of 500 µl glass beads in 1.5-ml screw-cap tube for 5 minutes at room temperature. 200 µl TE and 400 µl phenol-chloroform isoamyl alcohol (Invitrogen) was added to cell lysate minus glass-bead. Samples were then vortexed to mix. The aqueous and organic layer was separated by centrifugation at 16,000g for 5 minutes. 150 µl of the aqueous layer was transferred to a fresh 1.5-ml microtube and RNaseA-treated at 37°C for 10 minutes. Subsequently, ethanol precipitation of DNA was perfomed by adding 1ml 100% ethanol into the samples. Genomic DNA was pelleted by centrifugation at 16,000 for 5 minutes, washed with 70% ethanol and the supernatant was removed completely. DNA was air-dried and resuspended in 100 µl TE.

2.2.8 PCR

2.2.8.1 PCR amplification for cloning

Standard PCR reactions were performed using Phusion High-Fidelity DNA Polymerase (Thermo Scientific) in a total volume of 50 µl. For each PCR reaction, PCR components include 1-10ng plasmid DNA, 1X HF buffer, 200µM dNTPs, 0.5µM of forward and reverse primers and approximately 1U Phusion DNA polymerase. The cycling conditions are demonstrated as follows:

Table2.9: PCR condition for cloning

Cycle step	Temperature	Time	Cycles
Initial denaturation	98°C	30 seconds	1
Denaturation Annealing Extension	98°C 55-60°C 72°C	10 seconds 15 seconds 15-45 seconds	35
Final extension Hold	72°C 10°C	10 minutes -	1

2.2.8.2 Site-directed mutagenesis

In vitro site-directed mutagenesis was carried out using PCR amplification method to mutate the individual lysine (K) residues into the non-modifiable arginine (R) or glutamine (Q) residues that cannot be acetylated. This assay was performed using the protocol adapted from QuikChange® II XL site-directed mutagenesis kit (Stratagene®). Mutagenic primers were designed to make single, triple and quadruple mutations at the N-terminal acetylatable lysine residues of Htz1. A 50-µl PCR reaction contains 1 µl double stranded DNA template (10-20ng), 1X Pfu reaction buffer, 2.5ng/µl of each forward and reverse oligonucleotide primers (100ng/µl stock), 0.2mM dNTPs, 2.5U PfuUltra™ high-fidelity DNA polymerase and dH_2O to the final volume of 50 µl. The PCR cycling conditions were described as follows:

Table 2.10: PCR condition using in site-directed mutagenesis

Cycle step	Temperature	Time	Cycles
Initial denaturation	95°C	1 minute	1
Denaturation	95°C	50 seconds	18
Annealing	55-60°C	50 seconds	
Extension	68°C	4-5 minutes	
Final extension	68°C	7 minutes	1

Following the cycling amplification, each amplification reaction was treated with 1 µl *Dpn*I restriction enzyme (10U/µl), mixed thoroughly and spun down briefly in the centrifuge. The *Dpn*I-treated amplification reaction was incubated at 37°C for 1 hour 30 minutes. The mutagenised DNA plasmid was then transformed into competent XL1-Blue cells as previously described. Next day, a single colony was selected and the mutagenised plasmids were extracted using QIAprep® spin Miniprep Kit (Qiagen). The result of mutagenesis reaction was verified by DNA sequencing.

2.2.8.3 Yeast colony PCR

Yeast colony PCR was performed using whole yeast cells to screen transformants for gene-specific integrations or disruptions using primers that amplify PCR products of different size in wild type and target alleles. A miniscule scoop of cells was transferred to a PCR tube using a sterile pipette tip. Cells were lysed briefly in the microwave and immediately put on ice. 25 µl of PCR master mix containing Phire® hot start DNA polymerase (Thermo Scientific) was added to each PCR tube. All tubes were carefully mixed and spun down briefly before starting the cycling reaction.

Table 2.11: PCR condition for yeast colony PCR

Cycle step	Temperature	Time	Cycles
Initial denaturation	98°C	1 minute	1
Denaturation Annealing Extension	98°C 55-60°C 72°C	10 seconds 10 seconds 20 seconds	30
Final extension Hold	72°C 10°C	1 minutes -	1

2.2.9 RNA isolation and cDNA synthesis

Total RNA was extracted from yeast cells using RNeasy Kit (Qiagen) with glass-bead lysis method according to the manufacturers' instructions. On-column DNAse (Qiagen) treatment was also carried out for a complete genomic DNA removal. RNA samples are stored at -80 °C. The purified RNA concentration was measured and equal amount of RNA samples were reverse-transcribed into complementary DNA (cDNA) using SuperScript® III Reverse Transcriptase (Invitrogen). Each sample was performed with and without reverse transcriptase (+RT/-RT) to ensure the absence of genomic DNA contamination. These cDNA were used as a template for a linear PCR reaction or quantitative real time PCR with SYBR green master mix. A total volume of 10 µl cDNA synthesis reaction comprised of 5 µg of RNA in a total volume of 7 µl with RNase-free dH_2O, 1 µl of 50 µM Oligo $(dT)_{20}$, 1 µl of 300 ng/µl Random Primer 9 (NEB) and 1 µl of10 µM dNTPs. Samples were incubated at 65 °C for 5 minutes, followed by 1-minute incubation on ice. Subsequently, 10 µl of RT master mix was added to the reaction and placed on the PCR machine using the condition as follows: 25 °C 10 minutes, 50°C 50 minutes, 85°C 5 minutes. The synthesised cDNA is subjected to further Q-PCR analysis or stored at -20 °C.

2.2.10 Cell fractionation

Yeast cell pellet harvested from the culture equivalent to 80 OD units were resuspended in 1ml PSB buffer (20 mM Tris pH 7.4, 2 mM EDTA, 100 mM NaCl, 10 mM BME) in 2-ml microtubes (Starlab). Cells were briefly pelleted and supernatant was discarded. Subsequently, cells were resuspended in 1 ml SB buffer (20 mM Tris pH 7.4, 1M Sorbitol). 10 µl of cell suspension was set aside to photometrically examine pre-zymolase

treatment in the presence of 1% SDS. 25 µl Zymolase 100T (Zymo Research) solution (3mg/ml Zymolase, 10% glucose) was added to cell suspension. Samples were incubated at 30°C on a roller wheel for 30 minutes. After Zymolase treatment, 10 µl of cell suspension was examined photometrically in the presence of 1% SDS and visualised under the microscope to determine the success of enzymatic reactions of yeast cell wall. Spheroblasts (yeast cells without cell wall) were pelleted at 2000g for 5 minutes at 4°C, washed twice with 1ml pre-chilled SB solution and spun down. Cell lysis of outer membrane was performed using EBX buffer (20 mM Tris pH 7.4, 10 mM NaCl, 0.25% Triton X-100, 15 mM BME, 0.01% phenol red and 1X protease inhibitor cocktail) to the total volume 480 µl. The concentration of Triton X-100 was adjusted to 0.5% in a total volume of 500 µl with the addition of 7 µl dH_2O and 13 µl of 10% Triton X-100. Samples were incubated on ice for 10 minutes and 100 µl of total cell lysates (WCEs) were taken for further analysis. The EBX lysates were placed carefully on to of 1ml of NEB buffer (20 mM Tris pH 7.4, 100 mM NaCl, 1.2 M Sucrose, 15 mM BME and 1X protease inhibitor cocktail) in a 2-ml microtube and centrifuged at 13,000g for 15 minutes at 4°C to sediment nuclei from cytoplasmic fractions via sucrose gradient. 100 µl of upper layer containing cytoplasmic proteins was set aside for further analysis. The remaining supernatant was removed and nuclei were resuspended in 400 µl EBX buffer without phenol red. The concentration of Triton-X 100 was adjusted to 1% by addition of 38.75 µl dH_2O and 11.25 µl of 10% Triton-X 100. Samples were incubated on a nutator at 4°C for 10 minutes to lyse nuclear membrane. 100 µl of soluble nuclear samples were taken for further analysis. Chromatin and insoluble nuclear proteins were pelleted at 16,000g for 10 minutes at 4°C. After that, supernatant was discarded and insoluble chromatin materials were resuspended in 50 µl 100 mM Tris pH 8.0 and additional 50 µl 2X SDS-PAGE loading buffer (50mM Tris-HCl pH6.8, 10% glycerol, 2% SDS, 0.01% bromophenol blue, 10% beta-mercapto ethanol)

2.2.11 Yeast histone extraction

A pre-culture was diluted to OD_{600} = 0.05 in 1.5 L YPD media and grow to OD_{600} = 0.3 at 30 °C on a shaking platform incubator. Cells were harvested by centrifugation at 3000 g for 5 minutes at 4 °C. Next, cell pellets were washed with 200-400 ml ice-cold dH_2O and centrifuged at 3000g for 5 minutes. After the supernatant was discarded, cells were resuspended in 50 ml DTT/Tris solution (0.1 mM Tris, pH 9.4, 10 mM DTT), incubated at 4°C for 15 minutes and pelleted at 4,500 rpm. Subsequently, cells were washed with

Sorbitol/HEPES solution (1.2 M Sorbitol, 20 mM HEPES pH 7.4) and harvested by centrifugation. Cell pellets were weighed and resuspended in Sorbitol/HEPES solution. 2.75 mg of Zymolase was added to the samples per gram of pellets and samples were incubated at 30 °C for 45 minutes. Spheroblasts were washed with 100 ml cold Sorbitol/PIPES/$MgCl_2$ buffer (1.2 M Sorbitol, 20 mM PIPES pH 6.8, 1 mM $MgCl_2$) and pelleted at 3,500g for 5 minutes at 4 °C.

From this stage, all solutions used were pre-chilled and the experiment was carried out on ice. Spheroblasts were gently resuspended in 50 ml cold NIB solution (0.25 M sucrose, 60 mM KCl, 15 mM NaCl, 5 mM $MgCl_2$, 1mM $CaCl_2$, 15 mM MES pH 6.6, 1mM PMSF, 0.8% Triton-X 100, 30 mM sodium butyrate), incubated on ice water for 20 minutes and pelleted at 4000 g at 4 °C for 5 minutes. This step was repeated twice. Next, samples were washed twice in 50 ml A-wash solution (10 mM Tris pH 8.0, 0.5% NP-40, 75 mM NaCl, 30 mM sodium butyrate, 1 mM PMSF), followed by centrifugation at 4,000 g for 5 minutes. Next, pellets were resuspended in 50 ml B-wash solution (10 mM Tris pH 8.0, 0.1 M NaCl, 30 mM sodium butyrate, 1 mM PMSF) and incubated on ice for 5 minutes. After incubation, pellets were spun down at the same speed, resuspended in 25 ml B-wash solution, and re-pelleted again by centrifugation. Pellets were resuspended in 3 volumes of cold dH_2O and 5N HCl was added to the sample to final concentration of 0.25 N. Samples were incubated on ice for 30 minutes with occasional vortexing. After that, samples were then spun down at 30,000g at 4 °C for 10 minutes. The supernatant containing extracted histone was set aside. 100% TCA was added to the supernatant fraction to the final concentration of 20% and samples were incubated on ice for 30 minutes. After incubation, samples were centrifuged at 30,000g for 30 minutes at 4 °C and the supernatant was discarded. Protein pellets were washed with cold acid acetone solution (0.5% HCl acetone), spun down at 30,000 g for 5 minutes, and the supernatant was removed. Next, pellets were wash with cold 100% acetone, spun down at the same speed. The histone samples were air-dried and resuspended in 250µl of 10 mM Tris pH 8.0. The concentration of histones samples was determined using Bio-Rad DC™ protein assay.

2.2.12 Yeast cell lysis and chromatin isolation

All steps were performed on ice with pre-chilled solutions unless otherwise stated. Cell pellets were resuspended in 400 µl of 10mM ChIP lysis buffer (50mM HEPES/KOH pH 7.5, 10mM NaCl, 1mM EDTA, 1% Triton-X-100, 0.1% SDS, 0.1% sodium deoxycholate) containing 1X proteinase inhibitors cocktails (Roche). Cell suspensions were transferred to a 1.5-ml screw-cap tube containing ~400 µl 0.5 mm acid washed glass beads (Biospec

Products, Inc.) and lysed by vortexing on the FastPrep®-24 tissue and cell homoginizer (MP biomedicals) at 6.5 m/s for 20 seconds and 30 seconds rest at each cycle for the total of 6 cycles. Next, each tube was punctured by using red-hot 21-guage, 1 1⁄2-inch needle, placed on a 1.7-ml no-stick hydrophobic microtube and centrifuged at 2000g for 15 seconds. Crude cell lysate minus glass beads was collected and resuspended thoroughly for the lysate homogeniety. Chromatin was then sheared by sonication to an average size of 200- 500 bp using Bioruptor water bath sonicator (Diagenode) at 30 seconds on-and-off interval for a total of 15 cycles. The samples were then clarified by centrifugation at 16,000g for 5 minutes at 4°C. Crude yeast whole cell extract (supernatant) was transferred to a fresh no-stick microtube for further analysis or can be stored at -80°C.

2.2.13 SDS-Polyacrylamide Gel Electrophoresis (SDS-PAGE) and western blot analysis

Total cell lysates were prepared as mentioned in the previous method. Protein concentration was measured in relation to known concentration of BSA standard curve using Bio-Rad DC™ protein assay according to the manufacturer's protocol. Protein concentration was normalised to achieve equal amount. Protein samples were diluted in SDS-PAGE loading buffer and boiled for 5 minutes or 30 minutes (if samples were cross-linked). Protein samples were resolved on 12-15% SDS-PAGE gels (resolving: 0.375 M Tris pH 8.8, 0.075% SDS; stacking 0.125 mM Tris pH 6.8, 0.1% SDS) in SDS-PAGE running buffer (25 mM Tris pH 8.2, 192 mM glycine, 0.1% SDS) at 200V using Mini-PROTEAN Tetra Cell (Bio-Rad). Spectra™ Multicolor Broad Range Protein Ladder (Fermentas) was used to determine the molecular weight of proteins. After electrophoresis, protein samples were transferred to a Protran® nitrocellulose membrane (GE Healthcare Life Sciences) in Tris-Glycine transfer buffer pH 9.2 (48 mM Tris, 39 mM glycine, 0.05% SDS and 20% methanol) Subsequently, the protein-bound membrane was blocked with appropriate blocking agents (5% BSA/PBS or Li-cor blocking buffer) and probed with appropriate primary antibodies overnight at 4 °C. Immunodetection of proteins was carried out by using the Odyssey Imaging System (Licor Biosciences)

2.2.14 Affinity purification of acetyl-specific anti-Htz1 antibodies

The affinity purification comprised of two successive steps: negative and positive purifications using unacetylated and site-specific acetylated Htz1 peptides respectively. In the first step, affinity columns were prepared by coupling unacetylated Htz1 peptides to Ultralink® Iodoacetyl Gel (Thermo Scientific) in coupling buffer for the negative affinity purification. The peptide-conjugated gel was then blocked with L-Cysteine-HCl solution at room temperature for 15 minutes on a nutator. And the gel was further incubated without mixing for additional 30 minutes. The negative affinity column was washed with 10 gel-bed volumes of 10mM Tris pH 7.5, 100mM glycine pH 2.5, and 10mM Tris pH 8.8 respectively. The pH from the last wash was investigated to remain at pH 8.8. The column was equilibrated by washing with 10 gel-bed volumes of with 10mM Tris pH 7.5. A selected candidate antiserum was spun down, filtered and diluted 10-fold with 10mM Tris pH 7.5 and loaded to a column. The antibody flow-through was kept in a reservoir and re-passed to the column 3-5 times.

In the second step, an unbound, flow-through fraction from the first round of negative purification was incubated with appropriate singly acetylated Htz1 peptides conjugated to the gel and progress through the procedures as above. After that, the antibody-bound gel was transferred to a 15-ml falcon tube and washed twice with 10ml of 10mM Tris pH 7.5 for 5 minutes on a roller mixer at room temperature, following by washing twice with 10ml of 10 mM Tris pH 7.5/500 mM NaCl for 5 minutes each cycle. The gel was spun down at 500g for 30 seconds and the supernatant was removed and set aside. The gel was resuspended in the washing buffer before transferred back to the column. The gel was washed with 2 mM Tris and allowed to set in the column for 30 minutes at room temperature. Next, the bound antibody was eluted using 100 mM glycine buffer, pH 2.5. Prior to an elution step, 100µl of 1M Tris, pH 8.8 was aliquoted into 10 non-stick microtubes (Anachem Scientific Specialities Inc.) labelling E1-E10. This step was aim to immediately neutralise antibody fractions. 900µl of antibody was eluted into each prepared tube (E1-E10) by adding 10 gel-beds volumes of 10 mM glycine, pH 2.5 sequentially. The column was washed with 10 mM Tris, pH 8.8 and 10 mM Tris pH 7.5, and stored in the storage buffer containing 0.02% sodium azide. To determine the success of affinity purification and examine which fraction contained the majority of eluted antibodies, 10ul eluates from each fraction (E1-E10) was analysed on 12% SDS-PAGE gel; along with input, flow-through and all washing fractions. The gel were then stained with coomassie solution (0.1% (w/v) coomassie brilliant blue 7.5% (v/v) acetic acid 50% methanol) for 20

minutes and de-stained by boiling in dH_2O for 5 minutes up to 3 times. Once the fractions were identified, antibody-containing fractions were combined and exchanged into 1X PBS/50% glycerol buffer by dialysis using a Slide-A-Lyser® Dialysis cassette kit (Pierce) according to the product protocols. The affinity-purified antibodies were aliquoted and stored at - 20°C.

Table 2.12: Acetylated Htz1 peptide sequences

Peptide Names	Residues	Peptide sequences
H2A.ZK3ac	1-7	NH2-SGZ*AHGGC-COOH
H2A.ZK8ac	4-13	NH2-AHGGZ*GKSGAC-COOH
H2A.ZK10ac	4-13	NH2-CAHGGKGZ*SGA-COOH

Z* represents acetyl lysine sequence, (Dr Catherine Millar, unpublished)

2.2.15 Chromatin Immunoprecipitation (ChIP)

2.2.15.1 Yeast culture and formaldehyde crosslinking

Yeast cells were grown overnight to saturated stationary phase in 5ml YPD or an appropriate dropout media. OD_{600} was measured in each starter culture next day and cells were then diluted to an OD_{600} of 0.2/ml in the required volume of appropriate media in conical flasks. Cells were grown at 30°C at 200 rpm in the shaking incubator to an OD_{600} of 0.8 OD_{600} / ml (~2 doublings). Formaldehyde cross-linking of histones to DNA was performed by adding formaldehyde (Sigma-Aldrich) to the culture to the final concentration of 1%. Cells were cross-linked on a shaking plate at 120 rpm at room temperature for 15 minutes. After that, the cross-linking reaction was quenched by adding glycine to the final concentration of 125mM (2.5 ml of 2.5M glycine) for 5 minutes on the shaking plate. Yeast cells were harvested in the 50-ml Falcon tube by centrifuging at 4°C at 3000 g for 3 minutes and washed twice in 25 ml ice-cold sterile distilled water.

2.2.15.2 Chromatin Immunoprecipitation

Chromatin Immunoprecipitation (ChIP) contained appropriate amounts of a given affinity-purified anti- acetylated H2A.Z antibody specific to each lysine residue (K3, K8, K10 and K14) and 90-100 µl of cell lysate. Additionally, the IP may contain 500mM NaCl to enhance the performance of antibody. The bulk H2A.Z IP reaction contained 1µl of anti-HA Clone 12CA5 (Roche) or anti-660 antibody in 50 µl whole cell lysate. Chromatin fragments were immunoprecipitated from the WCEs as described in Section 2.2.12 overnight at 4°C on a nutator (VWR international). Next day, a suspension of 25 µl of 50% (v/v) of protein A Sepharose CL-4B and GammaBind^{TM} G sepharose (GE healthcare) was added to an acetylated H2A.Z IP reaction and bulk H2A.Z IP reaction respectively and the IP was further incubated for 2 hours. After 2-hr incubation, protein-A sepharose beads and GammaBind^{TM} G beads were pelleted by centrifuging at 500g for 30 seconds. The supernatant was discarded and beads were washed in 3 washing solutions sequentially on a nutator at room temperature as follows: i) 1-ml 500mM lysis buffer (50mM HEPES/KOH pH 7.5, 500mM NaCl, 1mM EDTA, 1% Triton-X- 100, 0.1% SDS, 0.1% sodium deoxycholate) for 15 minutes twice, ii) 1 ml deoxycholate buffer (10mM Tris-HCl, pH 8.0, 0.25M LiCl, 0.5% Igepal CA-630, 0.5% sodium deoxycholate and 1 mM EDTA, pH 8.0) for 5 minutes, and iii) TE (50 mM Tris-HCl, pH8.0, 19mM EDTA, pH 8.0) for 5 minutes. Beads were then collected by centrifugation at 500g for 30 seconds. Immunoprecipitated chromatin fragments associated to the beads were eluted in 50 µl of TE/1% SDS for 15 minutes at 65°C and the elution step were repeated one more time. Total 100-µl chromatin eluate was reverse-crosslinked at 65°C overnight. In addition, the input sample, containing 25 µl of whole cell lysate and 75 µl of TE/1%SDS, was reverse-crosslinked at 65°C overnight. The next day, the samples were treated with 5 µl proteinase K (100 µg) and incubated at 37 °C for 2 hours. Subsequently, DNA was extracted by conventional phenol/isoamyl alcohol/chloroform (Invitrogen) extraction. Aqueous layer (top) was separated from organic layer (bottom) by centrifuging at 16,000 g for 5 minutes before transferred to new 1.5-ml microtubes. This step was repeated once by adding equal volume to TE to the organic layer. The samples were combined and RNAase-treated (10µg RNaseA) at 37 °C for 30 minutes. Ethanol precipitation of DNA was carried out in the presence of glycogen and sodium acetate. The samples were incubated at -20 °C for >1 hour and centrifuged at the maximum speed for 30 minutes at 4°C. DNA pellets were washed once with 70% ethanol and pelleted at the same speed for 15 minutes. Immunoprecipitated DNA and Input DNA was air-dried and resuspended in 50 µl Tris, pH

8.0. Alternatively, as required, ChIP and Input DNA can be purified using Qiagen spin column after reversed cross-linked, RNAase and protease K treatment.

2.2.16 Real-time quantitative PCR (qPCR)

Since ChIP can be used to quantify the enrichment relative to a reference, input genomic DNA is used as the reference sample to normalise both background levels and the input chromatin into ChIP reaction. Immunoprecipitated DNA was analysed using qPCR and two primer sets were used: control and experimental primers. The control represents known Htz1-unenriched binding regions versus the known experimental Htz1-enriched binding regions. The enrichment of acetylated Htz1 was analysed on StepOne^{TM} qPCR (Applied Biosystems) in a 96-well plate (Starlab) format. Primers were optimised to assess the efficiency of each primer sets using standard curve from serial dilution of known DNA concentration. Immunoprecipitated DNA (~2 µl) or cDNA samples were subjected to qPCR reaction using Quantitect$^{®}$SYBR$^{®}$Green PCR Master Mix (Qiagen). For ChIP-qPCR, the data was normalised to input DNA and represented as the ratio of the percentage of input ($100*2^{-\Delta Ct}$) or fold enrichment ($2^{-\Delta\Delta Ct}$). PCR conditions are shown as follows:

Table 2.13: qPCR condition used in this study

Cycle step	Temperature	Time	Cycles
Initial denaturation	98°C	15 minutes	1
Denaturation	94°C	15 seconds	40
Annealing	55-60°C	30 seconds	
Extension	72°C	30 seconds	
Final extension	72°C	1 minutes	1
Hold	10°C	-	

2.2.17 ChIP and DNA microarray (ChIP-chip)

2.2.17.1 PCR amplification of immunoprecipitated DNA

ChIP was carried out according to Section 2.2.15. ChIP DNA is amplified using the protocol adapted from Affymetrix® Chromatin Immunoprecipitation Assay Protocol. This step was performed to increase the amount of DNA for probe labelling and hybridisation of DNA microarrays. The random priming PCR reaction was performed in a 0.2-ml thin wall microtube. PCR components containing 10µl of immunoprecipitated DNA, 4µl of 5X sequenase buffer, 40µM TPCR-A oligonucleotides (5'-GTTTCCCAGTCACGATCNNNNNNNNN-3') was denatured at 95 °C for 4 minutes. The sample was then placed on ice promptly while the temperature of PCR machine was set to decrease to 10°C and the PCR machine was then paused. 2.6 µl of PCR reaction mixture containing 0.625mM dNTPs, 5mM DTT, 0.1mg/ml BSA, and 1.3U-diluted Sequenase™ (USB Corporation) (1/10 from 13 U/µL stock) was added to the samples. The samples were put back to the PCR machine and incubated at 10 °C for 5 minutes. Annealing step was carried out by incrementing temperature from 10 °C to 37 °C over a period of 9 minutes and the elongation was obtained by incubating at 37 °C for another 8 minutes. Following this, the samples were denatured at 95 °C for 4 minutes and then put on ice. While the PCR machine was cooling down to 10 °C and paused, 1 µl of 1.3U Diluted Sequenase™ was added to the samples. The samples were incubated at 10 °C and repeated in annealing step again. These procedures were repeated for 2 more cycles (4 cycles in total). Subsequently, the PCR product was purified using QIAquick PCR purification kit (QIAGEN) as stated by manufacture's instructions. The sample was eluted in 60 µl QIAGEN buffer EB (10mM Tris-HCl, pH8.5). 20 µl of purified PCR product is used as DNA template in the second-round PCR step using conventional Taq polymerase (Invitrogen). PCR components consisted of 1X PCR buffer (20mM Tris HCl, pH 8.4, 50mM KCl), 2mM MgCl2, 1.25nmol TPCR-B oligonucleotide (5'-GTTTCCCAGTCACGATC-3'), 0.2375mM dNTPs+dUTP, and 10U of Taq polymerase in a final volume of 100 µl. The 30-cycle PCR reaction included denaturation at 95 °C for 30 seconds, two 30-second annealing steps at 45 °C and 55 °C respectively, elongation at 72°C for 1 minute and final extension at 72 °C for 10 minutes. 10 µl of amplified DNA was visualised on 1.5% agarose gel containing ethidium bromide. The average size of amplified DNA is 200-500 bp. After that, the samples were purified using QIAquick PCR purification kit and eluted in 50 µl buffer EB. DNA concentration was measured by using NanoDrop® ND-1000 spectrophotometer (Labtech International)

2.2.17.2 Probe labeling, hybridisation and DNA microarray processing

These procedures were performed using the methods and reagents according to the Affymetrix® Chromatin Immunoprecipitation Assay Protocol and were carried out by the Genomic Technology core facility at the Faculty of Life Sciences, University of Manchester.

2.2.18 ChIP and high-throughput sequencing (ChIP-seq)

ChIP was performed according to Section 2.2.15. Multiple ChIP reactions were carried out to obtain sufficient DNA amount. Subsequently, ChIP-qPCR was conducted to identify the enrichment at known target loci. The remaining samples were used for the following library preparation process (~10ng). Since it is difficult to measure ChIP DNA (<1ng/µl), it is recommended to quantify ChIP samples using flurometric-based method. In this study, ChIP DNA was quantified using Qubit (Invitrogen) according to manufacturers' instructions. The library construction and the following sequencing steps were performed by Genomic Technology staffs at the Faculty of Life Sciences, University of Manchester. Briefly, the library of Htz1, *htz1*-4KR and *htz1*-4KQ ChIP-Seq samples were constructed using TruSeq® ChIP Sample preparation protocol. 5-10ng ChIP and Input DNA samples were end-repaired (to convert the overhangs into blunt ends), adenylated at 3' end and ligated with adapters. Subsequently, adapter-modified DNA samples were amplified by PCR using primers annealed to the end of adapters. The amplified library DNA was purified and subjected to next-generation sequencing (NGS) using Illumina® Genome Analyzer II.

2.2.19 Bioinformatics and statistical analysis

Throughout this study, genome mapping and data normalisation of Htz1 ChIP-Seq was performed by Mr Muxin Gu. Sequence reads from ChIP and Input DNA was mapped to sacCer1 genome assembly using Bowtie software version 0.12.9. Following this, the mapped reads of Htz1 ChIP-seq were normalised to input sample for background subtraction. Normalised ChIP data in a wiggle format was visualised using Integrated Genome Browser (IGB) or UCSC genome browser (Kent *et al*., 2002; Nicol *et al*., 2009). For systematic quantification of ChIP datasets, normalised ChIP signals were separated into 150-200bp windows and the signal within each window was calculated. Data analysis and representation was carried out using Galaxy (*Goecks et al*., 2010), seqMiner (Ye *et al*.,

2010), Microsoft Excel and R. The standard deviation (*s*) or standard error (SE) was calculated from at least two independent experiments. The statistical significance, *P*-values, was determined using one/two tailed student's t test (TTEST function). The correlation between two datasets was calculated using the Microsoft excel function PEARSON and denoted as *r*.

CHAPTER 3: The co-occurrence of acetylated H2A.Z Lys 8, 10 and 14 marks across the yeast genome

3.1 Introduction

Eukaryotic chromatin domains can be altered by the dynamic equilibrium of histone acetylation and deacetylation. It has been widely recognised that euchromatic domains are associated with hyperacetylated histones while heterochromatic domains are associated with hypoacetylated histones. Distinct patterns of acetylation on histones can impact on distinct downstream biological processes such as transcription, nucleosome assembly, DNA replication and repair. (reviewed in Shabizian and Grunstein, 2007). *In vivo* profiling of site-specific histone acetylation has emerged to be a powerful tool to search for a downstream function by associating specific genomic features with characteristics of these modification patterns. Previous research demonstrated that similar patterns of acetylation status are associated with similar groups of genes as well as their expression profiles (Kurdistani *et al*., 2004). With regard to gene activity, acetylation of histones on the nucleosomes surrounding the TSSs has been associated with active transcription such as histone H3 and H4. Other studies have linked specific acetylation states of core histones with their occupancy in chromosomal domains such as promoter regions; for example, H3K9ac and H3K14ac marks are associated with 5'end of active genes and correlates well with transcription rates (Pokholok *et al*., 2005). However, high-resolution mapping suggested that that some acetylation sites may have distinct patterns at the nucleosome flanking the TSS such as H2AK7ac, H2BK16ac, H4K8ac and H4K16ac sites are hypoacetylated (Liu *et al*., 2005). Another example, perhaps the most distinct acetylation patterns, was observed within histone H4 N-terminal acetylation sites. Several lines of evidence have implicated H4K16ac is distinct from other acetylation sites of H4 (Dion *et al*., 2005). Furthermore, individual sites of acetylation or deacetylation may attract a specific set of enzyme targeted to chromatin (reviewed in Kurdistani and Grunstein, 2003). Therefore, characterising the association acetylation marks with genomic features provide important clues about the linkage to the functions.

H2A.Z (Htz1) is acetylated at four lysine residues (K3, K8, K10 and K14) at the N-terminus by KAT5 and KAT2 acetyltransferases (Millar *et al*., 2006; Barbiarz et al., 2006; Keogh et al., 2006). The reverse reaction is mediated by Hda1 histone deacetylase enzyme (Lin *et al*., 2008; Mehta *et al*., 2010). The acetylated H2A.Z at K14 (Htz1K14ac) is predominantly site in yeast and is associated with promoters of active genes (Millar *et al*.,

2006). However, other single acetylation sites of H2A.Z are less well characterised. It is not known whether acetylation at other N-terminal lysines of H2A.Z marks distinct chromosomal locations or overlaps with Htz1K14ac localisation profiles. It is likely that its distinct modification states may enable H2A.Z to perform multi-functional roles. Therefore, the possibility that differential acetylated Htz1 isoforms may be distinguished by their specific localisations and biological functions has led us to search for the acetylation patterns of all three acetylation sites on H2A.Z.

Investigations of biological significance of individual acetylation sites on histones and histone variants are often associated with site-specific antibodies. The requirement for quality of antibodies used to target specific residues is crucial because it specifically affects the interpretation of data. Therefore, the antibody characterisation procedures must be performed to obtain both specificity and high-affinity towards histone modification sites. In particular, validation of antibodies for the study of histone modification could face several concerns such as the specificity of the intended target histones, the specificity of selected residue (off-target) and the selectivity towards modified and unmodified states (for example: acetylated and deacetylated states) (Egelhofer *et al*., 2011). Therefore, these potential issues must be evaluated to minimise the cross-reactivity of such antibodies.

To understand the association of other individual acetylation sites of H2A.Z (K3, K8 and K10), I identified polyclonal antibodies specific to each acetylation site in the N-terminal region of H2A.Z (including anti-Htz1K3ac, anti-Htz1K8ac and anti-Htz1K10ac antibodies). These reagents were then subsequently used to explore genome-wide localisation of individual acetylated H2A.Z isoforms in relation to bulk H2A.Z. The global relationship of acetylated isoforms of H2A.Z was investigated. The result indicates that the genome occupancy of acetylated H2A.Z species at lysine K8 and lysine K10 are highly similar across the budding yeast genome.

3.2 Characterisation and purification of acetyl-specific H2A.Z antibodies

The outcomes of ChIP data depend crucially on the quality of the antibody used because the degree of enrichment of intended targets is achieved via this reagent. To achieve the minimal cross-reactivity, three main key criteria are required for characterising post-translational modifications of histones or histone variants should be considered. These include: i) the selectivity and affinity of antibody to the intended target histone or histone variant, ii) the specificity of an antibody to a specific modified residue and iii) the ability of an antibody to discriminate between modified and unmodified state of a particular mark.

To examine the global profile of individual acetylated lysines of Htz1, site-specific antibodies were required. The main objective was to characterise and purify antibodies that are specific to acetyl-lysine of Htz1 at lysine 3 (K3ac), lysine 8 (K8ac), and lysine 10 (K10ac) to use these reagents in ChIP experiments and subsequent genome-wide analysis. Rigorous screening and validation of antisera raised against each acetyl-lysine on Htz1 were performed to select the most sensitive and specific antibody for affinity purification and ultimately immunoprecipitation procedures.

For each antibody a specific peptide corresponding to individual acetylated Htz1 K3ac, K8ac, or K10ac (Section 2.2.14) was used as an antigen to immunise 8 rabbits in order to generate anti-Htz1K3ac, anti-Htz1K8ac and anti-Htz1K10ac antibodies. For each antigen, a total of 8 crude antisera were initially screened by Enzyme-Linked Immuno Sorbent Assay (ELISA) in the presence of a competitor (peptides corresponding to unacetylated state). This step was used to assess the specificity and relative binding strength of each antiserum (Dr. Catherine Millar; unpublished/data not shown). Furthermore, I tested all 24 antisera (K3ac*8; K8ac*8 and K10ac*8) by performing independent immunoblot analyses to determine relative affinities of individual antiserum. C-terminally TAP–tagged versions of wild type Htz1 (*HTZ1*-TAP) and lysine-to-alanine point mutations of Htz1 (*htz1K3A*-TAP, *htz1K8A*-TAP or *htz1K10A*-TAP) were purified from whole cell lysate using IgG sepharose (GE healthcare). Protein samples were then run on SDS-PAGE gels, blotted and probed with corresponding antisera. Equal gel loadings were confirmed by probing with anti-CBP antibody (data not shown). Following this, an antiserum candidate was chosen for each epitope based on the criterion that the relative western blot signals are higher in WT comparing to appropriately mutated recognition sites.

Together with the previous ELISA data (Dr Catherine Millar; unpublished), an antiserum candidate was selected and the double-affinity antibody purification was carried out

(described in Section 2.2.14 methodology) to increase the specificity and minimise cross-reactivity of antibodies in the downstream ChIP experiments.

Selected antisera were affinity-purified using column chromatography methods. The purification comprised two successive rounds: negative and positive purifications (Figure 3.1). Firstly, an antiserum was purified using unacetylated Htz1 peptide-containing column (negative purification) to select for antibody species that can only bind to a modified state of Htz1 (e.g. acetyl-K8), which wasn't expected to be retained in the column but rather pass through and locate in flow-through fraction. With this strategy, antibody species that can bind to unacetylated Htz1 were expected to remain bound to the column, thus reducing non-specific immunoreactivity. Secondly, the flow-through fraction underwent another purification step using an acetylated Htz1 peptide-containing column (positive purification). With this approach, we expect to enrich for antibodies that recognise specific acetyl-lysines of Htz1.

In this study, αHtz1K3ac, αHtz1K8ac and αHtz1K10ac antibodies were purified. To confirm the success of the purification (elution) steps, the antibody-containing fraction from each round was analysed on SDS-PAGE gel and stained with coomassie staining solution. This step was used to identify which eluted fraction contained the majority of purified antibody. In a denaturing SDS-PAGE gel, the presence of antibody was identified in two forms; ~50 kDa heavy chains and ~25 kDa light chains respectively. A sample result from the purification process is demonstrated in Figure 3.2A-B. Following this step, purified antibodies were combined and exchanged in a dialysis step to remove and buffer salts and concentrate the antibody. The success of antibody purification was re-examined on SDS-PAGE and visualised again after coomassie staining (Figure 3.2 C). These steps were applied to all three antibodies. These data indicate that the affinity purification of anti-acetylated Htz1 was successful.

As the desired application for these antibodies was ChIP experiments and specificity in ELISA or western blotting does not guarantee the specificity of antibodies in in vivo chromatin context (Suka *et al*., 2001), affinity-purified antibodies were further examined in ChIP using lysates from yeast strains expressing the C-terminally HA-tagged version of Htz1 in WT (*HTZ1*-HA) and from yeast strains carrying lysine-to-arginine point mutations allele (*htz1K3R-HA*, *htz1K8R-HA* or *htz1K10R-HA*). The extent of immunoprecipitation was measured using western blot analysis with anti-HA antibody. In addition, I extensively performed the optimisation for ChIP protocol with respect to buffers used and washing conditions. Without the presence of acetylatable lysine in the mutant

strains, we expected no reaction of antibody-antigen binding or, at least, a very minimal background.

In each case, I found that αHtz1K8ac and αHtz1K10ac antibodies are bound to acetylated Htz1 isoforms in WT when a specific acetyl-lysine is present but binding was abrogated to the background level when the lysine sites were mutated (Figure 3.3A). These data indicate that the antibody can recognise appropriate acetyl-lysine sites of Htz1 in the chromatin. However, after many trials, αHtz1K3ac failed in our IP-western blot experiments as it bound to acetylated Htz1 in WT and *htz1-K3R-HA* alleles at comparable affinity, suggesting the antibody cannot discriminate between modified and unmodified Htz1 (Figure 3.3B). Therefore, only ChIP experiments using αHtz1K8ac and αHtz1K10ac antibodies were carried out. It is worth noting that analogous ChIP experiment using αHtz1K14ac antibody was also performed as a positive control. However, αHtz1K14ac antibody used in this study was derived from the different batch from the one use in published work (Millar *et al*., 2006)

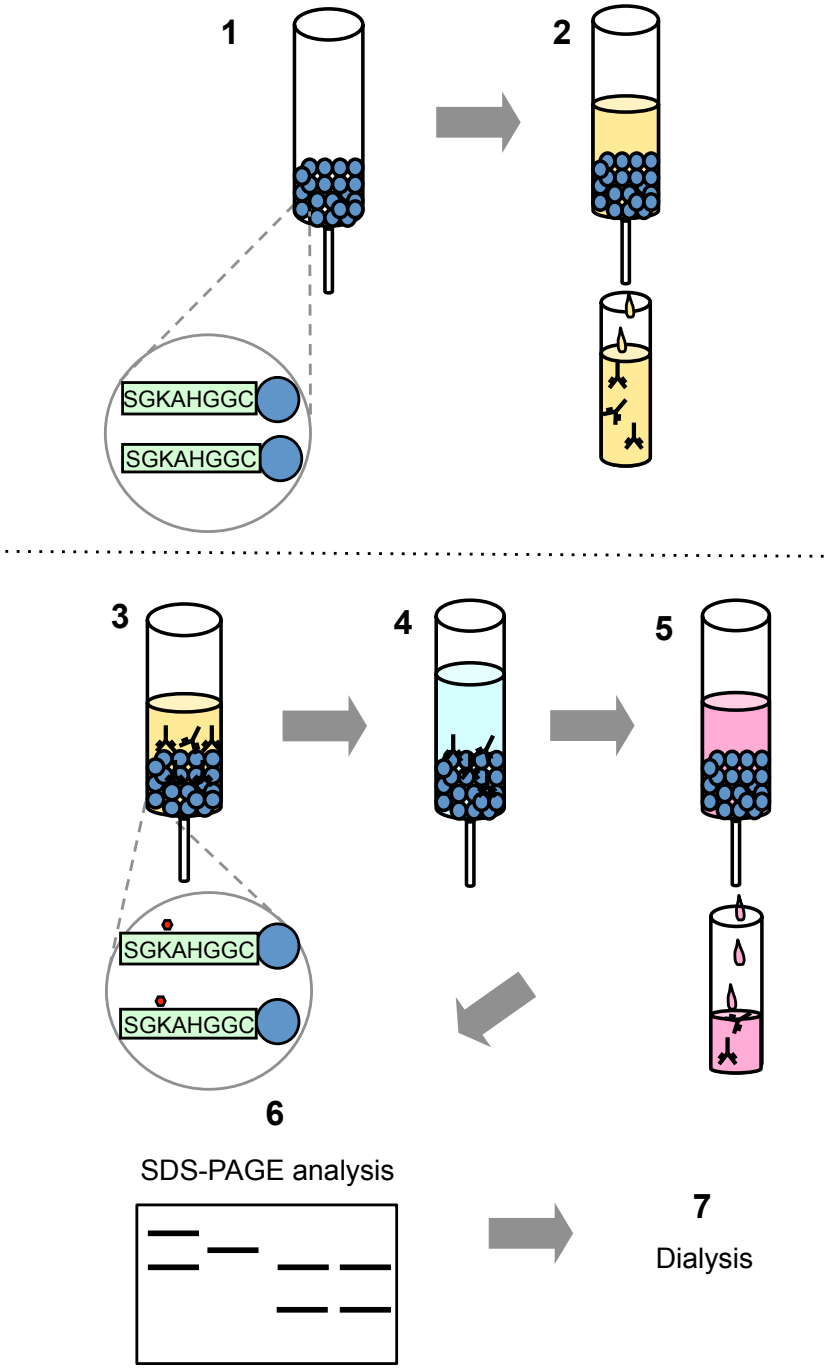

Figure 3.1. Schematic diagrams of double affinity purification of anti-acetyl-specific Htz1 antibodies

(A) Negative purification with an unacetylated Htz1 peptides-conjugated column

A column was coupled with peptides corresponding to N-terminal region of Htz1 where a specific lysine residue is unmodifiable (Step 1) and a selected antisera candidate is applied to the column (Step 2). The flow-through fraction is kept for the next step.

(B) Positive purification with an acetylated Htz1 peptides-conjugated column

Samples from step 2 are applied to a column containing specific actyl-lysine Htz1 peptides (Step 3) allowing specific antibody to bind to their recognized epitopes. The column is washed with buffers (Step 4) to remove unbound proteins. The antibody is eluted using low pH buffer (Step5) and samples are evaluated by SDS-PAGE (Step 6). Purified antibody is exchanged using the dialysis approach (Step 7)

Blue circles represent iodoacetyl beads. Peptides corresponding to Htz1 are shown in green boxes. Antiserum is show in yellow. Red dots represent a selective acetyl-lysine. Pale blue and pink represent washing and elution buffers.

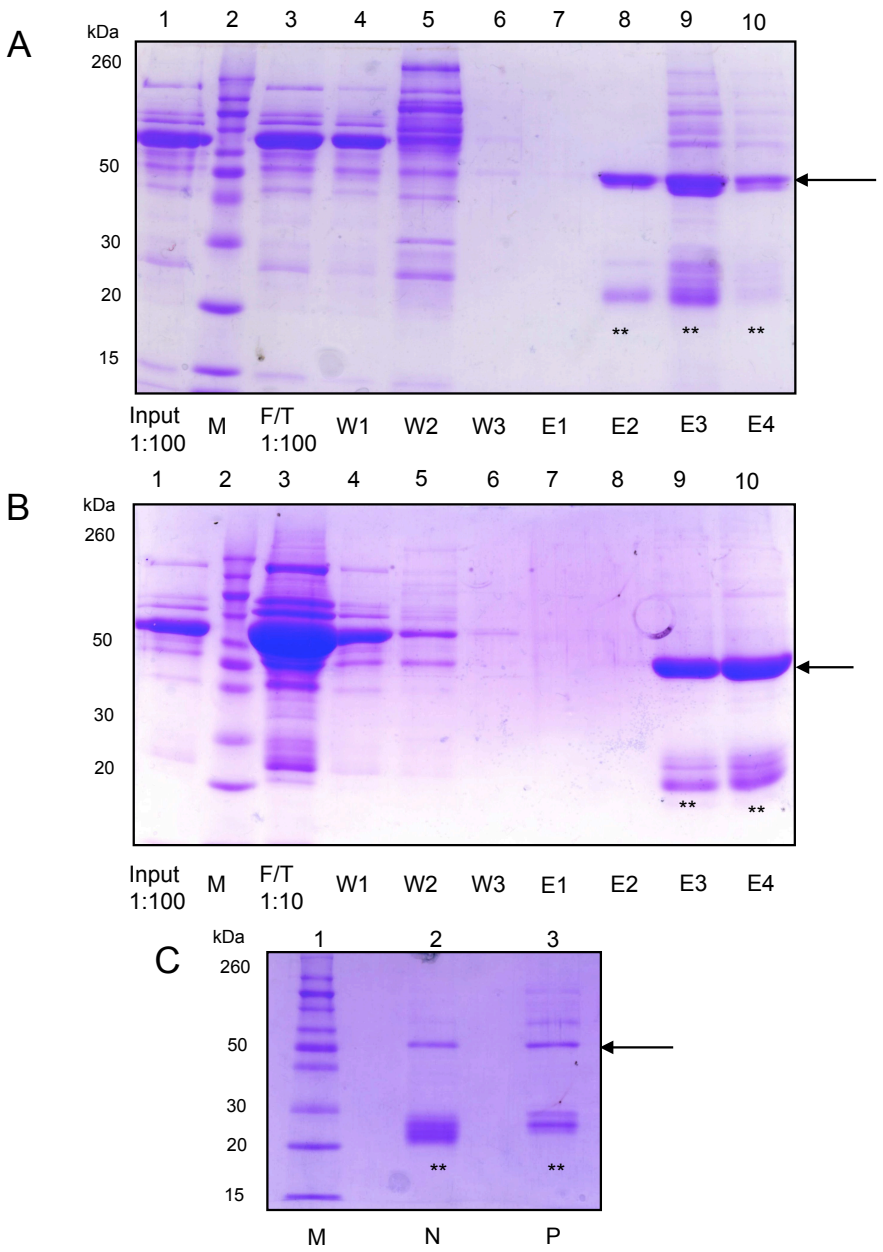

Figure 3.2 An example of double affinity purification of anti-acetylated Htz1 antibodies (anti Htz1K3ac antibody)

(A) and (B) A coomasssie-stained gel represents multiple fractions from the purification procedures

From left to right; lane 1= 1:100 dilution of serum (input), lane 2 = protein marker, lane 3 = 1:100 or 1:10 dilution of antibody flow-through, lane 4-6 = washing fractions W1-W3 respectively, lane 7-10 = eluted antibody fraction 1-4. Antibodies (IgG) were denatured in the presence of BME during the SDS-PAGE run and show in two forms: heavy and light chains around ~50 kDa and ~25 kDa respectively. Black arrows indicate heavy chains and ** indicate light chains of the antibody

(C) Final affinity purified anti-acetylated Htz1 antibody

From left to right; lane 1= protein marker, lane 2 = purified antibody fraction using site-specific unacetylated Htz1peptides (N), lane 3 = double purified antibody fraction using unacetylated and acetylated Htz1 peptides (P)

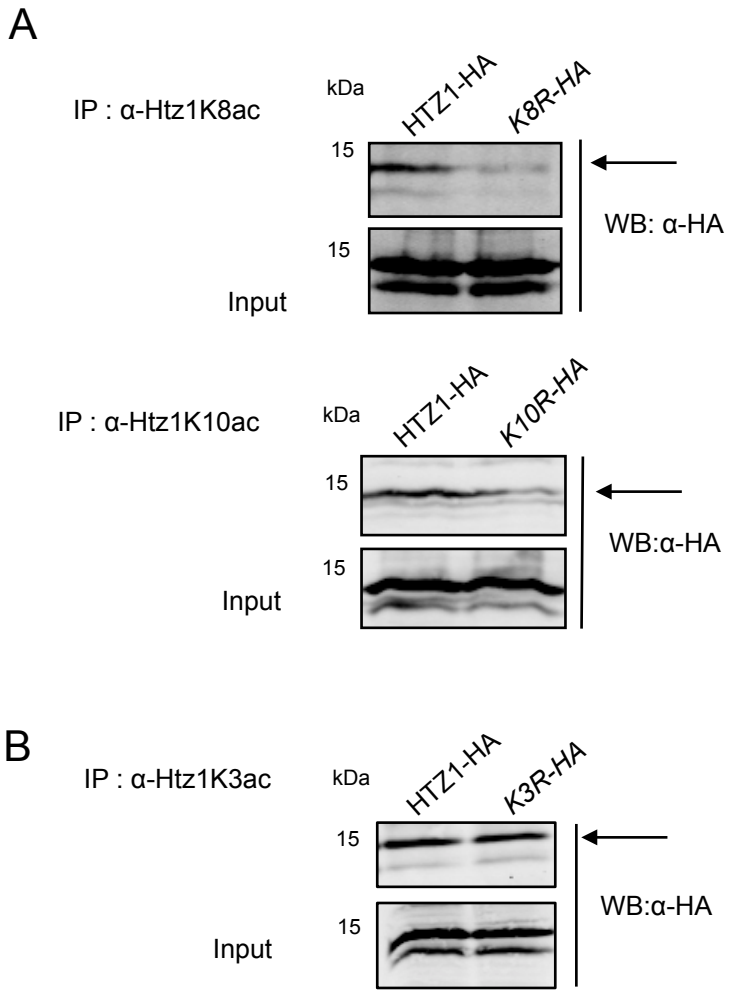

Figure 3.3 Specific lysine-to-arginine mutations abrogate the binding of α-Htz1K8ac and α-Htz1K10ac but not α-Htz1K3ac.
Whole cell yeast extracts prepared from cross-linked yeast strains expressing the C-terminally HA-tagged Htz1 and singly mutated lysine-to-arginine mutants (*htz1*K3R-HA, *htz1*K8R-HA and *htz1*K10R-HA) strains were immunoprecipitated using appropriate affinity-purified anti-acetylated Htz1 antibodies. Proteins recovered from IP were resolved by 15% SDS-PAGE and immunoblotted with anti-HA antibody. 5% input samples were also included in the analysis. Expected Htz1 bands were detected (~15kDa) and indicated by a black arrow.

3.3 Acetylated H2A.Z isoforms are co-localised and pervasive throughout the yeast genome

To determine the genome-wide distribution of steady-state Htz1 acetylation at K8ac and K10ac, I carried out ChIP experiments to enrich for acetylated Htz1 proteins using lysates harvested from an actively growing wild type yeast strain. As a control, an analogous ChIP experiment was also performed for bulk Htz1 using a polyclonal Htz1 antibody, recognising the C-terminal region of Htz1 (Millar *et al*., 2006). After immunoprecipitation, cross-links were reversed and the enriched DNA was purified and amplified by PCR. DNA samples were subjected to hybridisation to a DNA microarray. For detection of ChIP-enriched loci, samples were hybridised to GeneChip *S. cerevisiae* Tiling 1.0R Arrays which have a resolution of 5 bp (Affymetrix®). Peaks of acetylated Htz1 K8ac, K10ac and K14ac marks and bulk Htz1 were identified using Tiling Analysis Software (TAS) and mapped to the genome library SacCer 1 (October 2003). These data were visualised in Integrated Genome Browser (IGB) or UCSC genome browser (Kent *et al*., 2002). The resulting data indicate that acetylated Htz1 K8ac, K10ac and K14ac distributions are largely similar with one another across the yeast genome. An example of peak profiles from yeast chromosome 9 is shown in Figure 3.4. To visualise the global profiles of Htz1 at Trancription Start Sites (TSSs), all 5,143 yeast protein-coding genes (Xu *et al*., 2009) were aligned and ChIP-signals were clustered. Like Htz1 itself, K8ac, K10ac and K14ac isoforms are preferentially enriched near TSSs and depleted within ORFs (Figure 3.5 A). These results are consistent with the published works regarding the pattern of Htz1 (Guillemette *et al*., 2005; Li *et al*., 2005; Raisner *et al*., 2005; Zhang *et al*., 2005; Millar *et al*., 2006). To systematically assess the relationship between each acetylated Htz1 isoform, the enrichment signals were separated into bins of 150 bp (performed by Muxin Gu). The signal intensity from each bin was compared against each other using pair-wise comparison. I found that the global profile between K8ac and K10ac and between K8ac and K14ac are highly correlated (r = 0.83; r = 0.78 respectively) and to a lesser degree between K10ac and K14ac (r = 0.67) (Figure 3.5 B). It is important to point out that αHtz1K14ac antibody, which was derived from a different batch from the previous studies (Millar et al., 2006), shows higher noise signal than that of K8ac and K10ac signals (data not shown). All acetylated marks showed lower correlation to the bulk Htz1 than the correlation between each acetylated isoforms, except for K10ac which showed a relatively higher correlation to the bulk Htz1 (Figure 3.5 C).

The slightly higher correlation to bulk is likely due to the fact that certain population of Htz1-containing nucleosomes are deacetylated. To verify the microarray data, I performed ChIP-qPCR experiments at selected loci (Figure 3.6). The patterns were consistent with ChIP-chip experiments, indicating the reproducibility of these data. Taken together, these data suggest that acetylated Htz1 isoforms at lysine 8, 10 and 14 are not restricted to particular genomic regions, while co-localisation of the acetylated Htz1 isoform implies that they may confer a similar function.

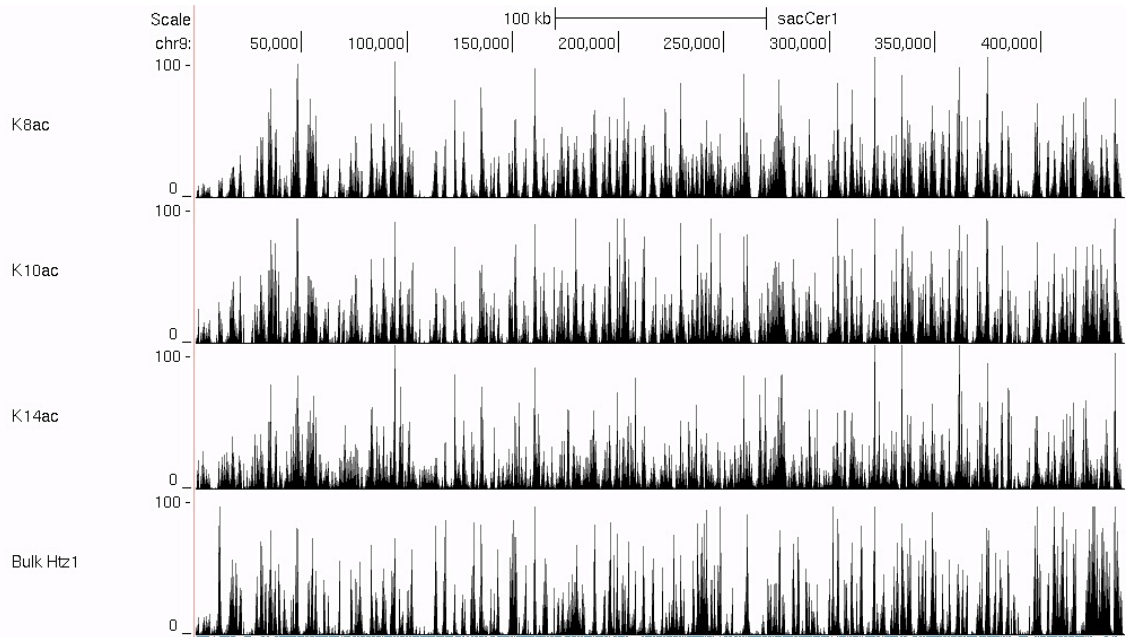

Figure 3.4 The global profiles of acetylated K8ac, K10ac and K14 are highly similar
ChIP-chip tracks show acetylated Htz1 isoforms are co-localised. A snapshot of localisation profiles of K8ac, K10ac and K14ac relative to bulk Htz1 after normalisation to input on the entire chromosome 9. Data was visualised using the UCSC genome browser. Numbers indicate the genomic coordinates.

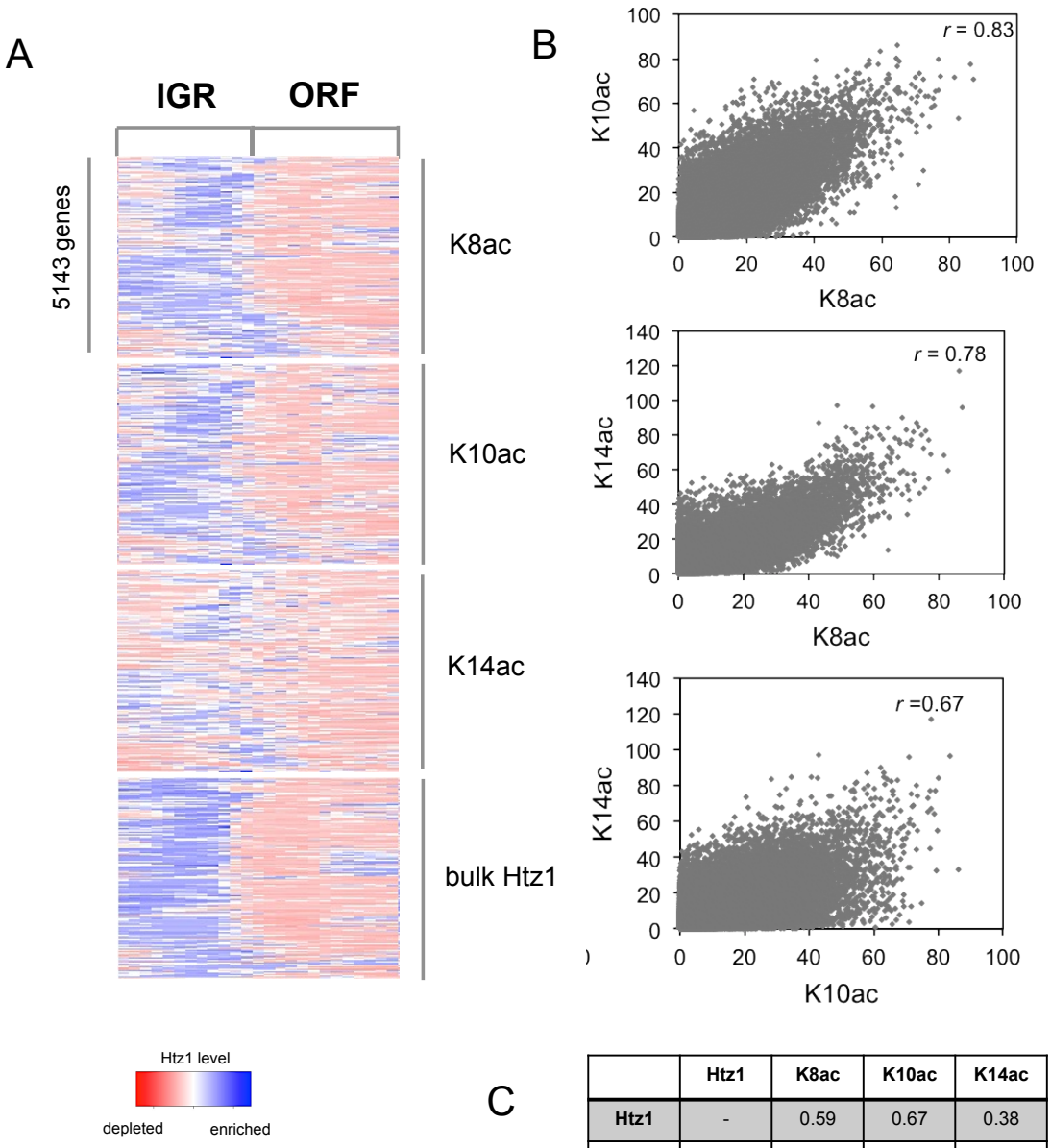

C

	Htz1	K8ac	K10ac	K14ac
Htz1	-	0.59	0.67	0.38
K8ac		-	0.83	0.78
K10ac			-	0.67
K14ac				-

Figure 3.5 Acetylation profiles of Htz1 at lysine 8, 10 and 14 sites are highly similar

(A) Groups of genes share similar acetylation patterns at lysine K8, lysine 10 and lysine K14 on their promoters. A heatmap diagram represents a color depiction of the enrichment ratios in ChIP on the intergenic regions (IGR) and 5' end of the open-reading frame (ORF). Blue color represents the positive enrichment versus red color for the negative enrichment. Each row represents a single gene (Xu *et al*., 2009)
(B) Scatter plot of ChIP enrichment signals on acetylated Htz1 at lysine 8, 10 and 14 (K8ac, K10ac and K14ac) using a window of 150 bp across the whole yeast genome. The global patterns of K8ac and at K10ac are highly correlated while K14ac is more similar to K8ac than K10ac. *r* = Pearson correlation coefficient
(C) A summary table demonstrates the correlation between ChIP-chip dataset in A) together with the bulk Htz1 data.

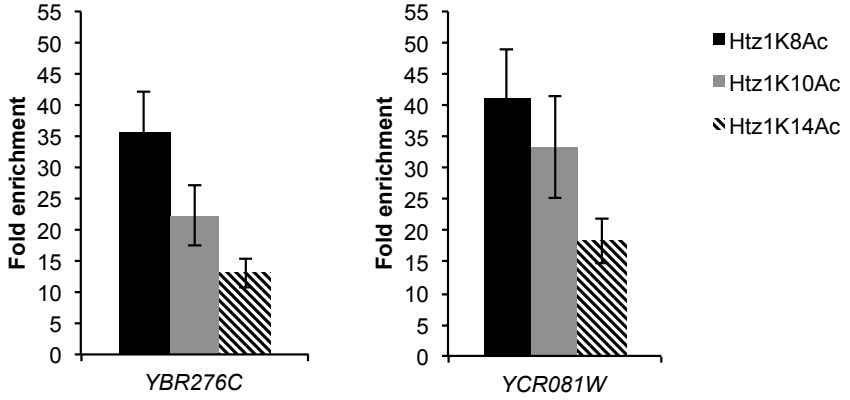

Figure 3.6 The pattern of acetylated Htz1 isoforms verified by qPCR is similar to ChIP-chip data.
Validation of tiling array data of acetylated Htz1 isoforms was carried out by ChIP-qPCR analysis using primers specific for the indicated loci. ChIP experiments were conducted using lysates from log-phase wild-type yeast strains. All ChIP samples were normalised with their input and *ARS317* (a known non-enrichment control) and displayed as fold enrichment. Error bars represents S.E. between three independent ChIP experiments (*n*=3)

3.4 Discussion

In this study, I characterised three acetylation site-specific Htz1 antibodies, which can be used in ChIP experiments. Using these reagents, I identified the co-existence of acetylated lysine K8, K10 and K14 isoforms of Htz1 across the yeast genome using ChIP-chip analyses. The resulting profiles showed that these acetylated Htz1 isoforms exhibit a similar global localisation patterns. This study revealed the positive relationship between these acetylation marks and suggests the co-existence of these marks throughout the yeast genome.

Previous genome-wide studies in yeast have demonstrated that Htz1 is predominantly localised at the promoters of genes transcribed by RNA polymerase II (Guillemette *et al*., 2005; Li *et al*., 2005; Millar *et al*., 2006; Raisner *et al*., 2005; Zhang *et al*., 2005). With these localisation profiles, Htz1 has been proposed to mediate a specialised chromatin state at promoter regions. Despite these established genomic profiles of Htz1, it remains unclear why Htz1 confers multifunctional roles. The possible explanations of multifunctional roles of Htz1 may be derived from the modified isoforms of Htz1 protein. Mapping of Htz1K14ac distribution relative to bulk Htz1 was demonstrated in budding yeast. It was reported that while Htz1 is preferentially associated with repressed loci, Htz1K14ac is preferentially localised at promoters of active genes (Millar *et al*., 2006). Consistent with the yeast study, acetylated H2A.Z isoforms were

reported to preferentially localise at the active promoter regions in chicken cells (Bruce *et al*., 2005) and at the bivalent promoters (containing H3K4me3 and H3K27me3) but not repressed loci in mouse embryonic and neural progenitor cells (Ku *et al*., 2012). Together, these findings suggested that acetylation of H2A.Z at the N-terminus is a key characteristics of active genes and that the pattern is conserved across species. However, there is no information about the individual sites of H2A.Z on a genomic scale.

In this chapter, I demonstrated the co-localisation of Htz1 K8ac, K10ac and K14ac relative to Htz1 and the strong correlation between these acetylation marks. Globally, these three acetylation marks appear to be a near-ubiquitous feature of Htz1 proteins. One possible explanation is that acetylation is a common feature of Htz1 molecule. Thus, the pattern is pervasive across the genome. It is important to note that the co-occurrence of Htz1 K8ac, K10ac and K14ac marks share similar genomic regions but this data cannot identify the simultaneous presence of each mark at the exact histone molecule. It would be tempting to test whether this event exists *in vivo* by performing re-ChIP using each acetyl-specific antibody sequentially. Nevertheless, the evidence observed indicates that the acetylation pattern of Htz1 is similar to other histones where there is a high correlation between different acetylation sites (Kurdistani *et al*., 2004). This has been observed for H3K9ac and H3K14ac acetylation at the promoter of active genes (Pokholok *et al*., 2005) and H4 K5ac, K8ac and K12ac marks that are normally associated with similar genomic regions.

Despite the careful purifications, a concern raised by these acetylated antibodies may recognise all Htz1 sites, meaning that they may still co-associate with unacetylated Htz1 or other acetylated histone tails. An antibody intended to recognise a specific modified residue might bind to adjacent modifications (Fuchs *et al*., 2011). This example was reported that site-specific antibodies for histone H4 preferentially bind to poly-acetylated histone substrate (Rothbart *et al*., 2012). Given the challenge in identifying acetylation site-specific antibodies, the result of ChIP experiment needed to be assessed with caution and additional alternative validation approaches have been suggested (Egelhofer *et al*., 2011). Peptide binding test (dot blots) or mass spectrometry could be considered as a secondary validation method to provide a confidence for antibody specificity (Landt *et al*., 2013). The possibility that *in vitro* peptide binding may not reflect the antibody binding on histone tails in the chromatin context is still on debate.

Alternatively, one could consider quantifying the degree of enrichment at a particular acetylation using the stable isotope labeling of amino acids in cell culture (SILAC) in combination with mass-spectrometric analysis. This approach has been reported to quantitatively evaluate the outcome of immunuoreactivity of ChIP antibodies. (Peach *et al*., 2012). An alternative reagent to acetyl-specific antibodies has been proposed such as DNA aptamer technology because the ease of production *in vitro*. Interestingly, these 3-dimensional oligonucleotides are capable of recognising H4K16ac (Williams *et al*., 2009).

N-terminal lysines of Htz1 are substrates of KAT5 (Millar *et al*., 2006; Barbiarz *et al*., 2006; Keogh *et al*., 2006) and Hda1 deacetylase (Lin *et al*., 2008; Mehta *et al*., 2010). It is possible that these modifying enzymes co-ordinately regulate the acetylation state of all acetylatable lysine sites on Htz1 at the same time. Therefore, they may not perform any distinct specialities towards these lysine sites at any given genomic regions. As a result, acetylation sites of Htz1 seem to function similarly.

It is worth noting that results from Mehta and colleagues (2010) were not known at the start of this project. These findings, however, provide supporting information towards the co-occurrence of acetylated Htz1 marks such that their global existences may explain the redundancy of individual acetylation sites. These data appear to rule out the different function that each acetylation site on Htz1 may carry. In support of my genome-wide results, a recent report has shown that individual lysine site of Htz1 is internally redundant (Mehta *et al*., 2010).

CHAPTER 4: Genetic and functional analyses of the H2A.Z N-terminal lysine acetylation sites

4.1 Introduction

Identifying and characterising pathways that regulate Htz1 acetylation and deacetylation is important for understanding not only the functional significance of modified Htz1 species, but also diverse roles of Htz1 in cells. An interesting aspect of Htz1 lysine acetylation sites is the potential of distinct modification states on individual lysine residue or combinatorial effects between these residues. The key question I aim to address is "Do individual acetylatable lysine residues confer Htz1 function in a site-specific manner?"

With the easy genetic manipulation in yeast, mutational analyses with amino acids substitution mimicking modified and unmodified states have been widely exploited to investigate the function of individual or multiple residues on histones. Strains expressing amino acid(s) substitution were used in a wide variety of phenotypic assays.

Budding yeast cells lacking Htz1 (*htz1*Δ) display a slow growth phenotype and sensitivity to a wide variety of cytotoxic agents such as hydroxyurea, formamide, MMS, caffeine and benomyl. These phenotypes have proven to be a useful tool to characterise the function of individual or multiple acetylation sites on Htz1. Furthermore, previous studies highlighted the roles of a specific residue; for example it was reported that cells expressing unacetylatable allele at K14 (K14R) of Htz1 were sensitive to microtubule destabilising agent, benomyl (Keogh *et al*., 2006; Lin *et al*., 2008). It was not known whether other acetylation sites carry any specific roles. These observations were, at least partly, motivated by the possibility that genetic and functional evidence can be linked to genome-wide information of Htz1 acetylation marks

To this end, I set out to define the role of the individual lysine acetylation sites on Htz1 by using genetic and functional studies to probe the contribution of each residue to Htz1 function. Site-directed mutagenesis of an individual acetylatable residue was carried out to block acetylation at a given lysine residue or at all lysine residues. The phenotype was then monitored by assessing contribution of each residue towards the fitness in a variety of stresses. Additionally, biochemical analyses were also conducted to assess the effect of mutations at N-terminal acetylation sites of Htz1 towards its protein levels.

4.2 Individual acetylatable lysine sites on H2A.Z N-terminus are functionally redundant

Based on the global profiling data of acetylated Htz1 isoforms, Htz1K8ac, Htz1K10ac and Htz1K14ac marks are prevalent across the yeast genome and their localisations are almost indistinguishable from each other. These data suggest that N-terminal lysine residues on Htz1 are generally modified by acetylation because these marks overlap well with each other and with Htz1. This evidence lends support to the general view that these acetylatable lysine residues perhaps serve to regulate similar functions because of their similar localisation. However, these data cannot precisely demonstrate the clear view of the function of these sites.

To address whether the known acetylatable lysine sites of Htz1 carry individually unique function, we used genetic studies to explore whether genetic interactions exist between these sites and other N-terminal acetylatable sites of core histones. Previous data in our lab showed that mutations of all four acetylatable lysine to arginine (HA-*htz1 K3, 8, 10, 14 R;* hereafter abbreviated as HA-*4KR*) which mimic constitutive deacetylation displays genetic interactions with mutations of histone H4 at lysine 16 to glutamine (H4K16Q) (Figure 4.1A) (Dr Catherine Millar, unpublished). These results imply that the lysine residues within the N-termini of Htz1 and H4 share an essential function for cell viability, which likely involves acetylation of lysines. I sought to determine whether the genetic interactions with H4K16Q exist when we mutate each lysine to arginine on Htz1. Similarly, in this experiment, we used a histone-shuffle yeast strain where both endogenous H3 and H4 (*HHT2-HHF2*) were deleted from the genome and the wild-type copy of H3-H4 was expressed under the *GAL1*-inducible promoter on a *URA3* plasmid. An endogenous *HTZ1* allele in the chromosome was then replaced by singly mutated lysine site to arginine (HA-*K3R*, HA-*K8R*, HA-*K10R* or HA-*K14R*) by homologous recombination. This strain was then transformed with a second plasmid (CEN-*TRP1*) that contains either wild-type H3-H4 (control) or mutated H4K16Q alleles (experimental). The experiments were performed under selective conditions where wild-type H3-H4 gene on a *URA3* selectable marker was lost and repressed by the presence of glucose. Serial dilutions of cells were plated on synthetic media lacking tryptophan with or without 5-fluorotic acid (5-FOA) to counter select the *URA3* plasmid. I found that singly mutated lysines on Htz1 do not recapitulate the phenotype of the unacetylatable *htz1* when combined with H4K16Q (Figure 4.1 B). It is known that any single lysine on Htz1 can buffer the function of another when one site is unavailable. These results indicate that the sites of acetylation of

Htz1 variant are important for the function of the protein with mutations on H4 tails but the individual site may act in a functionally redundant manner.

Given that these results were derived from epitope tagged strains, I next tested whether these phenotypes are similar or distinct when compared to an untagged version of *HTZ1*. To test that this is the case, I created other yeast strains where *HTZ1* was deleted from the chromosome in the similar histone shuffle strain as previously described and the sole source of Htz1, quadruple or triple mutants (*K8, 10,14 R* = K3ac etc.) was expressed on a plasmid. The cartoon diagram illustrates the steps of making these strains (Figure 4.2).

Unexpectedly, I was unable to detect a similar genetic interaction pattern between unacetylatable Htz1 and H4K16Q (Figure 4.3). The most likely explanation was that the synthetic lethality phenotype that I observed previously was derived from the combinatorial effect between the N-terminal epitope tagging and mutations on Htz1 tail.

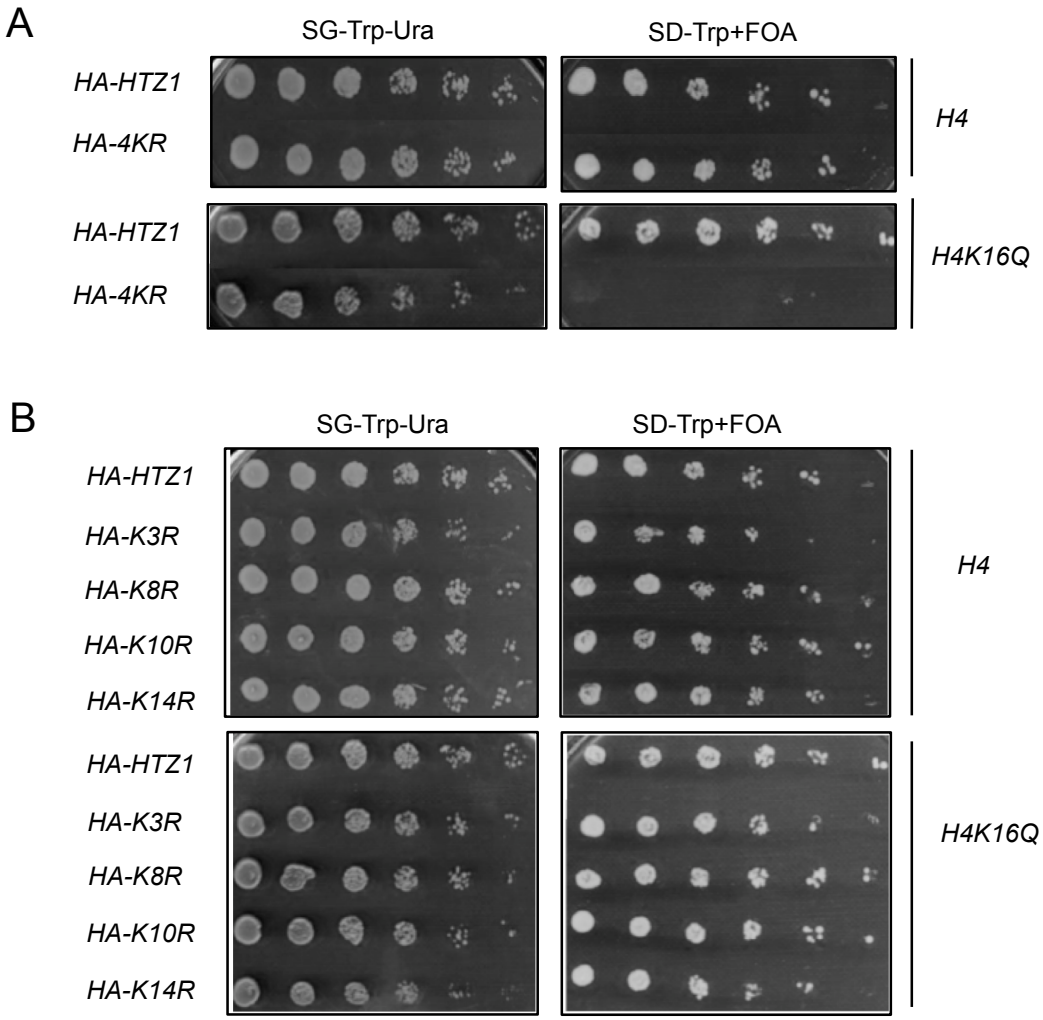

Figure 4.1 A completely unacetylatable allele (*HA-4KR*) of Htz1 displays synthetic lethality with an H4K16Q allele
(A) An *HA-4KR* allele of Htz1 (CMY279) is synthetically lethal with *H4K16Q*. (B) In contrast, the singly mutated htz1 alleles (*HA-K3R*, *HA-K8R*, *HA-K10R* and *HA-K14R*) show no genetic interactions with *H4K16Q* (CMY483, CMY486, CMY489 and CMY284 respectively). These data suggest the redundancy of the individual acetylatable sites of Htz1. Wild-type *HA-HTZ1*, *HA-K3R*, *HA-K8R*, *HA-K10R* and *HA-K14R* or HA-4KR were integrated in chromosomal DNA where wild-type H4 was carried on a *URA3* plasmid. These strains were transformed with either wild type H4 or *H4K16Q* on a *TRP* plasmid. Five-fold serial dilutions were spotted on either minimal medium lacking tryptophan and uracil or minimal medium lacking tryptophan and containing 0.1% FOA, to select against the *URA3* plasmid. Cells were grown at 30 °C for 3 days before imaging.

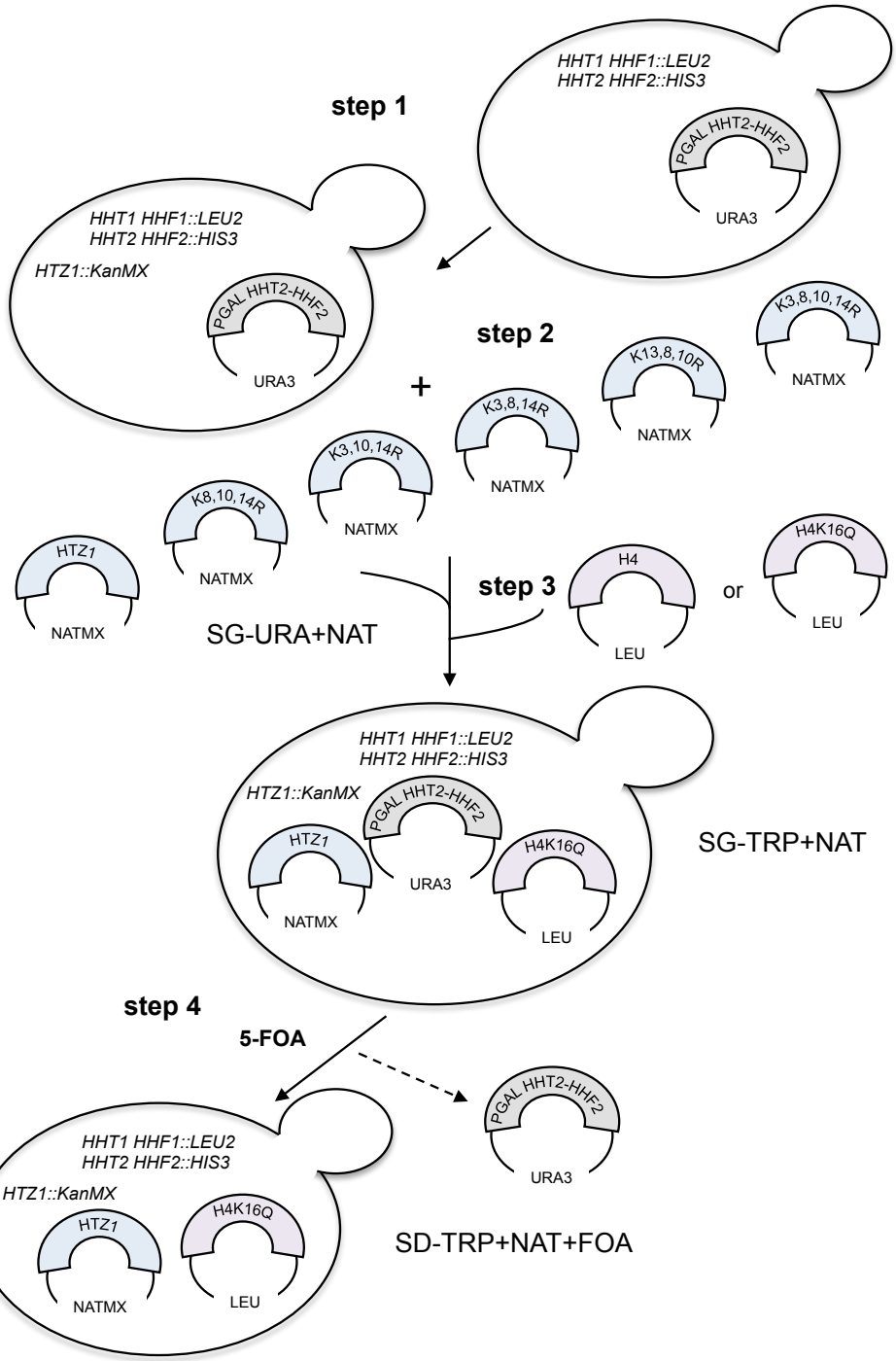

Figure 4.2 A schematic diagram of histone-shuffle yeast strain generation
HTZ1 was deleted from the chromosome in a histone shuffle yeast strain as described previously (CMY218) (step 1). This strain was transformed with a NAT plasmid (pRS418) expressing either wild type Htz1, quadruple or triple mutations (K8, 10, 14 R = K3ac etc.) (step 2) and grown on a clonNAT containing medium to select for the plasmid. Next, the *TRP* plasmids expressing either H3-H4 or H4K16Q were transformed (step 3) and counterselect by growing 5-FOA together repression by glucose (step 4)

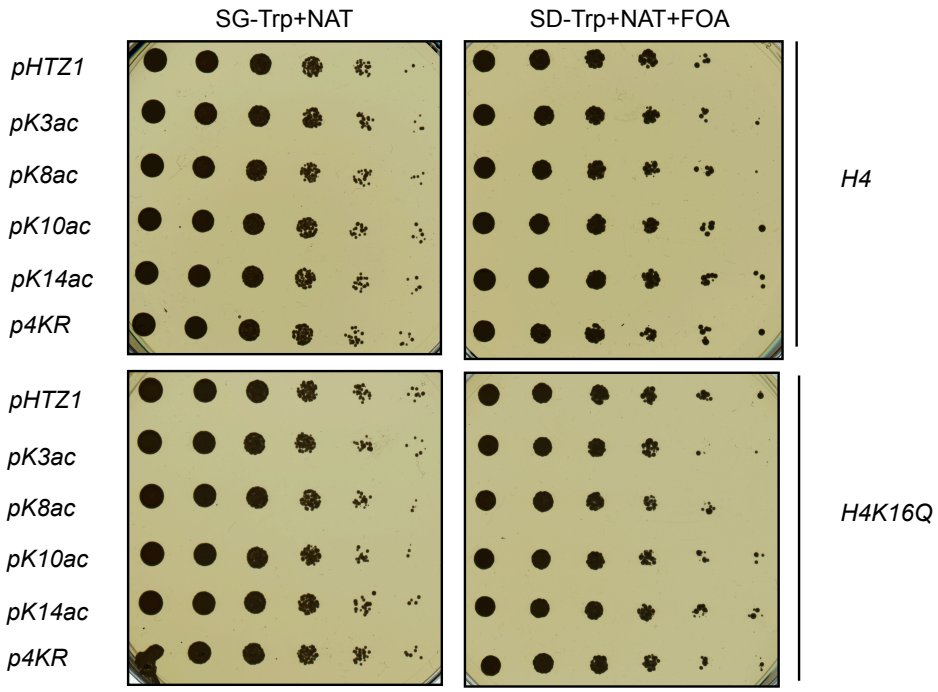

Figure 4.3 An untagged *4KR* allele of *HTZ1* displays no genetic interactions with *H4K16Q*

Untagged *4KR* alleles (CMY712) show no synthetic genetic interactions with H4K16Q in these analyses. Wild-type *HTZ1* and triple mutants (K3ac, K8ac, K10ac and K14ac) or *4KR* were expressed on the *NAT* plasmid in an *htz1* deletion background where wild-type H4 was carried on a *URA3* plasmid. These strains were transformed with either wild type H4 (Top) or H4K16Q (bottom) on a *TRP* plasmid. Cells were grown in the medium containing ClonNAT to select the NAT plasmid. Cells were spotted serially on either minimal medium lacking tryptophan and containing ClonNAT or minimal medium lacking tryptophan and containing ClonNAT and 0.1% FOA, to select against the *URA3* plasmid. Cells were grown at 30 °C for 3 days before imaging.

4.3 N-terminal HA epitope tagging disrupts H2A.Z protein levels and function

Next, I sought to determine how the N-terminal HA epitope tagging affects Htz1. I first checked the protein abundance of Htz1 in the presence and absence of HA tagging by western blot analysis using the specific Htz1 antibody, which recognizes the C-terminal region of Htz1 (Millar *et al*., 2006).

Whole cell lysate and histone samples harvested from untagged WT *HTZ1*, N-terminally HA-tagged Htz1 (*HA-HTZ1*) and *htz1Δ* which serve as a negative control were run on a 15% SDS-PAGE and probed with anti-Htz1 antibody (α660). Antibodies against tubulin and H4 were used as controls for equal gel loading. I found that the strain expressing *HA-HTZ1* allele (CMY231) displayed a marked decrease of Htz1 in the WCEs and purified histone samples (Figure 4.4 A). Given that HA epitope tagging is located at the N-terminal tail of Htz1, therefore it is unlikely that it would cause epitope disruption to the antibody. To rule out the possibility of an antibody issue, i.e. the antibody binding was blocked by post-translational modifications in the C-terminal region of Htz1, these observations were confirmed by comparing the N-terminally HA-tagged Htz1 with the C-terminally HA-tagged Htz1 (*HTZ1-HA*) by using an HA antibody. Similarly, the lower abundance of Htz1 was also observed in *HA-HTZ1* (Figure 4.4 B). In addition to this, the global depletion was also found in *HA-HTZ1* when comparing our ChIP-chip data, which were carried out in both HA-tagged and the untagged Htz1 (wild-type) strains (with anti-HA and anti Htz1 antibodies respectively). As expected, we observed the lower enrichment of *HA-HTZ1* in several regions (Figure 4.4 C). Taken together, these data suggest that the HA-epitope tagging perturbs gross Htz1 protein levels in the chromatin.

To further evaluate that the N-terminal HA epitope tagging disrupts Htz1 protein amount and function in yeast cells, *HA-HTZ1* was compared to the known decreased Htz1 protein amount side by side. Because truncating the promoter of genes can lead to the reduced mRNA expression and thus resulting in lowered protein levels, I constructed yeast strains with a CEN plasmid bearing *HTZ1* with a truncated promoter (crippled promoter) of 200 bp ($HTZ1^{cp200}$) or 100 bp ($HTZ1^{cp100}$) (Figure 4.5 A). A yeast strain, in which chromosomal *HTZ1* was deleted, was then transformed with a CEN-*URA3* plasmid expressing the crippled promoter of *HTZ1, HA-HTZ1* or WT construct. To determine the level of chromatin-associated Htz1, I used chromatin fractionation assay as shown in Section 2.2.10. Chromatin-associated samples were analysed by western blot using antibodies against Htz1 and H4. Indeed, truncating the promoter of *HTZ1* results in the reduction of chromatin-associated Htz1 protein levels to ~40% and ~3% of WT levels for

HTZ1^{cp200} and *HTZ1*^{cp100} respectively. In *HA-HTZ1* (CMY394), the level of protein was decreased to approximately 10% of WT levels (Figure 4.5 B).

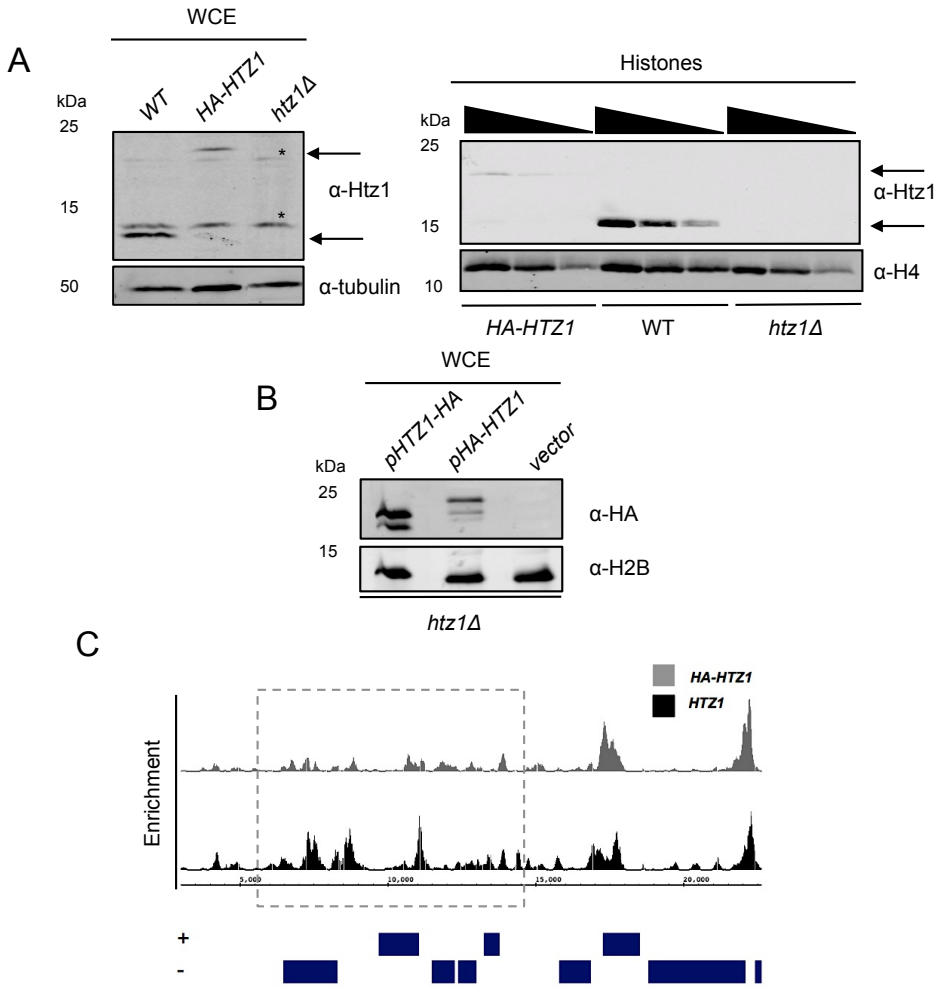

Figure 4.4. The N-terminally HA-epitope tagging of Htz1 affects Htz1 protein abundance in the chromatin fraction

(A) Total Htz1 protein levels are decreased in *HA-HTZ1 allele.* WCEs and purified histones samples from untagged wild type *HTZ1, HA-HTZ1 and htz1Δ* were separated by 15% SDS-PAGE and immunoblot analysis was performed for Htz1 using Htz1 antibody. Equal gel loading was confirmed by immunoblotting against tubulin for total Htz1 and H4 for histone extract samples. The molecular weight (MW) of Htz1 protein is ~14 kDa and the MW of N- and C-terminally HA tagged Htz1 are ~21 kDa and ~19 kDa respectively. Asterisks indicate cross-reactivity of Htz1 antibody to cytoplasmic proteins.

(B) Comparison of total protein levels of the C-terminally HA tagged Htz1 (*HTZ1-HA*) and the N-terminally HA-tagged Htz1 (*HA-HTZ1*). WCEs from the yeast strains with indicated genotypes were analyzed in a western blot analysis. Htz1 levels were examined using anti HA antibody and equal loading was confirmed by probing with anti H2B

(C) A snapshot view demonstrating localization profiles of wild type HTZ1 (black) and *HA-HTZ1* (Grey) on chromosome III (the genome coordination shown at the bottom). ChIP experiments were performed using anti HA (12CA5) and anti Htz1 (α660). The grey block indicates an example of the region where Htz1 is less abundant in *HA-HTZ1*. Blue blocks represent genes on Watson (+) and Crick (-) strands

Several lines of evidence have been demonstrated that yeast cells lacking Htz1 (*htz1*Δ) display growth defects upon exposure to a variety of cytotoxic agents (Mizuguchi *et al*., 2003; Kobor *et al*., 2004; Krogan *et al*., 2004). This suggests that Htz1 protein level plays a major role in these stress-inducing events. I asked whether a marked decrease of Htz1 protein level from *HA-HTZ1* alleles could lead to similar phenotypic defects upon exposing to different stress stimuli. Next, we tested the growth sensitivity of a strain bearing *HA-HTZ1* allele with $HTZ1^{cp200}$ and $HTZ1^{cp100}$ by serially plating on a variety of drugs that *htz1Δ* cells displayed growth defects including the TOR/ATM-ATR inhibitor-caffeine, DNA-damaging agent-methymethane sulfonate (MMS) and replication-stressed inducing agent-hydroxylurea (HU). Consistent with the previous evidence that cells lacking *HTZ1* display hypersensitivity to various cytotoxic agents, both cells expressing *HA-HTZ1* and $HTZ1^{cp100}$ (of which the Htz1 protein levels are less than 10% of WT) showed striking sensitivity to caffeine and MMS. It is noted that cells expressing $HTZ1^{cp200}$ are not more sensitive to these agents (Figure 4.6). Therefore, it is likely that a certain level of Htz1 protein is required for cells to respond to stresses caused by caffeine and MMS. However, except for the *htz1Δ* strain, none of the mutants displays sensitivities to HU, suggesting that the level of Htz1 protein is not required in HU-mediated response.

Since yeast cells lacking Htz1 shows growth defects when exposing to stresses, I wondered whether the overproduction of Htz1 protein would also impact the function of Htz1 in response to stresses. A yeast strain carrying the *GAL1*-regulated promoter upstream of *HTZ1* locus was constructed in the BY4741 background by chromosomal integration. In this experiment, the promoter is being shut down in the presence of glucose from the YPD medium while being induced in the presence of galactose from the YPG medium. Briefly, cells were grown in the rich YPD or YPG overnight and serially spotted on the media as described with or without the presence of MMS. As expected, cells lacking *HTZ1* either by shut-off promoter or deletion showed sensitivity to MMS (Figure 4.7 A) but over-expression does not result in any apparent growth defects in these analyses. (Figure 4.7 B). Collectively, these data demonstrate that Htz1 protein levels play a critical role in diverse biological processes.

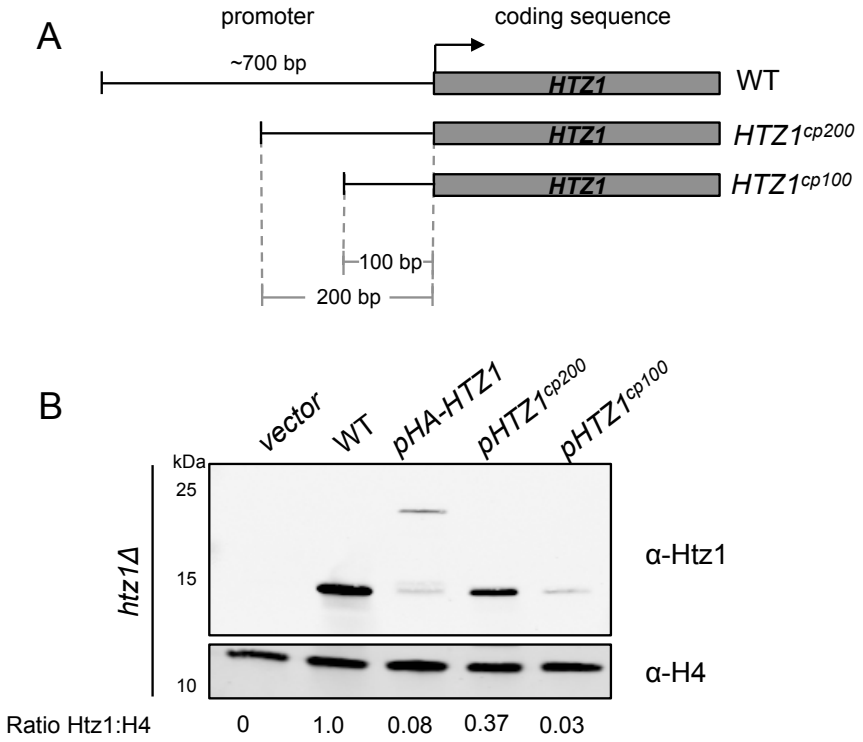

Figure 4.5. **Chromatin-associated Htz1 protein levels are reduced in the truncated *HTZ1* promoter strain (*HTZ1*^{cp}).**
(A) A Schematic diagram of the *HTZ1* constructs with the truncated *HTZ1* promoter. The black lines indicate the promoter sequence and grey bars represent the coding sequence of *HTZ1* locus. The numbers shown in the diagram denoted the promoter sequence in base pairs.
(B) Chromatin fractionation assay was performed in yeast strains with the indicated genotype. WT, *HA-HTZ1*, *HTZ1*^{cp200} , *HTZ1*^{cp100} *and vector were* expressed on *URA3* plasmids in yeast strain where chromosomal *HTZ1* is deleted.
Chromatin fraction samples were run on 15% SDS-PAGE and analyzed by western blotting using specific Htz1 antibody. Equal gel loading was confirmed by immunoblotting against histone H4. The ratio at the bottom shows the relative amount of Htz1 relative to WT after normalization to H4 (*n*=2)

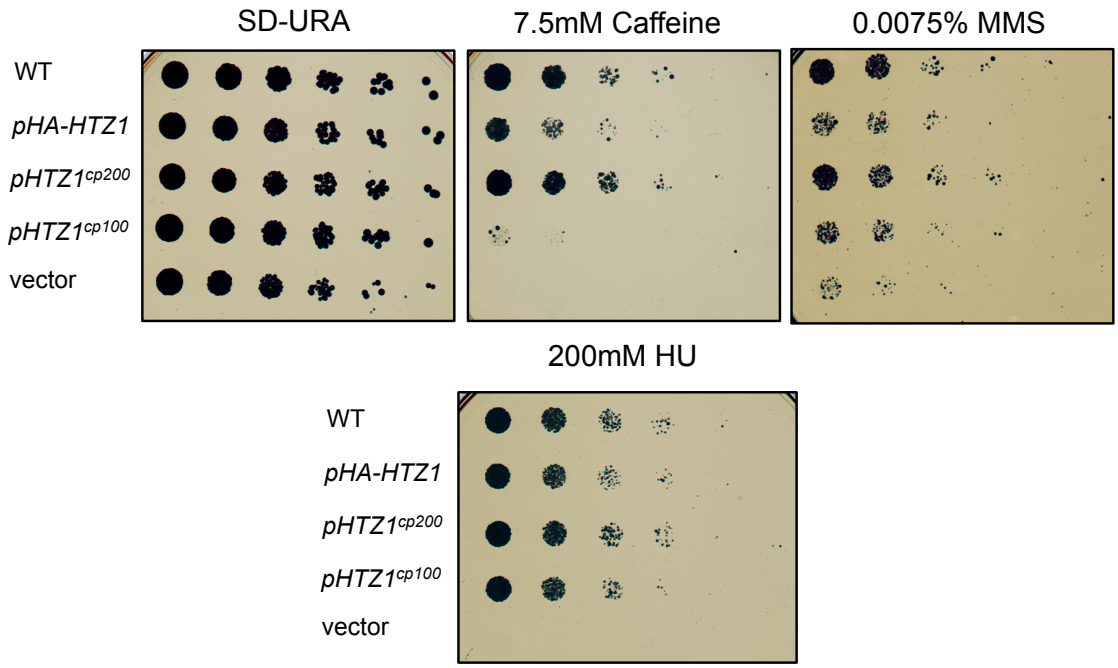

Figure 4.6. **Reduced Htz1 protein levels affect cells' sensitivity to cytotoxic agents**
Cell growth was retarded when Htz1 protein is removed (*htz1Δ)* or dramatically reduced (*HA-HTZ1 and HTZ1*^{cp100}*)* under stress conditions on caffeine and MMS but not HU. Wild type, *HA-HTZ1*, *HTZ1*^{cp200,} and *HTZ1*^{cp100} were carried on a *URA3* plasmid in the *htz1Δ* background. Five-fold serial dilutions of indicated genotype were spotted on SD-URA media and SD-URA media containing the indicated concentrations of caffeine, MMS or HU, Cells were grown at 30 °C for 3 days before imaging.

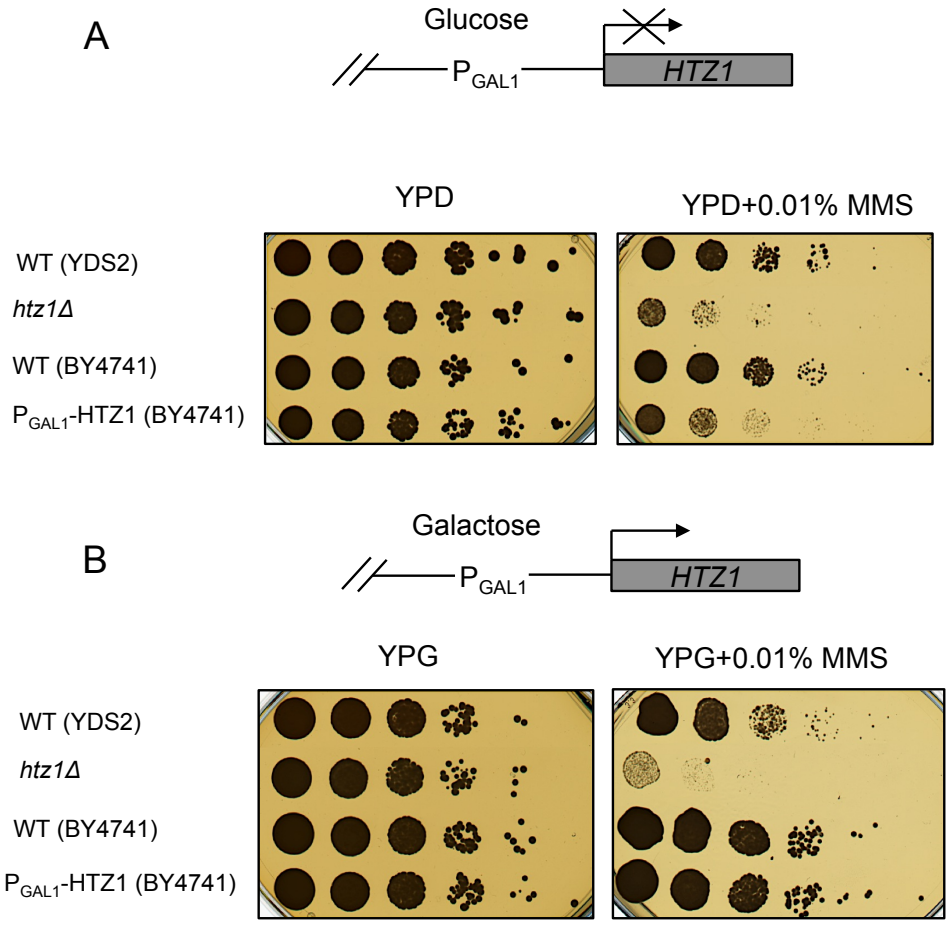

Figure 4.7. **Overexpression of Htz1 does not affect Htz1 function in MMS**
(A) Lack of Htz1 protein results in defective growth phenotype when cells are exposed to a DNA-damage inducing agent MMS.
(B) Conversely, MMS-sensitivity is not shown when Htz1 is overexpressed by galactose induction. Schematic diagrams represent *HTZ1* locus in a grey block and a black line with P-GAL1 for promoter of *GAL1*. The black arrows demonstrate whether the transcription is repressed in (A) or activated in (B). *GAL1*-inducible promoter of *HTZ1* was integrated into chromosomal DNA in BY4741 yeast strain background. Before spotting, indicated yeast strains were grown overnight in YPD to repress *GAL1*-promoter driven transcription of *HTZ1* by glucose or grown in YPG to induce transcription of *HTZ1* by galactose induction. Serial dilutions of cells were spotted on to YPD or YPD containing MMS in panel A and on to YPG or YPG containing MMS in panel B. Plates were incubated at 30 °C for 3 days before imaging.

4.4 The N-terminal acetylatable lysine residues is important for H2A.Z function

To address the potential role of Htz1 acetylation in cellular processes, I carried out further functional studies. Because the N-terminal epitope tagging compromised the function of Htz1, therefore I focused on studying the Htz1 acetylation using untagged Htz1 alleles. I generated yeast strains with a chromosomal-integrated *htz1 K3, 8, 10, 14 R*:: KanMX (hereafter abbreviated as 4KR) and an isogenic WT allele. The WT and 4KR allele were amplified from the plasmid construct containing the KanMX cassette. PCR products of WT and 4KR allele were then transformed into wild-type yeast strain YDS2. The resulting strains were screened by the G418 resistance and the genotype of theses strains was validated by DNA sequencing.

The phenotypes of Htz1 acetylation were investigated by comparing growth of the non-modifiable 4KR strain with the WT strain in different conditions. Growth curve analysis was performed as described in Section 2.2.5 to search for phenotypic defects in these mutant cells. Briefly, instead of spotting cells on solid media, I monitored growth kinetics of cells in liquid cultures with or without the presence of testing agents. I found that 4KR mutant cells were sensitive to caffeine (Figure 4.8), which phenocopied the growth defects in *htz1*Δ and recapitulated the phenotypes seen in *HA-HTZ1* and $HTZ1^{cp100}$. In addition, 4KR mutant cells displayed rapid growth, probably caused by bypassing cell cycle arrest, upon MMS exposure (Figure 4.8). Cell growths in YPD and YPD+DMSO served as the cell number control (Figure 4.8). Although, 4KR mutants showed prominent growth defects in caffeine and MMS, these mutant cells are moderately defective in growth in HU, formamide and a microtubule-destabilising agent benomyl (Figure 4.8). Taken together, these results indicated that acetylatable lysine sites on the Htz1 N-terminal tails were required to regulate Htz1 function under these conditions, highlighting the functional significance of Htz1 acetylation in diverse cellular processes.

In order to characterise the mechanistic involvement of Htz1 acetylation in different biological processes, I asked whether the phenotypic defects observed in the functional assay is a direct or indirect effect. Because the phenotype could be derived from other mutations occurred randomly in our mutants strains, I tested this by transforming a 2-micron-*LEU* plasmid expressing WT *HTZ1* allele into 4KR strain background and vice versa; following by further investigating whether expression of WT protein could rescue growth defects in response to caffeine and MMS. Interestingly, expression of acetylatable wild type Htz1 can partially alleviate the defective growth upon caffeine exposure (Figure

4.9). Unexpectedly, expression of 4KR into WT *HTZ1* allele background could disrupt the endogenous WT function in these assays; therefore I concluded that the 4KR allele conferred a dominant negative effect on endogenous Htz1 protein in these analyses.
However, I could not identify whether the phenotypic defects seen upon MMS treatment in 4KR strains can be rescued by expression of WT *HTZ1* allele. It was still unclear as the data were not reproducible due to cells undergoing flocculation in a minimal liquid media in the presence of MMS. It is possible that MMS caused gene expression changes including those that regulate cell wall integrity.

To determine the link between caffeine sensitivity in 4KR strains, I investigated this phenotype in other yeast strains where wild type Htz1 or mutant alleles were solely expressed on the plasmids. Since I revealed that reduced Htz1 abundance was involved in the defective growth during the caffeine treatment, I also included strain expressing reduced Htz1 levels with or without acetylation sites (*HTZ1*^{cp200} and *htz1-4KR*^{cp200}) in this experiment. The caffeine concentration was determined empirically to obtain the optimal concentration to distinguish different growth pattern between WT and *htz1* mutant alleles. In the presence of 10mM caffeine, 4KR displayed the growth defects comparing to WT while 4KQ and *HTZ1*^{cp200} were only modestly sensitive (Figure 4.10). Strikingly, the double mutant strain exhibited a synthetic slow growth defect, which was more severe than ether of the single mutant 4KR or *HTZ1*^{cp200} alone, suggesting the functional link of Htz1 acetylation sites and its protein abundance. Taken together, these findings recapitulated the synthetic effect of N-terminal epitope tagging with lysine-to-arginine mutants of Htz1, thereby supporting the idea that the Htz1 acetylation sites are critical for the fully functional Htz1 in response to stresses.

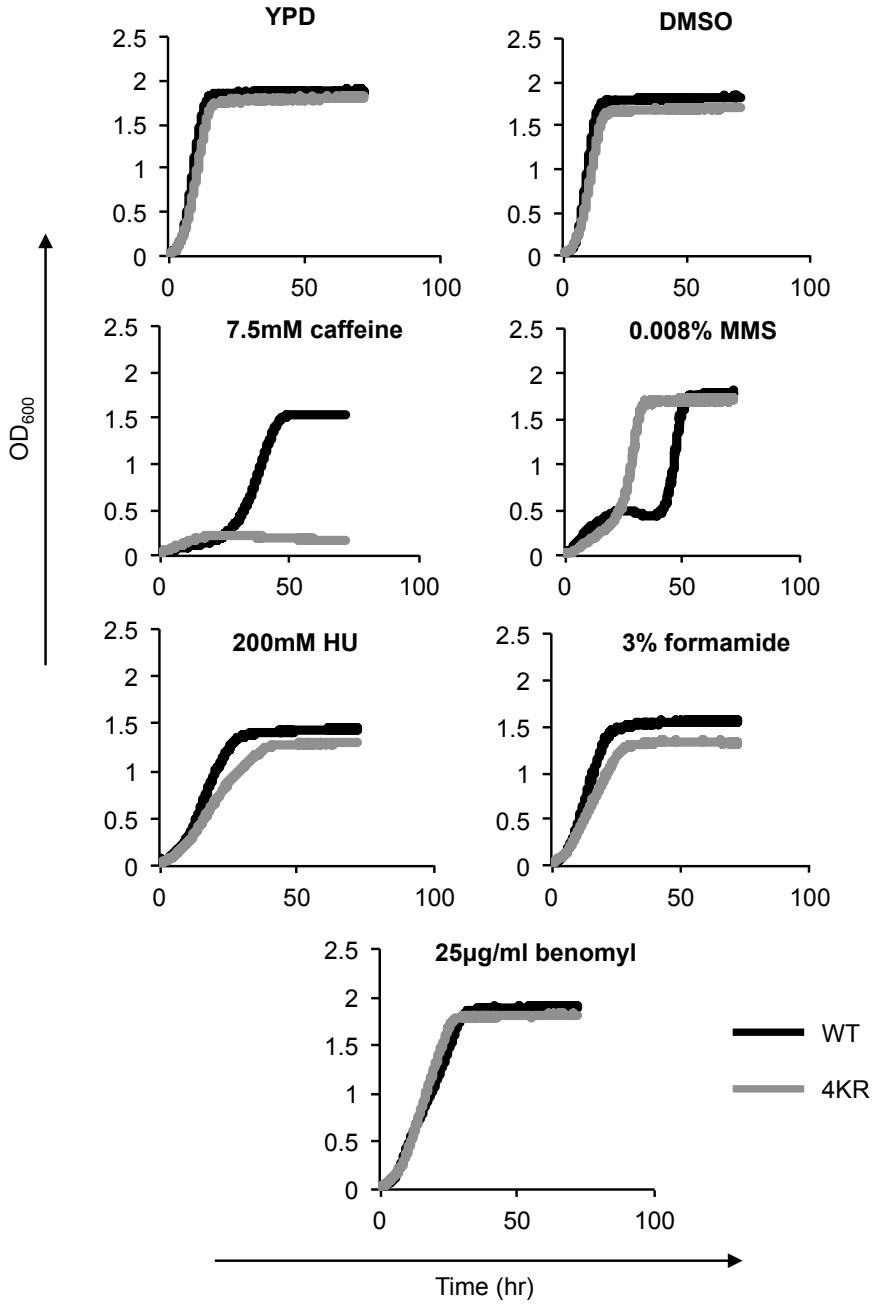

Figure 4.8. **Yeast strains bearing the *htz1*-4KR allele display atypical growth in the presence of caffeine and MMS.**
Yeast strains expressing the *htz1*-4KR allele (CMY743) shows anomalous growth when exposed to Caffeine and MMS but are only mildly sensitive to other agents. Growth curves of WT (CMY742) (blue lines) and 4KR (red lines) strains were analyzed on Bioscreen (Section 2.2.5 Materials & Methods) in the liquid media YPD and YPD containing appropriate agents at the indicated concentration. Cells were grown for 72 hours before data analysis was performed. The diagrams are representative of two independent experiments

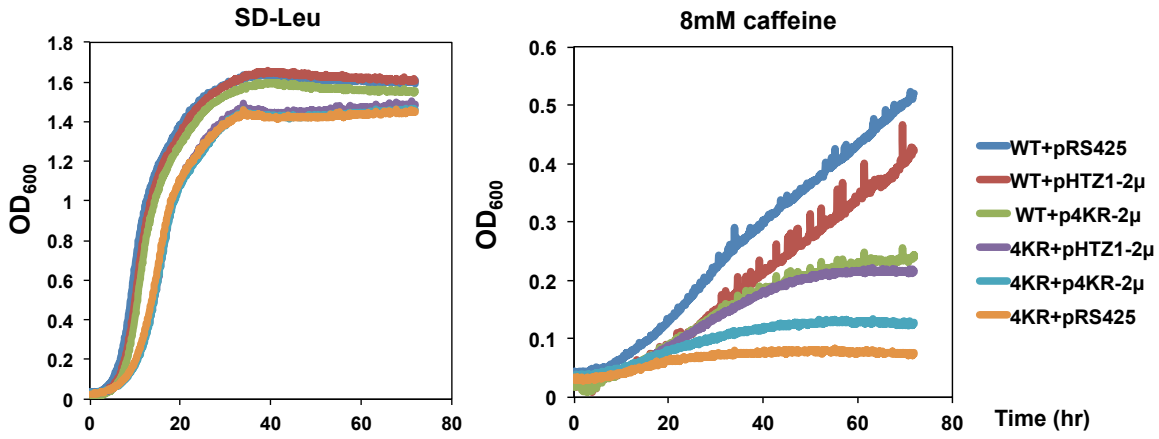

Figure 4.9. The caffeine sensitivity phenotype of the htz1-4KR strain can be partially rescued by overexpression of WT Htz1
Yeast strains expressing wild type or 4KR alleles were transformed with a 2-micron *LEU*-plasmid expressing either WT or *htz1*-4KR and empty vector.
Growth curves of all strains were analyzed in the minimal media lacking leucine and media containing 8mM caffeine. Cells were grown for 72 hours before data analysis was performed. The diagram is representative of two independent biological experiments.

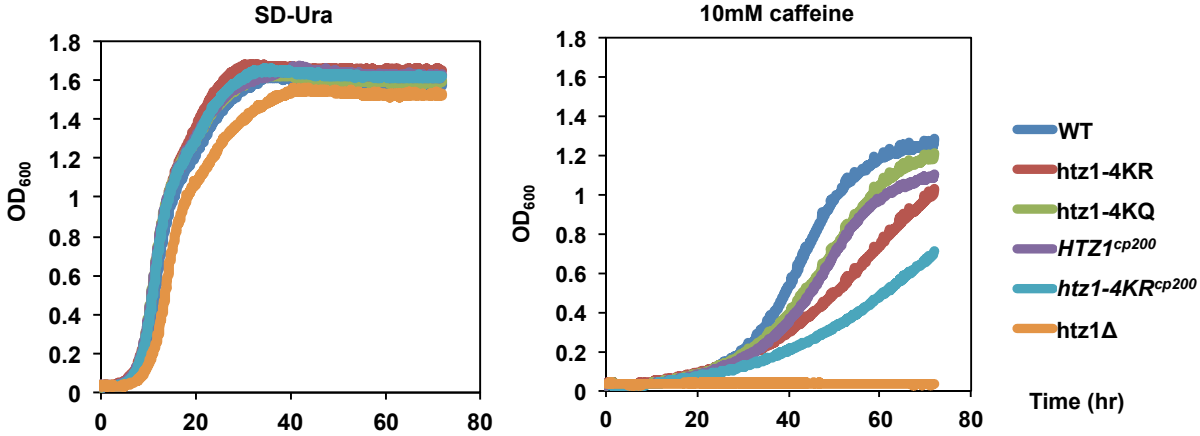

Figure 4.10. Yeast strains bearing the *htz1*-4KR allele exhibit growth defects when exposing to caffeine and display enhanced sensitivity when Htz1 level is compromised.
Yeast strains expressing the *htz1*-4KR allele shows growth sensitivity when exposed to 10mM caffeine and the phenotype is worsen in cp200*htz1*-4KR strain. In contrast, *htz1*-4KQ and cp200HTZ1 strains are only mildly sensitive to this agent. Growth curves of indicated yeast strains were analyzed on Bioscreen (Section 2.2.5 Materials & Methods) in the liquid minimal media lacking uracil with and without the presence of caffeine. Cells were grown for 72 hours before data analysis was performed. The diagrams are representative of four independent experiments (WT, *htz1*-4KR, *htz1*-4KQ, cp200HTZ1 and *htz1Δ*) and two independent experiments with cp200*htz1*-4KR.

4.5 Chromatin-associated H2A.Z levels are reduced in 4KR strains

To understand why the absence of acetylation sites in the 4KR strain led to phenotypic defects of these cells in our functional studies, I asked whether these phenotypes are due to the levels of Htz1 being altered, thereby affecting the growth in response to stresses such as caffeine and MMS.

In this experiment, I generated a yeast strain with a chromosomal-integrated allele where all four acetylatable lysines on Htz1 are mutated to glutamine *htz1*K3, 8, 10, 14 Q::KanMX (hereafter abbreviated as 4KQ). The 4KQ mutation is mimicking the constitutive acetylation state of Htz1 serving as an extra control in this experiment.

To determine the abundance of Htz1 in the chromatin, I performed chromatin fractionation assay and analysed Htz1 levels by western blot. Chromatin fractionation results revealed that both 4KR and 4KQ were chromatin-associated. Unexpectedly, I reproducibly found that the Htz1 abundance was reduced by approximately 40% in the 4KR strain while the decrease was not apparent in the 4KQ strain in relation to the Htz1 levels in the isogenic WT cells (Figure 4.11 A), suggesting that the N-terminal lysine residues are required to regulate the level of chromatin-bound Htz1. Consistent with this result, I also identified the decrease of Htz1 in 4KR in the chromatin in independent yeast strains where Htz1 was expressed on a CEN-NAT plasmid as a sole source in *htz1Δ* background (Figure 4.11 B), thus confirming the reproducibility of these findings. Additionally, I performed ChIP experiments using an antibody against Htz1 and analysed the DNA by qPCR with the primer specific for *GAL10* coding sequence, which was known for Htz1 enrichment (Millar *et al*., 2006; supplemental information). As expected, I detected a decrease of Htz1 level in the 4KR strain (Figure 4.11C), which correlated well our chromatin fractionation data. Subsequently, I checked whether these mutations affected Htz1 at the transcription levels, thus resulting in a decrease in Htz1 protein abundance. RT-qPCR analysis showed that Htz1 transcripts from the 4KR and 4KQ strains are similar to the WT counterpart (Figure 4.12). Collectively, these data suggest that N-terminal lysines regulate Htz1 level in the chromatin.

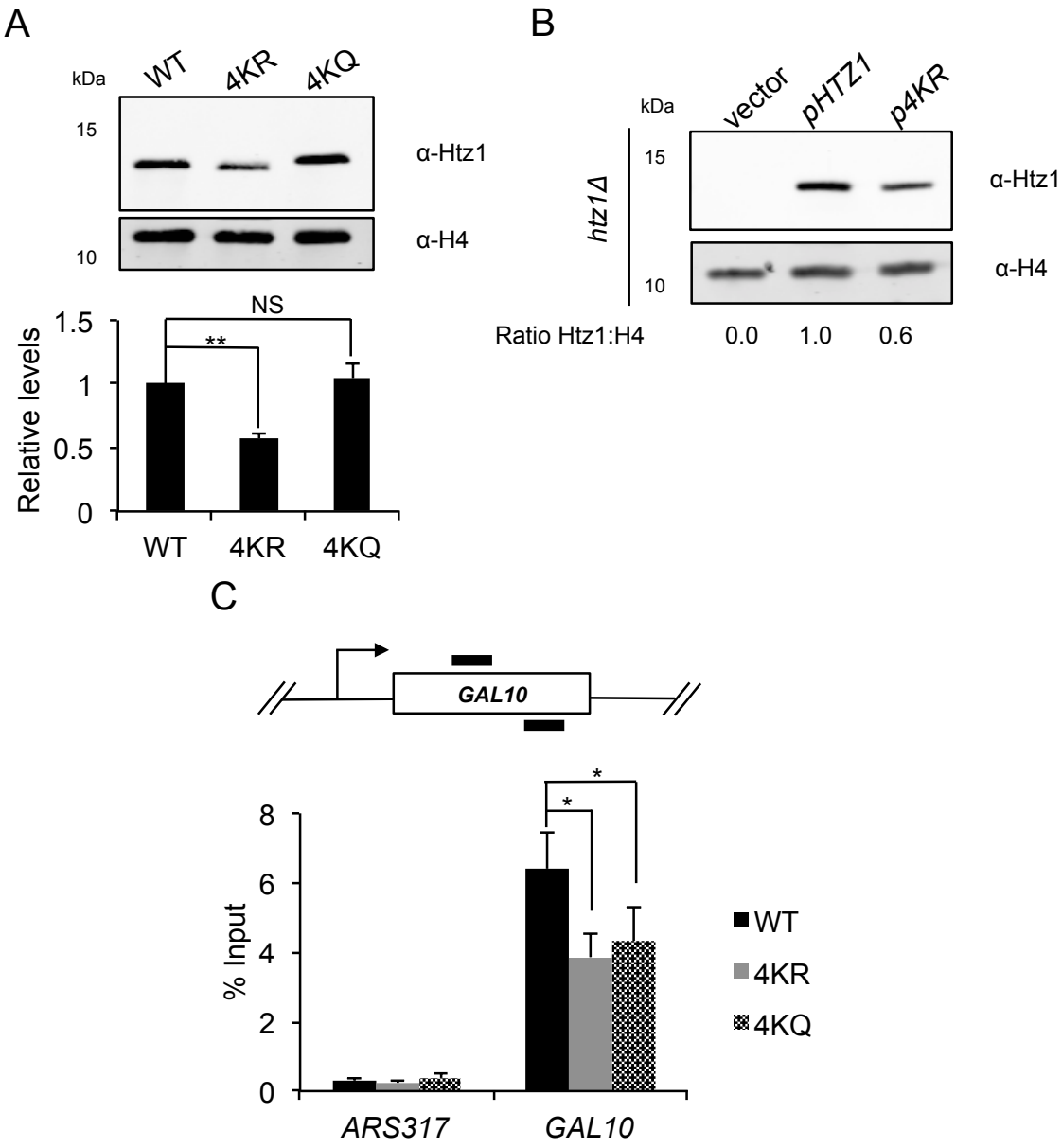

Figure 4.11. **Chromatin-associated Htz1 protein levels are reduced in 4KR**
Western blot analysis of Htz1 protein levels in strains with chromosomal-integrated
(A) or plasmid-borne alleles (B). Amount of Htz1 was normalised to histone H4 and expressed as a ratio relative to WT. A bar graph demonstrates the quantification of western blot signal as mentioned.
(C) ChIP-qPCR experiment confirms the reduction of 4KR in the chromatin.
ChIP DNA from immunoprecipitation using anti-Htz1 was analysed by PCR using *GAL10* primers as shown in a schematic diagram above. The enrichment of Htz1 at *ARS317* locus serves a negative non-enrichment control. Samples were normalised with their corresponding input chromatin and represented as percentage of input.
The error bars indicates S.E. from 5 independent experiments (*n*=5) for panel A and three independent experiments (*n*=3) for panel C. Asterisks indicates the statistical confidence using student's t-test (P value; * <0.05; ** <0.01) The number under figure B is the calculated ratio from two independent experiments (*n*=2).

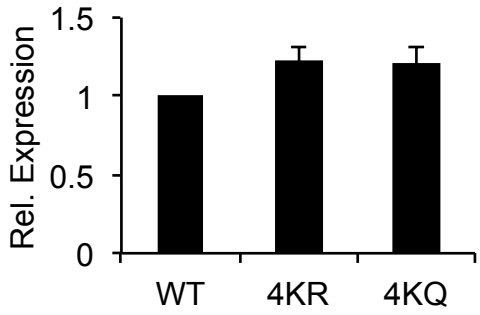

Figure 4.12. mRNA levels of Htz1 are relatively unaltered by mutations at the N-terminal lysines
Real time qPCR was performed after reverse transcription of the total RNA harvested from yeast strains as indicated. Htz1 mRNA was normalized to Actin mRNA and expressed relative to WT. The error bars represent S.E. from three independent experiments.

4.6 Discussion

Acetylation at lysine 3, 8, 10 and 14 of Htz1 within the N-terminus has been implicated in various cellular processes that Htz1 is involved. Understanding how an individual acetylation site of Htz1 function would allow us to visualise a bigger picture of how it regulates Htz1 function. Many studies suggest that mutations of the N-terminal acetylatable lysines phenocopy *htz1*Δ strain. Keogh and colleagues demonstrated that *K14R* mutant cells exhibit benomyl sensitivity and an increase rate of chromosome loss (Keogh et al., 2006) that is similar to *htz1*Δ strains. Other studies showed that 4KR mutant cells displayed deposition defects and aberrant heterochromatin spreading at the boundary protection (Millar *et al*., 2006; Barbiaz *et al*., 2006). Recent work has reported that acetylation sites of Htz1 are important for the induction of *GAL1* gene (Halley *et al*., 2010).

Large-scale gene expression and genetic evidence in *S. pombe* support an important role of acetylation in chromosome segregation (Kim *et al*., 2009). These works have uncovered multifunctional roles of H2A.Z and highlight the crucial involvement of acetylation sites to regulate H2A.Z. Despite this notion, the functional significance of this modification to H2A.Z protein remains unclear.

In this work, I aimed to identify whether each individual acetylatable lysine site could mediate any specialised function. The results presented in this study demonstrated that

mutation of all four lysine residues within the Htz1 N-terminal tail is synthetically lethal with H4K16Q only when combined with an HA-tagged allele of Htz1. It has been shown that quadruple mutations of Htz1 displayed genetic interactions with H4 K5, 8, 12 R (Babiarz *et al*., 2006). These findings indicated that Htz1 and H4 acetylation share an essential role in cell viability because cells can only be viable when one of these tails can be acetylated, suggesting the degree of redundancy between acetylatable lysines sites of the variant Htz1 and histone H4.

Analysis of mutations of individual lysine site of Htz1 in an N-terminal HA tagging allele revealed the functional redundancy of these sites since any single lysine site on Htz1 N-tail is sufficient to mediate the function with mutations of H4 lysine 16. Genetic evidence also demonstrated that these lysine sites (K8, K10 and K14) are functionally redundant as they share similar genetic patterns and are co-regulated by the same enzymes, namely Hda1 deacetylase and KAT5 acetyltransferase (Mehta *et al*., 2010). To our surprise, in this study, I identified the consequence of the N-terminal epitope tagging on Htz1. In particular, the genetic interactions of Htz1 mutants and H4K16Q was seen when Htz1 allele underwent HA epitope tagging. It has been reported that the N-terminal GFP epitope tagging of *D. melanogaster* H2A.Z disrupts acetylation and impairs heat-shock gene responsiveness (Tanabe *et al*., 2008). Moreover, N-terminal HA tagging leads to Htz1 being poorly acetylated in *S. cerevisiae* (Mehta *el al*., 2010). My research provides an alternate explanation that, in fact, tagging Htz1 at the N-terminus caused a marked decrease in Htz1 protein abundance. However, this finding cannot exclude the possibility that N-terminal HA tagging can interfere with modifying enzymes and thus affecting the acetylation directly. In addition, HA-tagging may signal an elevated histone degradation pathway on Htz1. The mechanistic detail of epitope tagging which negatively impact Htz1 protein abundance has yet to be established. If the phenotypic defects caused by the insufficient Htz1 supply in the chromatin, ones would predict that overexpression of HA-tagged Htz1 could rescue the phenotypes.

Moreover, phenotypic data revealed that the levels of Htz1 protein are crucial when cells are exposed to particular stresses. In the literature, it is formally accepted that many *htz1*Δ mutant phenotypes are likely due to SWR-C because deleting *SWR1* in *htz1*Δ mutants *(htz1*Δ *swr1*Δ) can suppress the phenotype seen in *htz1Δ* strain (Halley *et al*., 2010; Morillo-Huesca *et al*., 2010). Based on the data from this study, I propose that the dosage of Htz1 itself may contribute to these phenotypes at least to a certain extent. Despite the availability of Htz1 protein from *HA-HTZ1* and *HTZ1*^{cp100}, mutant cells still exhibited similar phenotypes to *htz1*Δ strain. Therefore, it is plausible that there is a synergistic

effect of fine-tuning between Htz1 level and SWR-C. Since Htz1 can be incorporated and evicted by SWR-C (Mizuguchi *et al*., 2003; Watanabe *et al*., 2013), it will also be of interest to decipher the relationship between SWR-C and Htz1 levels in greater detail.

While the sites of acetylation on Htz1 seemed to be functionally redundant, they all together play an integral role in Htz1 regulation. In this work, I examined the impact of acetylation on the resistance of cells to a variety of agents and found cells expressing the 4KR allele displayed caffeine sensitivity and atypically rapid growth on MMS. The enhanced caffeine-sensitive phenotype was observed when Htz1 protein level was compromised, indicating the interplay between these two pathways. The mechanistic details on how N-terminal acetylation regulates the Htz1 function are awaiting further investigations.

Additionally, I also showed that the chromatin abundance of Htz1 was reduced when all acetylation sites were abolished by lysine-to-arginine mutations. However, mutations of lysine-to-glutamine in Htz1 moderately affect the amount of Htz1 in the chromatin. Decrease in chromatin abundance was not derived from altered transcription as mRNA levels in *htz1*-4KR and *htz1*-4KQ strains appeared to be comparable mRNA to WT. Also, it is notable that the lower abundance of Htz1 alone cannot shed the light on caffeine sensitivity observed in *htz1*-4KR mutant cells because the level of Htz1 in 4KR, relative to WT, was more than Htz1 protein levels observed in $HTZ1^{cp200}$. Therefore, it is likely that the impact of Htz1 acetylation sites is required for caffeine resistance but the reason why this is the case has not yet been established.

My phenotypic analyses revealed that acetylation of Htz1 is required to regulate Htz1 dynamics in a certain cell signalling pathway and that it is crucial to have such functional Htz1 in this pathway when cells are exposed to caffeine. Like other mutations on other histone tails, it is possible that the mutations of all lysines on Htz1 tails may impact the transcription of multiple genes and that in turn contribute to the defective growth upon caffeine exposure. Furthermore, previous analyses have identified that the variant Htz1 act to prevent the spread of heterochromatin (Meneghini *et al*., 2003) and acetylation of Htz1 is required to establish this boundary (Babiarz *et al*., 2006). Since defects in boundary protection in unacetylatable mutants were not as severe as that of *htz1*Δ, I reasoned that perhaps my results presented here supported an interesting possibility that the lower abundance of Htz1 caused by mutations at all N-terminal lysines may cause this defect.

In summary, the N-terminal acetylation can directly regulate Htz1 function. This data argue that the four acetylatable lysine residues mediate the property of Htz1 that involves its abundance in the chromatin.

CHAPTER 5: Global analysis of H2A.Z lysine acetylation sites and their interplay with chromatin remodelling complexes

5.1 Introduction

Biochemical, genetic and phenotypic assays strongly suggest that the N-terminal acetylation sites of Htz1 are critical for the functional Htz1 molecules. Since my biochemical evidence showed that the chromatin-associated Htz1 level was significantly reduced when the N-terminal acetylatable lysine sites were substituted by arginine but not glutamine, the question was raised on how these lysine-to-arginine mutations affected the global localisation of Htz1. Does this reflect the specific loss in particular genomic loci? Or does the mutations affect the global reduction of Htz1 but not restricted to any chromosomal domains? For instance, the overall reduction of Htz1 level may be derived from the altered distribution patterns at promoter nucleosomes where Htz1 is preferentially bound or it could affect Htz1 binding in a non-uniform manner across the genome.

Because the phenotype observed in the mutant is related to chromatin abundance, it is also hypothesised that the cooperation between acetylation sites and the dedicated Htz1 deposition machinery, SWR-C (Mizuguchi *et al*., 2004; Krogan *et al*., 2004; Kobor *et al*., 2003) may exist. In addition, the eviction pathway of Htz1 by INO80-C (Papamichos-chronakis *et al*., 2011) may be co-regulated by these acetylation sites on Htz1. It is important to determine how all of these factors communicate with the N-terminal acetylatable lysine sites on Htz1. Based on these observations, it is possible that the unacetylatable Htz1 molecules may be further removed or inefficiently reassembled after they have been evicted, thus affecting the dynamics balance of Htz1 assembly-reassembly kinetics. This connection is also in agreement with previous reports that suggested that acetylation was required for Htz1 occupancy at *PHO5* promoters (Millar *et al*., 2006), However, it is still unclear how this regulation plays out mechanistically on a global scale. So far the assays used to investigate the contribution of N-terminal acetylation sites have been performed at a locus-specific level. It was not known how these acetylation sites contribute to the genome-wide localisation of Htz1. Mechanistically speaking, how acetylation sites coordinate with the incorporation and eviction of Htz1 in a concerted or independent fashion has not been established.

Having confirmed that both *htz1*-4KR and *htz1*-4KQ mutants are chromatin-bound, I set out to investigate the *in vivo* genome-wide relationship between Htz1 chromatin association and its N-terminal lysine acetylation. To explore the genome distribution of

Htz1, I performed Chromatin Immunoprecipitation in combination with high-throughput sequencing (ChIP-Seq) to map the position of Htz1 and its N-terminal mutants across the yeast genome under the steady-state growth conditions. Two N-terminal mutant Htz1 strains were used along with a wild type control including: all four N-terminal lysine residues of Htz1 were mutated to arginine (*htz1*-4KR), which mimics constitutively unacetylated state while retaining the similar charge of lysine or glutamine (*htz1*-4KQ), which mimics constitutively acetylated state.

In this chapter, the high correlated distribution profiles between N-terminal acetylation mutants and WT suggest that the location of Htz1 is not dependent on N-terminal lysine acetylation sites. Additionally, this study uncovers the interplay between acetylation sites of Htz1 and the SWR-C and INO80-C chromatin remodelling enzymes and proposes an alternative pathway in relation to Htz1 chromatin abundance.

5.2 Global H2A.Z localisation patterns in unacetylatable mutants are highly similar to the wild type profiles.

To identify the effect of mutations at acetylatable lysines on the localisation pattern of Htz1, I took the advantage of using genome-wide studies to search for distinct Htz1 localisation patterns that can be modified or unmodified by acetylation. Briefly, wild type, *htz1*-4KR and *htz1*-4KQ were harvested from log-phase growing YPD cultures, fixed with formaldehyde. Cross-linked cells were lysed and the chromatin was sheared by sonication. Chromatin Immunoprecipitation was conducted with anti-Htz1 antibody recognising the C-terminal regions of Htz1 (Millar *et al*., 2006). Input and immunoprecipitated DNA from each strain was submitted to sequencing using Illumina® platform. ChIP data were subtracted with input DNA and normalised read counts (performed by Muxin Gu).

In this study, two biological replicates were performed and high reproducibility between experiments was confirmed (Appendix A). The sequencing depth of the second experiment was lower than the first experiment but the average intensity was higher than the first one (data not shown). Although the ChIP-seq analysis of Htz1 has been demonstrated in budding yeast before (Albert *et al*., 2007), the data presented in previous studies did not include the contribution of Htz1 acetylation sites in determining the localisation pattern of Htz1. Consistent with published results; Htz1 binds to all 16 yeast chromosomes. The overall pattern of Htz1 in *htz1*-4KR and *htz1*-4KQ was not altered by these mutations. Figure 5.1A shows an example of Htz1 binding profiles in WT (top panel), *htz1*-4KR (middle panel) and *htz1*-4KQ (bottom panel) across chromosome 5. Htz1

is preferentially localised at the promoter regions downstream of Transcription Start Site (TSSs) (Figure 5.1A gray background). However, the global view of these localisation profiles did not reveal any distinct Htz1 binding patterns between WT, *htz1*-4KR and *htz1*-4KQ.

Further examination of ChIP enrichment patterns was carried out quantitatively by plotting normalised Htz1 ChIP intensity between each strain against the WT dataset. The genome was divided into 150-bp windows and ChIP signals in each window were calculated. Pair-wise correlation between datasets showed that the global enrichment profiles of Htz1 in *htz1*-4KR and *htz1*-4KQ cells were highly similar to that of WT (Figure 5.1B) Pearson correlation coefficient of each pair-wise comparison are 0.96 (WT versus *htz1*-4KR), 0.95 (WT versus *htz1*-4KQ) and 0.93 (*htz1*-4KR versus *htz1*-4KQ), suggesting the global localisation profiles of Htz1 were almost indistinguishable.

Despite the high similarity of Htz1 localisation between WT and unacetylatable mutants, the question was raised whether the localisation differences are located to particular regions of the genome. It is possible that small differences between each profile might not be seen. To this end, I attempted to dissect the profiles of Htz1-occupied regions by regions across the genome. Initially the Htz1 distribution around the TSS was examined to search for any possible altered abundance in the most Htz1-enriched feature. To characterise the profiles of *htz1*-4KR and *htz1*-4KQ surrounding the TSS more closely, I analysed their patterns by comparing the average signal intensity of Htz1 among these strains in the 200bp bins around TSS of 5,143 yeast genes using Seqminer software (Ye *et al*., 2010). As expected, the patterns of Htz1 distribution in *htz1*-4KR and *htz1*-4KQ mutants are almost identical to that of WT around the TSS (Figure 5.2 A).

In addition, the distribution of Htz1 in WT and unacetylatable mutants were assessed in various genomic features. The resulting profiles were almost identical to WT (Figure 5.2 B), suggesting the N-terminal acetylatable lysine residues are not important for Htz1 genome distribution. However, the global distribution of Htz1 was not consistent with biochemical observations that indicated the altered chromatin abundance in the *htz1*-4KR strain. Therefore, I turned to look for other possibilities to explain how the acetylation lysine sites contribute to Htz1 global distribution.

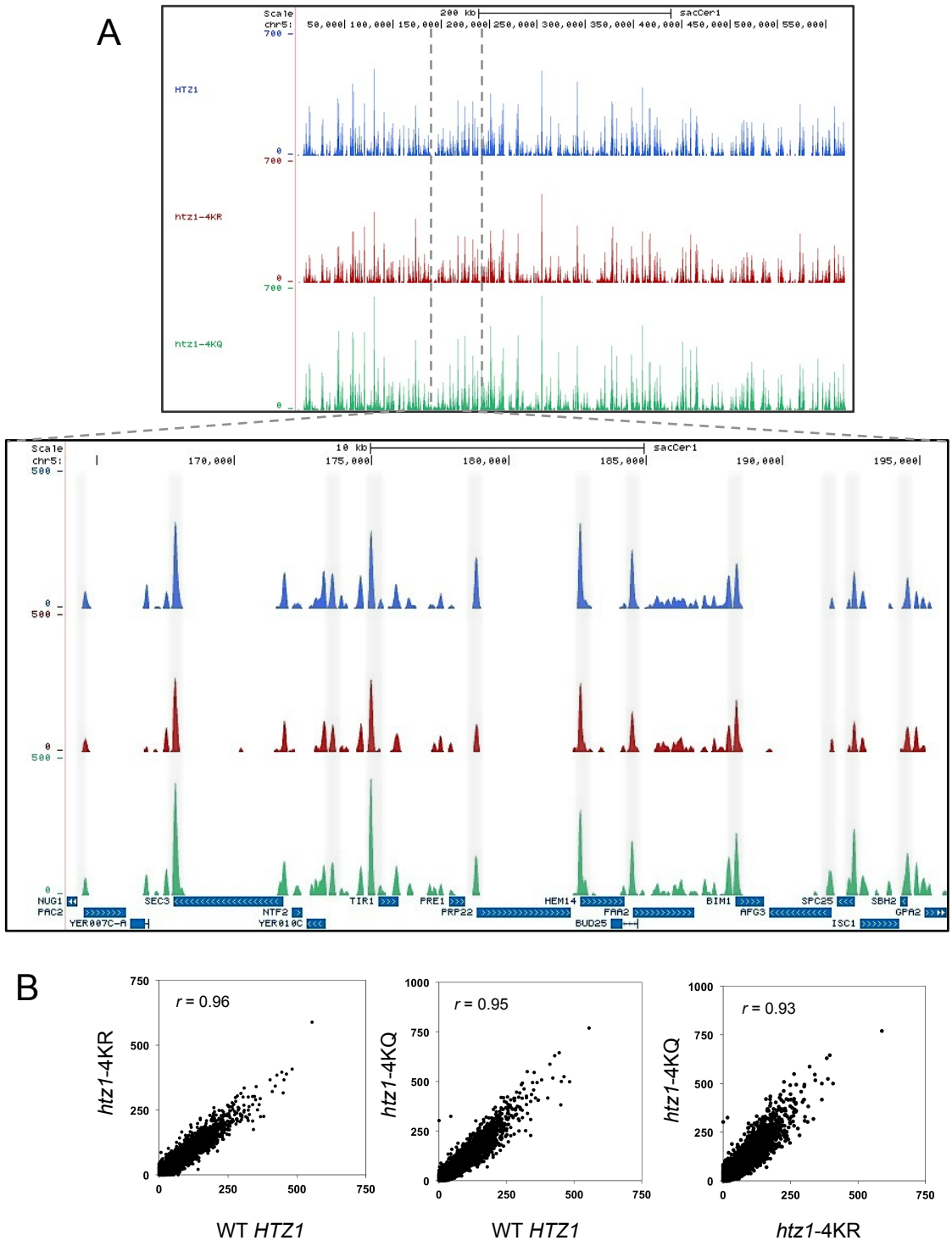

Figure 5.1 Localisation patterns of Htz1 in *htz1*-4KR and *htz1*-4KQ are highly similar to WT across the yeast genome

(A) Snapshot views of ChIP-Seq tracks from UCSC genome browser illustrate similar localisation profiles of WT Htz1 (blue), *htz1*-4KR (red) and *htz1*-4KQ (green) on the entire chromosome 5 (Top panel)

Htz1 is preferentially occupied at 5' end of genes surrounding the TSS. A close-up representation of ChIP-Seq tracks on chromosome 5 between coordinates: 165,000-195,000 indicates the predominant Htz1 localisation at TSS (gray background). Blue blocks indicate SGD genes and the white arrows within each block indicate its orientation (Bottom panel)

(B) Scatter plot comparing each ChIP-Seq signals between each strain using a window of 150 bp across the whole yeast genome. The global patterns of Htz1, *htz1*-4KR and *htz1*-4KQ are highly correlated. *r* = Pearson correlation coefficient

A

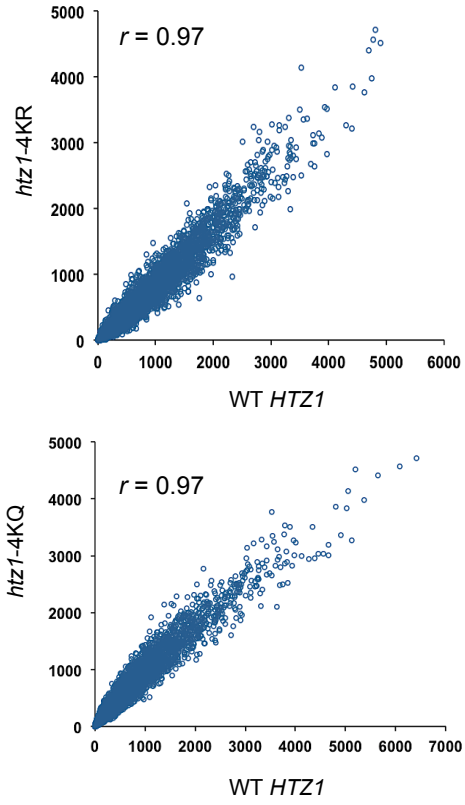

B

	WT	*htz1*-4KR	*htz1*-4KQ
Promoter	67.4%	68.1%	66.9%
Intergenic	8.6%	7.9%	7.5%
CDS	12.4%	12.5%	14.2%
3'end	11.6%	11.5%	11.5%

Figure 5.2 Distribution profiles of Htz1 are not affected by mutations at N-terminal lysines
(A) Quantitative comparison of signal intensities of ChIP-Seq signals between WT Htz1, *htz1*-4KR and *htz1*-4KQ surrounding the TSSs within the 200-bp bins around the peaks. Tag densities from ChIP-Seq dataset 1 were plotted using seqMiner (Ye *et al*., 2010) (TSSs = 5' end of annotated genes derived from Xu *et al*., 2009).
(B) A table representing the of Htz1 distribution across different genomic features in WT, *htz1*-4KR and *htz1*-4KQ (data in B were quantified by Muxin Gu)

5.3 Altered H2A.Z enrichments by lysine-to-arginine mutations are not associated with particular genomic loci

As the genome organisation of Htz1 in the unacetylatable lysine mutants were not affected by these mutations, this raised the question how the reduced total amount of Htz1 was observed. Genome-wide data provide not only the localisation pattern but the enrichment level of Htz1 as well. Instead of monitoring at the distribution, I turned to examine the intensity of ChIP signals between each strain. After the whole genome was divided into 150-bp and low signals were removed, the normalised ChIP-signal datasets were plotted against each other (Figure 5.3A). The overall intensity profiles showed that Htz1 ChIP signals in *htz1*-4KR were slightly lower than WT while normalised *htz1*-4KQ signal was almost equivalent to WT. Therefore; these data support the idea of global Htz1 loss in the *htz1*-4KR strain. Further investigations have shown distinctive enrichments of Htz1 at different regions such as Transcription Start Site (TSS) and Transcription Termination Site (TTS). The different enrichments of Htz1 were observed in promoter regions surrounding the TSSs (Figure 5.3B) and 3' downstream of TTSs (Figure 5.3C) in the *htz1*-4KR strain. Further comparison of average ChIP-signals revealed that other moderate Htz1-occupied regions such as intergenic and coding sequences were also affected (Figure 5.4A). This finding suggested that the reduction of Htz1 level in *htz1*-4KR strains was not restricted to any particular genomic loci but rather widespread. In agreement with this, the inverse relationship was observed between the degree of Htz1 enrichments and the differential enrichments of WT and *htz1*-4KR (Figure 5.4B), supporting the altered abundance of Htz1 was not preferentially associated with high Htz1-enriched regions. Taken together, these data confirmed the partial loss of Htz1 in *htz1*-4KR was widespread across the genome, suggesting that N-terminal acetylation sites regulate Htz1 amount in non-targeted fashion.

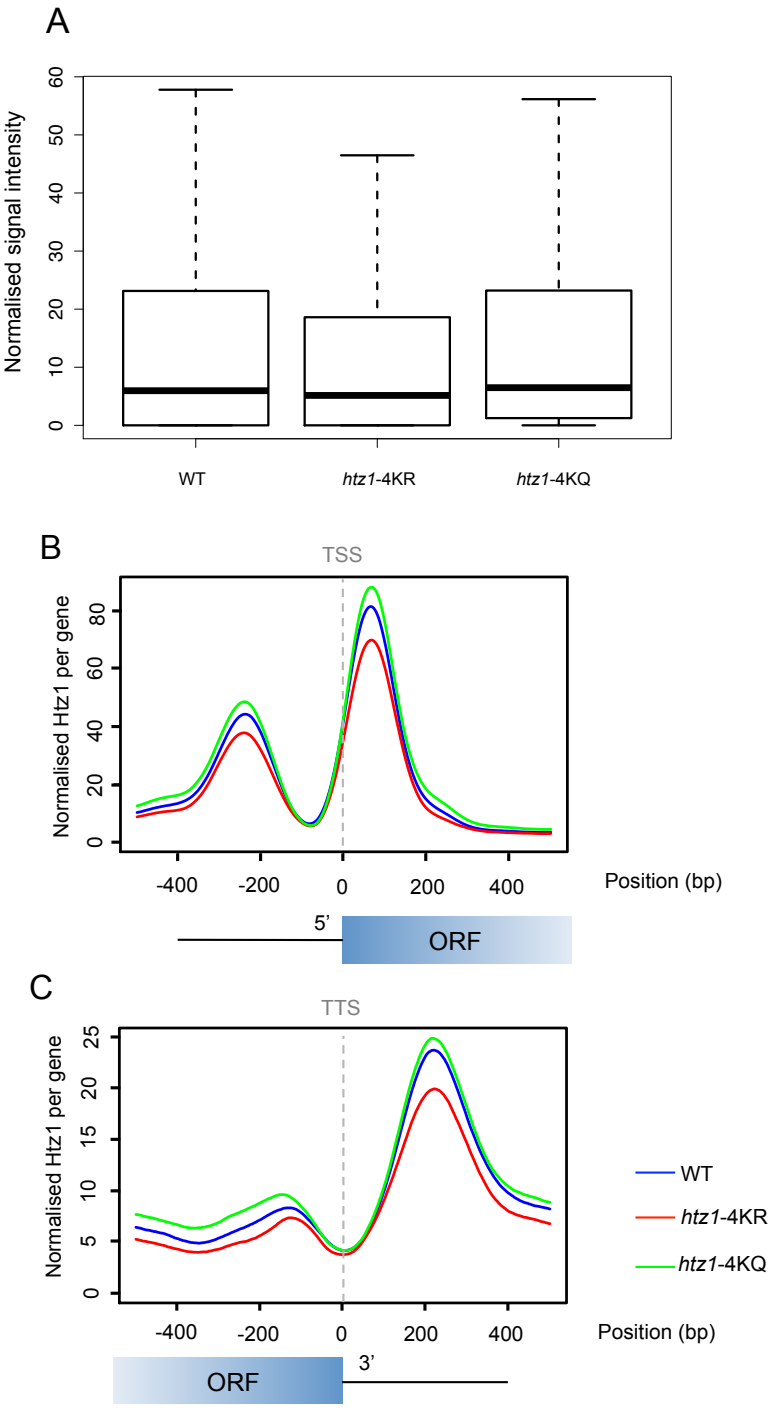

Figure 5.3 *In vivo* altered enrichments of Htz1 are not restricted to particular genome regions

Overall intensity of Htz1 in WT, *htz1*-4KR and *htz1*-4KQ strains is plotted against each other and relative to the TSS and TTS of genes across the genome.

(A) The altered Htz1 enrichment was detected in the *htz1*-4KR strain. Normalised ChIP-signals from 150bp bins are shown.

(B) Overall patterns of Htz1 enrichments surrounding the TSSs. All genes were aligned according to their TSSs and the average levels of Htz1 are illustrated for each base pair in every 200-bp moving bin

(C) Analogous patterns of Htz1 enrichment around TTSs were plotted as (A)

The alignments were performed by Muxin Gu

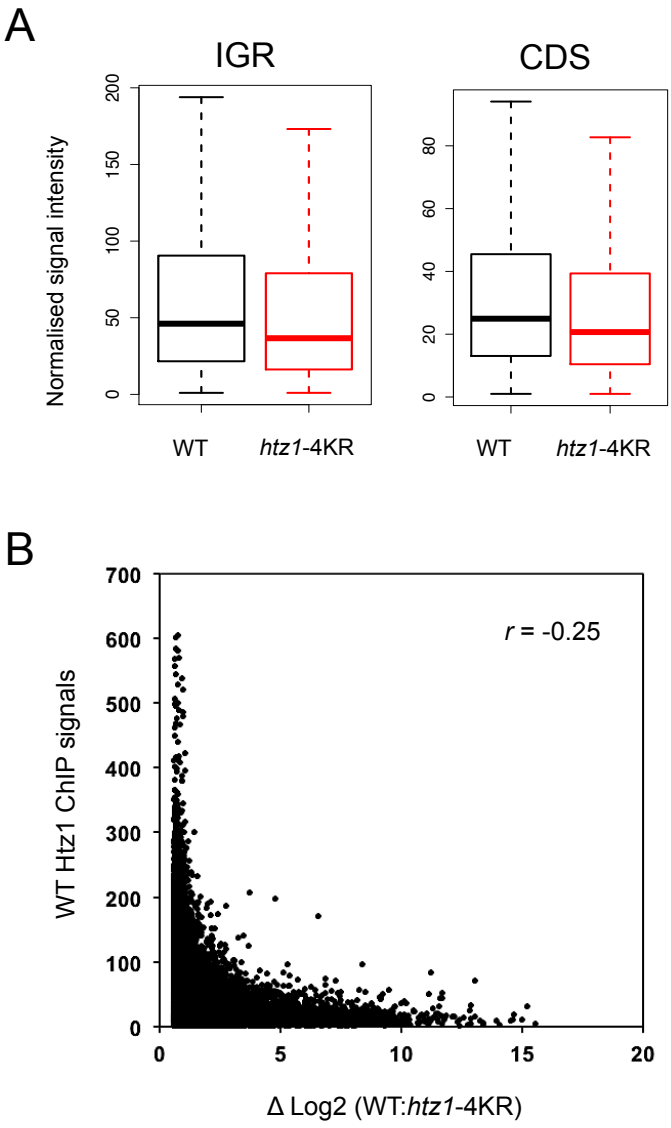

Figure 5.4 Altered Htz1 binding profiles were detected in other genomic regions and these patterns are inversely proportional to the Htz1 occupancy
(A) ChIP signals of Htz1 in the *htz1*-4KR strain is reduced in both intergenic regions (IGR) and coding sequences (CDS). Box plot of signal intensities in 20-bp windows are shown for WT (black) and *htz1*-4KR (red)
(B) Scatter plot of log 2 fold change of WT: *htz1*-4KR ChIP signals (only shown those that are greater than 1.5-fold) versus wild type HTZ1 binding levels. ChIP-Seq dataset of the indicated yeast strains using a window of 20-bp across the whole yeast genome.
r = Pearson correlation coefficient

To validate my ChIP-Seq data, a range of genomic loci were investigated and primer specific for these regions were designed. These primers were selected based on the differential enrichments of Htz1 between wild type and *htz1*-4KR strains, including various genomic features such as those that located at -2, -1 and +1 nucleosomes within the promoter regions, coding sequences and 3' end of genes from different yeast chromosomes. Additionally, two other loci, whose Htz1 occupancy was comparable between WT and *htz1*-4KR strain, were also chosen. Two independent ChIP from two biological replicates of WCEs were performed with anti-Htz1 (α660) antibody. Immunoprecipitated DNA was subjected to qPCR analysis. The qPCR results from 9 random genome locations demonstrated that the amount of Htz1 in *htz1*-4KR strain was lower than WT at several loci but still retained in others (Figure 5.5), indicating a precise consistency with ChIP-Seq results. These findings confirmed that data were biologically reproducible and consistent with the partial yet widespread loss of chromatin-bound Htz1 in *htz1*-4KR.

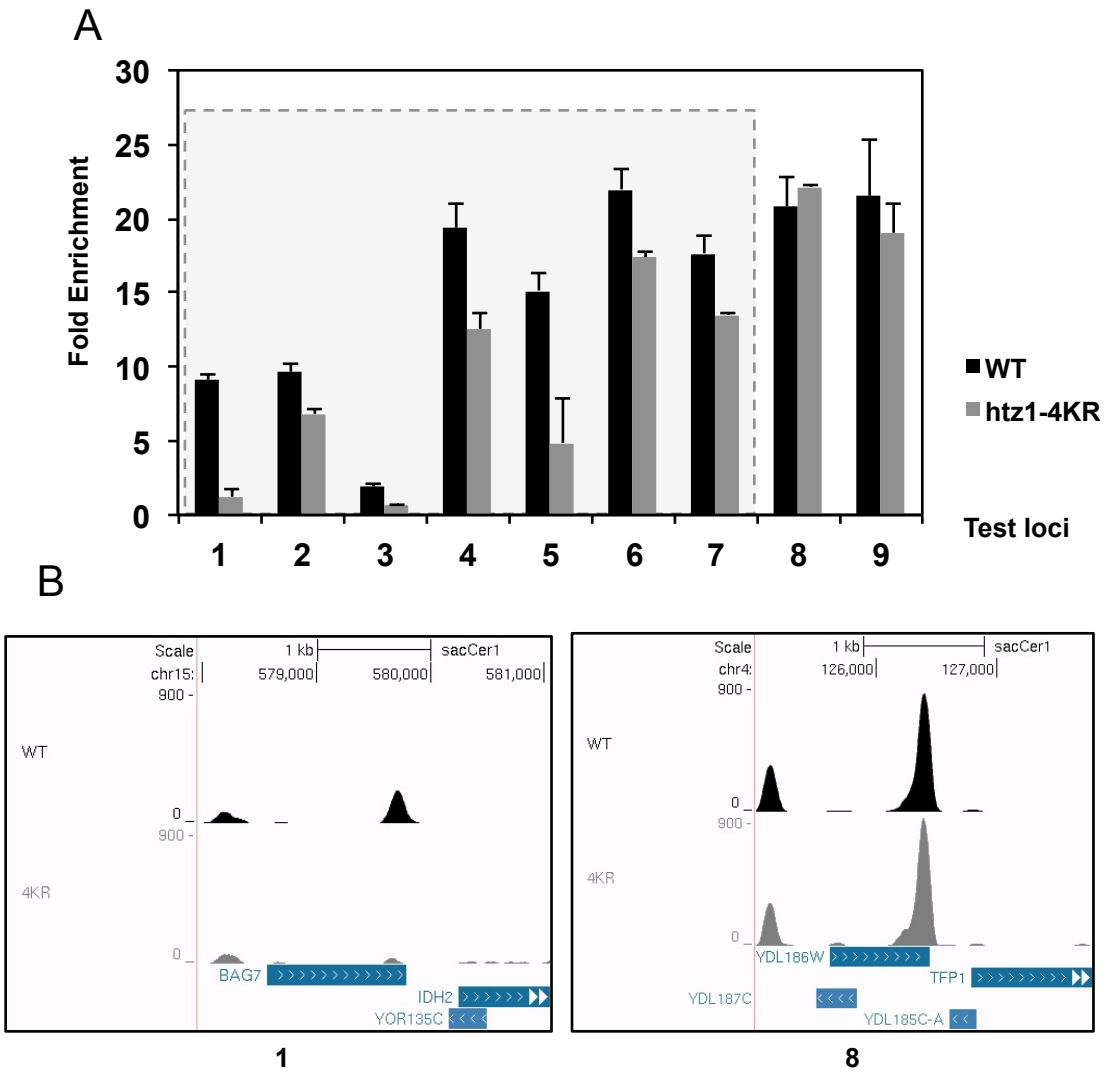

Figure 5.5 Differential Htz1 enrichment patterns in WT and *htz1-4KR* are biologically reproducible

(A) Immonoprecipitated DNA was analysed by qPCR on selected regions. Primer sets (1-9) were chosen to represent various chromosomal locations and enrichment levels of WT and *htz1*-4KR in ChIP-Seq experiments. Primers set 1-7 indicate differential Htz1 enrichments (in a gray box) and Primers set 8-9 indicate similar Htz1 enrichments. Error bars denote standard errors of two independent qPCR experiments (*n*=2) performed in triplicates.

(B) Examples of snapshot view from UCSC genome browser of WT and *htz1*-4KR represent genomic regions associated with primer sets 1 and 8. Numbers above each track indicate chromosome coordinates. The blue bar indicates SGD genes.

Each primer pair is listed as follows: **1** = chrXV: 579652-579754 (3'End), **2** = chrIV: 148204-148309 (Promoter +1 Nuc), **3** = chrX: 152102-152206 (CDS), **4** = chrXV: 611966-612078 (Promoter +1 Nuc), **5** = chrXIV: 258421-258534 (3'End), **6** = chrX: 60066-60168 (Promoter -2 Nuc), **7** = chrXVI: 360149-360298 (Promoter +1 Nuc), **8** = chrIV: 126348-126450 (3'End), **9** = chrVIII: 360542-360643 (Promoter, -1 Nuc).

5.4 Lysine acetylation sites on H2A.Z independently regulate its chromatin abundance from SWR-C and INO80-C remodelling complexes

The genome-wide distribution, biochemical and genetic evidence of Htz1 and its N-terminal acetylation site mutants point to a general pathway that affects Htz1 levels in chromatin. These data suggested the interplay between lysine acetylation sites for regulating its abundance and function. However, it is still unclear how these four acetylatable sites are involved in these roles in mechanistic details.

In budding yeast, Htz1 deposition is known to be highly dependent on the SWR-C complex. The SWR-C catalyses the exchange of H2A-H2B dimers with Htz1-H2B via the catalytic subunit Swr1 (Mizuguchi *et al*., 2004; Krogan *et al*., 2004; Kobor *et al*., 2003). Swc2 is the subunit that interacts directly with Htz1 while Swc5 is required for the efficient association of the complex with Htz1-H2B dimers (Wu *et al*., 2005). Molecular evidence indicated that Swr1, Swc2, and Swc5 are important for the incorporation of Htz1 in chromatin (Mizuguchi *et al*., 2004; Krogan *et al*., 2004; Morillo-Huesca *et al*., 2010).

Based on these observations, it is hypothesised that the effect of decreased Htz1 levels in *htz1*-4KR strain may be involved in this specific incorporation pathway. In addition, recent evidence reported that INO80-C catalyses the removal of Htz1 (Papamichos-Chronakis *et al*., 2011). Therefore, the reduced Htz1 abundance via it N-terminal acetylation sites could also be regulated by the specific eviction pathway e.g. the reduced Htz1 chromatin levels being the result of over-eviction.

To gain better insights into the functional connection of mechanisms involved in Htz1 abundance in the chromatin, I turned to the known pathways for Htz1 incorporation and eviction by specific activities of SWR-C and INO80-C chromatin remodelling enzymes. So far, it is not known whether the SWR-C or INO80-C can distinguish between acetylated and unacetylated Htz1 molecules and selectively deposit or remove one or the other from chromatin. It is possible that the N-terminal acetylation sites may facilitate Htz1 incorporation or eviction pathway by interacting with SWR-C or INO80-C complex leading to a steady-state Htz1 level in the chromatin. To this end, I set out to investigate whether the deposition of Htz1 by SWR-C or the eviction by INO80-C was affected by the N-terminal lysine-to-arginine mutations.

It is hypothesised that if SWR-C and lysine acetylation sites of Htz1 functioned in a common pathway for Htz1 chromatin abundance, one could argue that inactivation of SWR-C catalytic activity or other key subunits in conjunction with mutating acetylatable lysine sites would result in no further loss of chromatin-associated Htz1. In contrast, if the

eviction pathway by INO80-C was influenced by lysine-to-arginine mutations leading to the eviction defects, inactivation of INO80-C should rescue the chromatin loss in the *htz1*-4KR strain. To test these hypotheses, yeast strains carrying mutations that either lack of individual subunits of SWR-C (*swr1*Δ, *swc2*Δ or *swc5*Δ) or the INO80-C (*arp8*Δ) were combined with *htz1*-4KR or *htz1*-4KQ mutations to investigate the impact of Htz1 acetylation sites in these combination mutants. Isogenic wild type strain with *swr1*Δ, *swc2*Δ or *swc5*Δ and *arp8*Δ were also generated as a control. In order to determine relative Htz1 abundance, chromatin fractionation assays were conducted to evaluate the chromatin-bound Htz1 levels in these combination mutant strains relative to wild type strains. The levels of Htz1 were assayed by immunoblotting using anti-Htz1 antibody. The results demonstrated successful fractionation procedures showing each compartment across these strains (Appendix B).

In particular, the effects of acetylation sites in these combination mutants were analysed at chromatin levels. As expected, the absence of Htz1 acetylation sites and components of SWR-C including Swr1, Swc2 and Swc5 caused a pronounced decrease of chromatin-associated Htz1 fractions (Figure 5.6A; compare lane 1 with lane 4, 7 and 10). However, deleting these genes does not totally abolish Htz1 in the chromatin, suggesting that a pathway of Swr1-independent incorporation of Htz1 may exist. Substitution of Htz1 N-terminal lysine to glutamine in combination with deleting SWR-C components resulted in a comparable Htz1 amount to that of WT (Figure 5.6A; compare lane 3 with lane 6, 9 and 12). These results indicate that SWR-C is directly responsible for chromatin-bound Htz1 irrespective of its acetylation state. Interestingly, inactivating SWR-C in the *htz1*-4KR background exacerbated Htz1 loss in the chromatin (Figure 5.6A; compare lane 2 with lane 5, 8 and 11). These results suggest lysine acetylation sites and SWR-C share overlapping function for the steady-state levels of chromatin-bound Htz1.

In contrast, deletion of Arp8, a subunit important for chromatin remodelling activities of INO80-C (Papamichos-Chronakis *et al*., 2011), caused almost no change in chromatin-associated Htz1 level (Figure 5.6B; compare lane 1 to lane 4). No difference in Htz1 abundance was observed between combination mutants of *arp8* Δ carrying either *htz1*-4KR or *htz1*-4Q (Figure 5.6B). These findings indicate that Arp8 is not required for the reduced Htz1 levels in *htz1*-4KR strain.

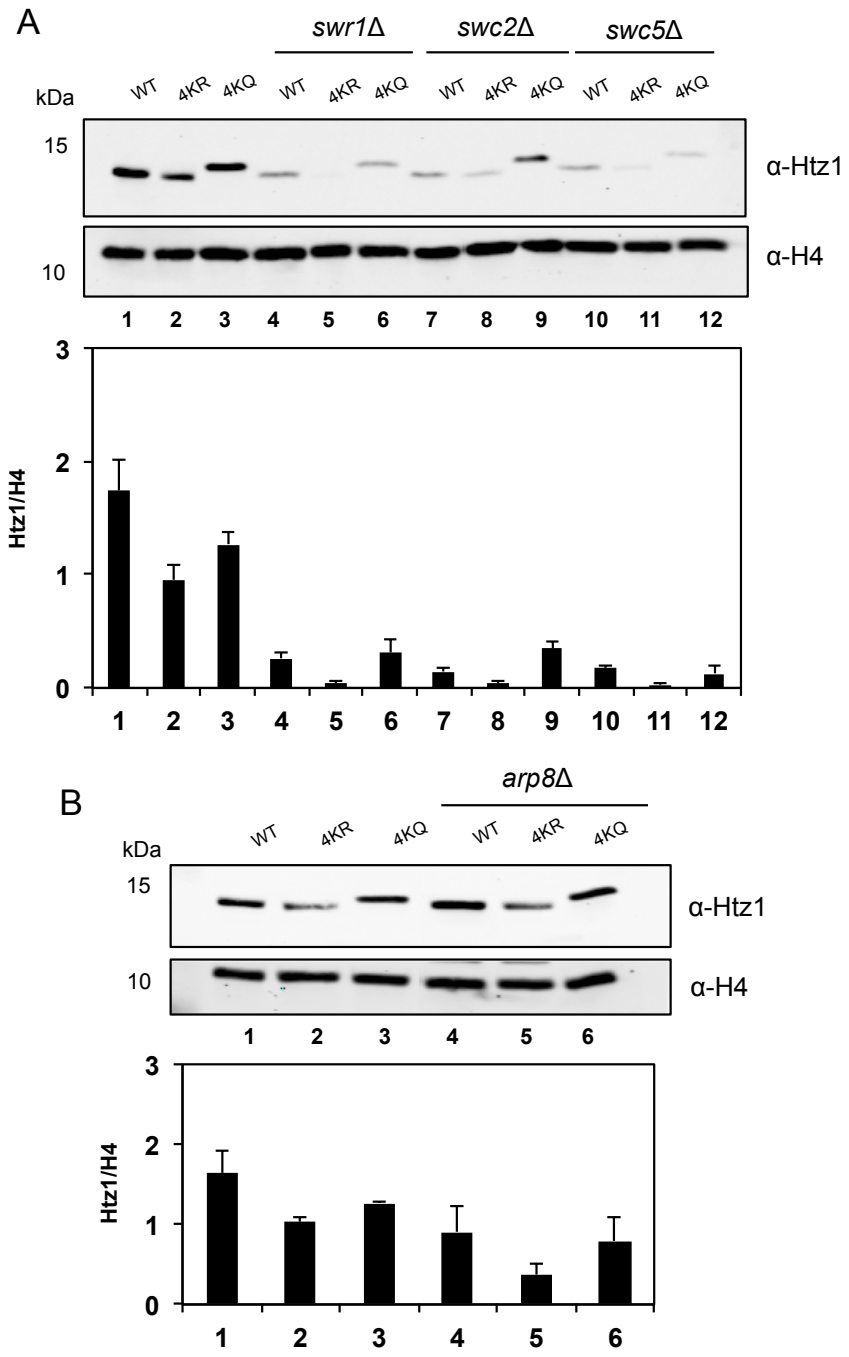

Figure 5.6 The amount of chromatin-bound Htz1 is markedly decreased when combined *htz1*-4KR with SWR-C mutants but remains relatively similar when *htz1*-4KR combined with an INO80-C mutant.
Cell fractionation experiments were carried out in yeast strains with the indicated genotypes. Chromatin fractions from these strains were analysed side-by-side by western blotting with anti-Htz1 antibody (upper panel). Anti-H4 antibody (lower panel) was used as sub-cellular compartments and equal gel loading control. Representative data from two independent experiments are shown (*n* = 2). Quantification of enrichment values (Htz1/H4) is shown in bar graphs underneath. Error bars indicate standard deviation of two experiments.

To integrate these findings, a model regarding the contribution of acetylation sites towards Htz1 abundance is proposed. In the absence of SWR-C activity (*swr1*Δ, *swc2*Δ or *swc5*Δ), Htz1 sub-populations are still incorporated into chromatin (Figure 5.6; lane 4, 7 and 10), supporting the notion of the existence of SWR-C independent Htz1 deposition. Notably, the majority of Htz1 populations that aren't incorporated are known as SWR-C dependent. In an analogous situation, in reduction of chromatin-associated Htz1 level was observed in *htz1*-4KR mutants (Figure 5.6; lane 2). Therefore, these Htz1 species are incorporated in an acetylation-independent manner (most likely SWR-C dependent). Inhibition of these two compensatory pathways that converge on the same function for Htz1 chromatin abundance leads to dramatically decreased Htz1 abundance (Figure 5.6; lane 5, 8, 11). These findings indicate that the acetylation sites and SWR-C can function independently but share overlapping function for the level of chromatin-bound Htz1. An alternative pathway that favours acetylated Htz1 species may exist and this pathway contribute to maintain a steady state Htz1 in the chromatin (Figure 5.7).

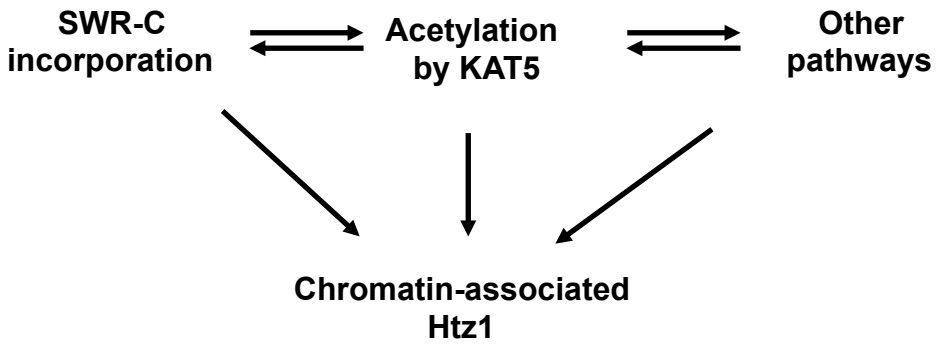

Figure 5.7 A schematic model of pathways involved in the regulation of Htz1 chromatin abundance
The diagram illustrates the functional link between Htz1 acetylation and SWR-C. Double arrows suggest the coordination between these factors. An alternative pathway that co-regulates the homeostatic level of Htz1 in chromatin may exist.

5.5 Discussion

Through comprehensive analysis of Htz1 via genome-wide and biochemical studies, these findings revealed that the overall distribution of Htz1 was not dependent on its N-terminal acetylation sites because the localisation pattern was unaffected by when these sites are mutated from lysine to arginine or to glutamine. The high correlation of Htz1 localisation profiles of *htz1*-4KR and *htz1*-4KQ strains with wild type strain indicates that these four acetylation sites together are not determinants for Htz1 distribution patterns. Despite their high similar profiles, the altered degree of enrichments between Htz1 and *htz1*-4KR could still be detected by ChIP-Seq experiment even after data normalisation. The biological reproducibility of these data confirmed that the altered Htz1 levels in *htz1*-4KR were not due to data normalisation in genome-wide studies. These data revealed the variable effects of lysine-to-arginine mutations such that *htz1*-4KR was lost the in some genomic regions while it was still retained other loci. If one function of acetylation sites is to control the kinetics of association and disassociation then unacetylatable Htz1 molecules are thought to be defective in chromatin abundance across the whole genome. Therefore, Htz1 deposition is likely to be independent from N-terminal lysines. Since defects in chromatin abundance were not observed in *htz1*-4KQ mutants, it is possible that the dynamic alteration of Htz1 molecule by charge modulation may underlie the ability of Htz1 to serve as a platform for a protein-binding site. It is worth noting that the global Htz1 distribution observed in this study was not comparing the different kinetics between acetylatable and unacetylatble state of htz1 but their occupancy. Thus, it will be interesting to performed competition ChIP (Lickwer *et al*., 2012) between acetylated and unacetylated Htz1.

SWR-C and Htz1 acetylation sites are both intimately associated with Htz1 protein levels in the chromatin. Using mutational analyses, I showed that combination mutants of SWR-C components and *htz1*-4KR drastically disrupted chromatin-bound Htz1. One possible explanation is that the deposition and the acetylation of Htz1 works in parallel pathways to cycle functionally acetylated Htz1 into chromatin. NuA4 (KAT5) shares components with SWR-C (Kobor *et al*., 2004) and these two complexes reflect a physical merge of human TIP60 complex (Auger *et al*., 2008), highlighting the functional and physical connection between two pathways. This study lends a further support to an alternative pathway for Htz1 deposition. It is possible that this pathway preferentially incorporates acetylated Htz1 species into chromatin. However, further works will be required to resolve the mechanistic details on how Htz1 acetylation regulates this pathway.

In summary, these data suggest that N-terminal acetylation sites of Htz1 are not a key determinant for the Htz1 localisation patterns. However, these acetylation sites function in a combinatorial manner to regulate Htz1 level in the chromatin.

CHAPTER 6: GENERAL DISCUSSION

6.1 Summary

The evolutionarily conserved histone variant H2A.Z has been implicated in multiple cellular processes including transcriptional regulation, DNA replication and repair, chromosome segregation, heterochromatin conformation and protection of heterochromatin spreading. H2A.Z is an indispensable component of the genome in most organisms as its absence is lethal but not in budding and fission yeast. So far, the reason why H2A.Z possesses multiple specialised roles remain unknown. It is likely that the spatial and temporal arrangements of H2A.Z in the genomes may influence its central function. The PTMs on the H2A.Z have been characterised within the N- and C- terminal tails including acetylation, ubiquitination and sumolyation. Therefore, these modifications may vary H2A.Z function to facilitate additional regulatory roles.

Mechanisms for regulating H2A.Z localisation profiles are conserved and have been extensively investigated across organisms from yeast to man. A dedicated chromatin remodelling complex, the SWR-C (SRCAP/p400) complex, has evolved to deposit H2A.Z into chromatin (Mizuguchi *et al*., 2004; Kobor *et al*., 2004; Krogran *et al*., 2004; Cai *et al*., 2005; Ruhl *et al*., 2006; Wong *et al*., 2007). Importantly, the unique genomic location of H2A.Z is highly conserved. It has become evident that H2A.Z is preferentially enriched at 5' in the promoter regions of genes near the TSS. (Guilletmette *et al*., 2005; Raisner *et al*., 2005; Zhang *et al*., 2005; Li *et al*., 2005; Millar *et al*., 2006; Albert *et al*., 2007; Barski *et al*., 2007; Hardy *et al*., 2009; Jin *et al*., 2009). At promoter regions, H2A.Z is co-localised with the active histone marks such as H3K4me3 where the turnover rate of nucleosomes is high (Dion *et al*., 2007; Barski *et al*., 2007). In addition to promoter regions, H2A.Z is found in other regulatory elements such as enhancers and insulators (Bruce *et al*., 2005; Jin *et al*., 2009; Hardy *et al*., 2009), where it could contribute to gene regulation.

The genome localisation profile of acetylated H2A.Z isoforms have been documented and provided extra information to the biology of H2A.Z. Acetylated H2A.Z molecules are associated with active-transcribed regions in yeast and vertebrates (Millar *et al*., 2006; Bruce *et al*., 2005; Hardy *et al*., 2009, Valdes-Mora *et al*., 2011, Ku *et al*., 2012), suggesting that acetylated H2A.Z is a feature of active genes and perhaps involved in transcriptional regulation. In contrast, hypoacetylated H2A.Z isoforms are associated with heterochromatin (Bruce *et al*., 2005; Hardy *et al*., 2009), which is similar to ubiquitinated

H2A.Z subspecies locating at repressed loci such as inactive X chromosome (Sarcinella *et al*., 2007). H2A.Z that is both acetylated and ubiquitinated is found at bivalent domains in mouse ES cells, which may represent a functionally distinct sub-population for H2A.Z molecules (Ku *et al*., 2012).

Importantly, genetic and functional studies in budding and fission yeast showed that the N-terminal acetylation sites of H2A.Z are indeed critical for H2A.Z function in maintaining chromosome stability (Keogh *et al*., 2006; Kim *et al*., 2009), *GAL1* gene induction (Halley *et al*., 2010) and protecting the euchromatic regions from heterochromatin spreading (Barbiaz *et al*., 2006).

Given that the H2A.Z acetylation plays an important part in a number of cellular processes that H2A.Z is involved, the main aim of this project was to investigate the functional significance of Htz1 acetylation sites to dissect how acetylation regulates H2A.Z function. While it is known that four-lysine residues (K3, K8, K10 and K14) in the budding yeast Htz1 are acetylated, only the genome-wide distribution of one acetylated isoform (K14ac) is reported so far (Millar *et al*., 2006). It is still unknown whether the distribution of acetylation at the other sites is distinct from or overlaps with the profile of K14ac. The key initial question I attempted to address was 'What is the global localisation profile of other acetylation sites (K3ac, K8ac and K10ac)?' The strategies were to investigate the function of other acetylatable lysine sites by approaching them from genome-wide investigation to gain an insight into whether these acetylation sites marks the same or distinct locations as K14ac and relate these global profiles to their potential functions. Site-specific antibodies recognising each individual acetyl-lysine sites were characterised and validated for use in ChIP experiments and subsequent microarray analysis. In addition, independent genetic and functional studies were conducted to identify the functions of individual acetylation sites on Htz1 and overall acetylation-dependent roles.

The data presented in this thesis demonstrate that lysine acetylation is a general feature of Htz1 as global distribution profiles of K8ac, K10ac and K14ac are almost indistinguishable. Individual acetylation marks are co-localised with each other across the yeast genome. However, N-terminal acetylation sites do not affect the global distribution pattern of Htz1. Genetic studies indicate that these acetylatable lysine sites of Htz1 are internally redundant but altogether these acetylation sites confer essential function on Htz1. Additionally, the consequence of N-terminal epitope tagging was identified. Finally, a role for Htz1 acetylation in the maintenance of Htz1 levels in chromatin was reported.

6.2 The redundant roles of individual acetylatable lysines on H2A.Z

One objective of this project was to characterise the function of each single acetylation site on H2A.Z N-terminus. Using genetic studies of acetylation point mutants that altered all four lysines to arginine (on the HA epitope-tagged allele) in combination with mutations at H4 lysine 16, I showed that an intact acetylation site at any given lysine residue on Htz1 can compensate for the function when other sites become unavailable, suggesting the functional redundancy of acetylation sites. However, this study wasn't taken further because there were confounding effects of the epitope-tagged allele in yeast trains I used. In addition to this, during this study, a report from other laboratories suggested that individual acetylatable lysine sites on Htz1 are functionally redundant (Mehta *et al*., 2010). Mehta et al analysed genome-scale genetic interaction profiles of singly mutated or triply mutated Htz1 acetylation sites and showed that they exhibited highly similar profiles to wild type (Mehta *et al*., 2010), suggesting the non-specialised roles between each acetylation site.

Genome-wide studies of histone modifications have been widely used to provide a global view of distribution patterns and to relate these to potential biological functions. Additional information regarding the functional redundancy was drawn from the co-localisation pattern of acetylated Htz1 marks in my genome-wide studies. This result raised the possibility that acetylated Htz1 isoforms who share particular genomic loci may serve compensatory function for each other. The overall conclusion is that individual acetylatable lysine sites on Htz1 are functionally redundant, implying that there would be a high degree of combinatorial effect of Htz1 acetylation sites *in vivo.*

How are they redundant? One explanation for the redundancy on Htz1 acetylation sites could be due to the fact they share similar acetyltransferase and deacetylase enzymes. Acetylation and deacetylation of Htz1 is mediated by the action of KAT5 (NuA4) and Hda1 respectively (Millar *et al*., 2006; Barbiarz *et al*., 2006; Keogh *et al*., 2006; Lin *et al*., 2008; Mehta *et al*., 2010). It is tempting to speculate that the co-regulation between KAT5 and Hda1 activity and their substrate non-specificity on all lysine sites (with the exception of K3) on Htz1 perhaps support the tendency for functional redundancy similar to histone H4 acetylation sites. The reason that I excluded K3 site because I could not rule out the possibility that other modifying enzymes may regulate this site without Htz1K3ac acetyl-specific antibody.

It is worth noting that cells expressing a completely unacetylatable Htz1 allele, exhibit synthetic interactions with acetylation sites on histone H4 (K5, 8, 12 R), and *eaf1*Δ (subunit of NuA4 requires for H4 acetylation), suggesting the essential requirement of either acetylatable lysines on Htz1 or H4 for viability (Barbiarz *et al*., 2006). These works also support the idea that not only acetylation sites on Htz1 are internally redundant but it also demonstrates functional redundancy with acetylation sites on other histones (Babiarz *et al*., 2006). In concordance with previous findings, molecular evidence of *GAL1* gene induction demonstrated that *GAL1* induction is not dependent on acetylation at any individual lysine site as single lysine-to-arginine mutant strains exhibit *GAL1* expression similar to WT strain (Halley *et al*., 2010).

It has been hypothesised that regulation of N-terminal acetylation sites on histones may be linked to either charge-neutralisation or protein binding effects. So far, there is no evidence supporting that any distinct groups of proteins are associated with Htz1 in either acetylated or deacetylated state. It will be interesting to investigate this further by mass-spectrometry. Also, it is possible that charge-dependent effect may be attributed by the dynamic actions of acetylation-deacetylation on Htz1 tails. In this study, it is likely to be the charge modulation because other functional evidence pointed to the difference between lysine-to-arginine and lysine-to-glutamine mutations. This will be discussed in section 6.4.

While the sites of acetylation on Htz1 appear to play essential and functionally redundant roles, it is still unknown how they are important for Htz1 function. In yeast, the redundancy between distinct residues on histones has been proposed as 'histone redundancy hypothesis' (Kim *et al*., 2012). This proposal could be applied to the internal redundancy between acetylation sites on Htz1, meaning that instead of relying solely on the function at particular lysine sites, the total number of acetylatable lysine residues account for the functional impact.

6.3 Maintaining global H2A.Z protein abundance: an emerging role for H2A.Z regulation

The absence of Htz1 influences downstream functional outcomes such as gene expression and genome instability (Morillo-Huesca *et al*., 2010). As such, the mechanisms involved in the insertion and removal of chromatin-bound Htz1 must be tightly controlled to maintain the levels of Htz1. Imbalance in these processes can affect the level of Htz1 proteins and the capability to perform their proper functions. Consequently, the regulation of Htz1 levels in chromatin is critically important.

An unexpected result from this study was that the N-terminal HA-tagged version of Htz1 (*HA-HTZ1*) disrupts Htz1 abundance and function. My biochemical evidence showed that Htz1 protein level was markedly lower in the *HA-HTZ1* allele comparing to the untagged WT allele. Interestingly, this reduced Htz1 abundance is insufficient for the function of Htz1 in cells, as cells with reduced Htz1 exhibit defective growth upon exposure to a variety of stresses. Therefore, it is apparent that the maintenance of Htz1 at physiological levels in cells is essential.

How can the N-terminal epitope tagging affect the protein abundance? It is possible that this could be due to the effect of alteration of transcript levels, although this has not yet been addressed. Alternatively, additional regulation in post-transcriptional controls could be altered. Firstly, the HA-tagged Htz1 may be inherently unstable due to the disruption at the N-terminus by the HA epitope leading to altered conformation stability and that could influence the association of Htz1 with chaperones. Since the Nuclear Localisation Signal is located at the Htz1 N-terminus and is responsible for Htz1 nuclear import (Straube *et al*., 2010), it is possible that epitope tagging disrupts this interaction, resulting in interfering with the transfer to the SWR-C complex. Secondly, since H2A.Z N-terminus harbours four acetylatable lysines, it was proposed by other laboratories that the epitope tagging might interfere with the physical interaction of KAT5 enzyme leading to improper acetyltransferase activity and reduced acetylation levels (Mehta *et al*., 2010; Tanabe *et al*., 2008). These studies compared the levels of acetylated H2A.Z isoforms in the strains expressing the N- and C-terminal epitope-tagging version of H2A.Z and found the dramatic decrease of acetylated H2A.Z in the strain expressing the N-terminally epitope-tagged allele. It is arguable that this effect is most likely due to the substantial decrease in protein abundance because the effect is more pronounced than a completely unacetylatable allele (Figure 4.4A and 4.5B). Thirdly, the targeting of HA-tagged Htz1 protein may be disrupted. It is possible that *HA-HTZ1* is not targeted to their cognate sites or loosely associated with chromatin. Genome-wide examination of *HA-HTZ1* in this study showed that the distribution patterns between untagged and *HA-HTZ1* allele was relatively similar, although there are certain regions that showed the altered Htz1 enrichment levels as a result of epitope tagging (Figure 4.4C). Finally as a result of those possibilities mentioned above, the impaired proteins may cause aberrant degradation regulation. Interestingly, it has been reported that the steady state of histone abundance is tightly regulated to prevent deleterious effects in the genome (Gunjan and Verreault, 2003). Canonical histones can be degraded via a phosphorylation/ubiquitinylation/proteasome degradation pathway (Singh *et a*l., 2009). Recently, the ubiquitin-mediated proteolysis

specific for a centromeric H3 variant (Cse4) has been identified (Ranjitkar *et al*., 2010). In budding yeast, Psh1, an E3 ubiquitin ligase, is responsible for the degradation of Cse4 and prevent its mislocalisation in euchromatin (Ranjitkar *et al*., 2010). It will be interesting to explore whether there is such a regulator mediating H2A.Z degradation. Additionally, it is possible that the Tyrosine (Y) present in the HA peptides (YPYDVPDYA) is phosphorylated and targeting the protein for rapid degradation. This could be simply tested by using specific tyrosine phosphatase inhibitors or knockout known tyrosine-specific phosphatase enzyme.

Using the epitope-tagged proteins provide alternative and the tight control for immunoprecipitation specificity, I found that these strategies are unlikely to be ideal as the epitope tagging of Htz1 interferes with the function of the protein, especially at the N-terminus. Although, it is not clear by which mechanism N-terminal epitope tagging affects the Htz1 abundance, it is apparent that the N-terminal epitope tagging functionally impairs Htz1 function via the perturbation of its protein levels. Furthermore, my functional studies have revealed new facets about overexpression of Htz1 (Figure 4.9). Cells expressing excessive Htz1 amounts display defective growth compared to the endogenous WT (Figure 4.9). Therefore, overexpression of Htz1 while cells undergoing stress such as caffeine treatment led to markedly delayed growth, illustrating that cellular homeostatic maintenance of Htz1 is important to prevent the potential adversity in the genome upon stress exposure.

The key message here is that the dynamic balance of Htz1 abundance in cells is crucial. An excessive or insufficient Htz1 levels may affect the downstream Htz1functions in cells.

6.4 The essential role of H2A.Z acetylation

The overall aim of this project was to identify how N-terminal lysine acetylation sites regulate the function of H2A.Z. The idea that sites of acetylation are involved in H2A.Z regulation can be supported by a number of observations. First, these modified residues have essential functions in cells upon exposure to stresses. In the functional studies, cell lacking acetylatable lysines are sensitive to caffeine and exhibit atypical growth upon exposure to MMS. It was reported that Htz1 is deacetylated in response to MMS (Bandyopadhyay *et al*., 2009), suggesting the functional connection of the regulation of acetylation in response to DNA damage. Furthermore, yeast cells lacking ino80 (Papamichos-chronakis *et al*., 2011) or ies6 (Chambers *et al*., 2012) displayed markedly

reduced Htz1K14ac isoforms. These findings suggest the functional links of Htz1 deacetylation during DNA damages or when cells exhibit higher rates of genomic instability.

The caffeine-sensitive phenotype was significantly enhanced when Htz1 protein abundance was compromised (crippled promoter), indicating the synthetic defects Htz1 protein abundance and a completely unacetylatable mutant allele on Htz1 (Figure 4.10). However, Babiarz et al (2006) demonstrated that no growth defects were observed during the caffeine treatment. The discrepancies between the results presented in this study from previously published data are most likely due to the different yeast strains used. Throughout functional studies I used untagged Htz1 allele because the influence of epitope tagging may account for different phenotypic effect while Babiarz et al examined drug sensitivity in the C-terminally flag-tagged Htz1. Another possibility was due to different methods used between this study and previous study. I investigated the stress-sensitive phenotypes by measuring cell kinetics cell growth in liquid media in the presence of absence of drugs. The liquid culture approach appears to be more sensitive than the spot-test approach because it detects better kinetics and allow investigators to differentiate growth between strains that are modestly severe but significantly different than the wild - type counterpart.

Second, the alteration of steady state chromatin-bound Htz1 when all acetylatable lysine sites were mutated was observed. These data strongly suggest that the chromatin-associated Htz1 has been globally altered. Third, the involvement of SWR-C and acetylation for Htz1 deposition was suggested (Figure 5.7).

In this work, I showed that the Htz1 is not fully functional when all acetylatable lysine sites were mutated from lysine to arginine. Conversely, lysine-to-glutamine mutants show the phenotypes that are comparable to wild-type cells throughout the analyses. The mechanism through which Htz1 acetylation mediates general functions of Htz1 has not yet been established. Alteration by point mutations at the N-terminal tails of Htz1 may impact the conformation of unstructured tails. Given that acetylation of histone tails has been demonstrated to be an important regulator of transcriptional activation in eukaryotic cells and the acetylation of H2A.Z can also affect transcription of genes upon induction (Tanabe *et al*., 2008; Wan *et al*., 2009; Halley *et al*., 2010), the caffeine-sensitive phenotype in *htz1*-4KR and cp200-4KR cells is likely to be due, at least in part, to a transcriptional effect. So, what could happen upstream of transcription defects? It is plausible to speculate that N-terminal acetylation may modulate its Htz1- nucleosome dynamics in assembly and reassembly and that defects in this process could lead to the failure in global gene

induction. Millar et al (2006) showed by ChIP experiment that the deposition defects of Htz1 in *htz1-4KR* strain at *PHO5* promoter during the induction of *PHO5* after the phosphate-containing media shift, suggesting a role of acetylation in the efficient association and disassociation of Htz1 protein at *PHO5* promoter (Millar *et al*., 2006). It would be interesting to observe the enrichment of *htz1-4KR* mutant at multiple time-point ChIP experiments in the presence of caffeine.

Mapping the genomic distributions of quadruple point mutants (*htz1*-4*KR* and *htz1-4KQ*) of Htz1 versus acetylatable wild-type alleles demonstrated that they are highly similar, indicating that acetylation sites are not required for the global distribution for the variant H2A.Z. However, the enrichment patterns are altered in the *htz1-4KR* strains. Similarly, biochemical data also detected the global loss of Htz1 from the chromatin as a result of lysine- to-arginine mutations.

Recent investigations have revealed that that SWR-C can modulate the dual eviction pathway as a result of H3K56 hyperacetylation (Watanabe *et al*., 2013). In this hypothetical case, the series of events may occur if somehow unacetylatable 4KR mutants can activate H3K56ac and, in turn, this would promote a removal of Htz1 nucleosome, thereby indirectly controlling the overall Htz1 levels in chromatin. Since the effect that we see is rather modest, it is unlikely that this event would occur throughout the genome. Furthermore, it is possible that unacetylatable lysine residues may attenuate the interactions of Htz1-containing nucleosomes with SWR-C prior to deposition or unacetylatable Htz1 may stimulate the increased kinetics of a removal pathway, such as INO80-C (Papamichos-chronakis *et al*., 2011). Instead of using co-IP assay to identify these interactions, I sought to explore the contribution of SWR-C and INO80-C genetically by deleting essential subunits to inactivate their catalytic activities in the WT and unacetylatable *htz1* mutant backgrounds. The results from biochemical assays showed that SWR-C and acetylation might be independently responsible for Htz1 incorporation into chromatin. Without these two key regulatory features, the levels of chromatin-bound Htz1 were severely reduced (Figure 4.11)

Finally, since the total amount of Htz1 that associated with the chromatin is altered, it is likely that a balance between the degradation and turnover of Htz1 variant may be affected. It was reported that Htz1 acetylation was not involved in the turnover of Htz1 (Mehta *et al*., 2010). This study investigated the half-life (t½) of acetylated Htz1 species using transcription repression in galactose inducible system by glucose. The authors measured the disappearance of acetylated Htz1 species in time-course experiments and suggest that acetylated Htz1 species decayed in the similar rate. Additionally, the decay rates in mutant

cell lacking acetylation sites or Hda1 (hyperacetylation) were comparable to wild type cells. However, these experiments were carried out in a strain expressing the C-terminally HA-tagged Htz1. Therefore, it is possible that epitope tagging may contribute to the degradation kinetics. It will be interesting to test this hypothesis in an untagged strain background in presence or absence of MG132, a specific proteasome inhibitor. Alternatively, it would be intriguing to further investigate the specific enzyme involved in the degradation of Htz1 and the contribution of Htz1 acetylation sites. Most importantly, a pathway for acetylation-associated degradation of core histones has recently been identified in sperms and somatic cells in response to DNA damage (Qian *et al*., 2013). During spermatogenesis, histones become hyperacetylated and acetylation of H4K16ac is thought to promote histone removal. This step was followed by the replacement of transition proteins and protamines (Hammoud *et al*., 2009; Lu *et al*., 2010). Qian et al (2013) demonstrated the proteasome activator PA200 and its yeast ortholog Blm10 catalysed acetylation-dependent degradation of histones during the DNA damage and spermatogenesis (Qian *et al*., 2013). Since the proteasome activator is also present in yeast and the mechanism underlying Htz1 has not been identified, it is possible that altered Htz1 abundance in the *htz1*-4KR strain may be caused by the perturbation of a similar pathway, which remains to be characterised. This study suggests alternative mechanism of interplay between lysine acetylation sites to maintain appropriate levels of Htz1. While several plausible explanations to account for the reduction of Htz1 levels were proposed, it is attractive to speculate that the maintenance of Htz1 levels via its acetylation sites might not simply be answered by the disequilibrium of deposition and eviction pathways but rather involved, at least partly, in other acetylation-dependent regulatory mechanisms such as protein stability. This regulation requires further characterisation in the future.

In summary, this study provides a novel aspect of the acetylation sites on Htz1. These data indicate that acetylation sites of Htz1 are necessary for maintaining the level of H2A.Z in the chromatin in an unperturbed condition and become functionally crucial in response to stresses. The importance of maintaining Htz1 homeostasis in the yeast genome is underscored in this study as more insights are gained into acetylation-mediated pathways. Since the altered levels of H2A.Z are observed in many types of cancers (Hua *et al*., 2008; Svotelis *et al*., 2010) in conjunction with deregulation of H2A.Z acetylation (Valdes-Mora *et al*., 2011), it illustrates that these processes must be tightly controlled to regulate the H2A.Z function in higher eukaryotes. Notably, acetylated H2A.Z isoforms are largely responsive to suberoylanilide hydroxamic acid (SAHA), a clinical KDAC inhibitor (Choudhary *et al*., 2009), implying that may be of interest in clinical application.

Seemingly, the N-terminal H2A.Z acetylation is an important determinant for the functional H2A.Z. Understanding the molecular basis of acetylation-mediated control of H2A.Z will allow us to gain insights into the complex biology of H2A.Z in cells.

REFERENCE:

Abbott, D.W., Ivanova, V.S., Wang, X., Bonner, W.M., and Ausio, J. (2001). Characterization of the stability and folding of H2A.Z chromatin particles: implications for transcriptional activation. J Biol Chem 276, 41945-41949.

Adam, M., Robert, F., Larochelle, M., and Gaudreau, L. (2001). H2A.Z is required for global chromatin integrity and for recruitment of RNA polymerase II under specific conditions. Mol Cell Biol 21, 6270-6279.

Ahmad, K., and Henikoff, S. (2002). The histone variant H3.3 marks active chromatin by replication-independent nucleosome assembly. Mol Cell 9, 1191-1200.

Ahn, S.H., Diaz, R.L., Grunstein, M., and Allis, C.D. (2006). Histone H2B deacetylation at lysine 11 is required for yeast apoptosis induced by phosphorylation of H2B at serine 10. Mol Cell 24, 211-220.

Aihara, H., Nakagawa, T., Yasui, K., Ohta, T., Hirose, S., Dhomae, N., Takio, K., Kaneko, M., Takeshima, Y., Muramatsu, M., et al. (2004). Nucleosomal histone kinase-1 phosphorylates H2A Thr 119 during mitosis in the early Drosophila embryo. Genes Dev 18, 877-888.

Albert, I., Mavrich, T.N., Tomsho, L.P., Qi, J., Zanton, S.J., Schuster, S.C., and Pugh, B.F. (2007). Translational and rotational settings of H2A.Z nucleosomes across the Saccharomyces cerevisiae genome. Nature 446, 572-576.

Allahverdi, A., Yang, R., Korolev, N., Fan, Y., Davey, C.A., Liu, C.F., and Nordenskiold, L. (2011). The effects of histone H4 tail acetylations on cation-induced chromatin folding and self-association. Nucleic Acids Res 39, 1680-1691.

Allard, S., Utley, R.T., Savard, J., Clarke, A., Grant, P., Brandl, C.J., Pillus, L., Workman, J.L., and Cote, J. (1999). NuA4, an essential transcription adaptor/histone H4 acetyltransferase complex containing Esa1p and the ATM-related cofactor Tra1p. EMBO J 18, 5108-5119.

Allfrey, V.G., Faulkner, R., and Mirsky, A.E. (1964). Acetylation and Methylation of Histones and Their Possible Role in the Regulation of Rna Synthesis. Proc Natl Acad Sci U S A 51, 786-794.

Allis, C.D., Berger, S.L., Cote, J., Dent, S., Jenuwien, T., Kouzarides, T., Pillus, L., Reinberg, D., Shi, Y., Shiekhattar, R., et al. (2007). New nomenclature for chromatin-modifying enzymes. Cell 131, 633-636.

Allis, C.D., Glover, C.V., Bowen, J.K., and Gorovsky, M.A. (1980). Histone variants specific to the transcriptionally active, amitotically dividing macronucleus of the unicellular eucaryote, Tetrahymena thermophila. Cell 20, 609-617.

Allis, C.D., Richman, R., Gorovsky, M.A., Ziegler, Y.S., Touchstone, B., Bradley, W.A., and Cook, R.G. (1986). hv1 is an evolutionarily conserved H2A variant that is preferentially associated with active genes. J Biol Chem 261, 1941-1948.

Altaf, M., Auger, A., Covic, M., and Cote, J. (2009). Connection between histone H2A variants and chromatin remodeling complexes. Biochem Cell Biol 87, 35-50.

Arnaudo, A.M., and Garcia, B.A. (2013). Proteomic characterization of novel histone post-translational modifications. Epigenetics Chromatin 6, 24.

Auger, A., Galarneau, L., Altaf, M., Nourani, A., Doyon, Y., Utley, R.T., Cronier, D., Allard, S., and Cote, J. (2008). Eaf1 is the platform for NuA4 molecular assembly that evolutionarily links chromatin acetylation to ATP-dependent exchange of histone H2A variants. Mol Cell Biol 28, 2257-2270.

Ausio, J., and Abbott, D.W. (2002). The many tales of a tail: carboxyl-terminal tail heterogeneity specializes histone H2A variants for defined chromatin function. Biochemistry 41, 5945-5949.

Babiarz, J.E., Halley, J.E., and Rine, J. (2006). Telomeric heterochromatin boundaries require NuA4-dependent acetylation of histone variant H2A.Z in Saccharomyces cerevisiae. Genes Dev 20, 700-710.

Bandyopadhyay, S., Mehta, M., Kuo, D., Sung, M.K., Chuang, R., Jaehnig, E.J., Bodenmiller, B., Licon, K., Copeland, W., Shales, M., et al. (2010). Rewiring of genetic networks in response to DNA damage. Science 330, 1385-1389.

Barber, C.M., Turner, F.B., Wang, Y., Hagstrom, K., Taverna, S.D., Mollah, S., Ueberheide, B., Meyer, B.J., Hunt, D.F., Cheung, P., et al. (2004). The enhancement of histone H4 and H2A serine 1 phosphorylation during mitosis and S-phase is evolutionarily conserved. Chromosoma 112, 360-371.

Barski, A., Cuddapah, S., Cui, K., Roh, T.Y., Schones, D.E., Wang, Z., Wei, G., Chepelev, I., and Zhao, K. (2007). High-resolution profiling of histone methylations in the human genome. Cell 129, 823-837.

Barth, T.K., and Imhof, A. (2010). Fast signals and slow marks: the dynamics of histone modifications. Trends Biochem Sci 35, 618-626.

Beckouet, F., Hu, B., Roig, M.B., Sutani, T., Komata, M., Uluocak, P., Katis, V.L., Shirahige, K., and Nasmyth, K. (2010). An Smc3 acetylation cycle is essential for establishment of sister chromatid cohesion. Mol Cell 39, 689-699.

Bell, S.P., and Dutta, A. (2002). DNA replication in eukaryotic cells. Annu Rev Biochem 71, 333-374.

Bird, A.W., Yu, D.Y., Pray-Grant, M.G., Qiu, Q., Harmon, K.E., Megee, P.C., Grant, P.A., Smith, M.M., and Christman, M.F. (2002). Acetylation of histone H4 by Esa1 is required for DNA double-strand break repair. Nature 419, 411-415.

Borges, V., Lehane, C., Lopez-Serra, L., Flynn, H., Skehel, M., Rolef Ben-Shahar, T., and Uhlmann, F. (2010). Hos1 deacetylates Smc3 to close the cohesin acetylation cycle. Mol Cell 39, 677-688.

Boudreault, A.A., Cronier, D., Selleck, W., Lacoste, N., Utley, R.T., Allard, S., Savard, J., Lane, W.S., Tan, S., and Cote, J. (2003). Yeast enhancer of polycomb defines global Esa1-dependent acetylation of chromatin. Genes Dev 17, 1415-1428.

Brickner, D.G., Cajigas, I., Fondufe-Mittendorf, Y., Ahmed, S., Lee, P.C., Widom, J., and Brickner, J.H. (2007). H2A.Z-mediated localization of genes at the nuclear periphery confers epigenetic memory of previous transcriptional state. PLoS Biol 5, e81.

Bruce, K., Myers, F.A., Mantouvalou, E., Lefevre, P., Greaves, I., Bonifer, C., Tremethick, D.J., Thorne, A.W., and Crane-Robinson, C. (2005). The replacement histone H2A.Z in a hyperacetylated form is a feature of active genes in the chicken. Nucleic Acids Res 33, 5633-5639.

Buchanan, L., Durand-Dubief, M., Roguev, A., Sakalar, C., Wilhelm, B., Stralfors, A., Shevchenko, A., Aasland, R., Ekwall, K., and Francis Stewart, A. (2009). The Schizosaccharomyces pombe JmjC-protein, Msc1, prevents H2A.Z localization in centromeric and subtelomeric chromatin domains. PLoS Genet 5, e1000726.

Byeon, B., Wang, W., Barski, A., Ranallo, R.T., Bao, K., Schones, D.E., Zhao, K., Wu, C., and Wu, W.H. (2013). The ATP-dependent Chromatin Remodeling Enzyme Fun30 Represses Transcription by Sliding Promoter-proximal Nucleosomes. J Biol Chem 288, 23182-23193.

Carmen, A.A., Milne, L., and Grunstein, M. (2002). Acetylation of the yeast histone H4 N terminus regulates its binding to heterochromatin protein SIR3. J Biol Chem 277, 4778-4781.

Carr, A.M., Dorrington, S.M., Hindley, J., Phear, G.A., Aves, S.J., and Nurse, P. (1994). Analysis of a histone H2A variant from fission yeast: evidence for a role in chromosome stability. Mol Gen Genet 245, 628-635.

Chadwick, B.P., Valley, C.M., and Willard, H.F. (2001). Histone variant macroH2A contains two distinct macrochromatin domains capable of directing macroH2A to the inactive X chromosome. Nucleic Acids Res 29, 2699-2705.

Chambers, A.L., Ormerod, G., Durley, S.C., Sing, T.L., Brown, G.W., Kent, N.A., and Downs, J.A. (2012). The INO80 chromatin remodeling complex prevents polyploidy and maintains normal chromatin structure at centromeres. Genes Dev 26, 2590-2603.

Chen, I.Y., Lypowy, J., Pain, J., Sayed, D., Grinberg, S., Alcendor, R.R., Sadoshima, J., and Abdellatif, M. (2006). Histone H2A.z is essential for cardiac myocyte hypertrophy but opposed by silent information regulator 2alpha. J Biol Chem 281, 19369-19377.

Cheung, P., Tanner, K.G., Cheung, W.L., Sassone-Corsi, P., Denu, J.M., and Allis, C.D. (2000). Synergistic coupling of histone H3 phosphorylation and acetylation in response to epidermal growth factor stimulation. Mol Cell 5, 905-915.

Chew, Y.C., Camporeale, G., Kothapalli, N., Sarath, G., and Zempleni, J. (2006). Lysine residues in N-terminal and C-terminal regions of human histone H2A are targets for biotinylation by biotinidase. J Nutr Biochem 17, 225-233.

Choi, J., Heo, K., and An, W. (2009). Cooperative action of TIP48 and TIP49 in H2A.Z exchange catalyzed by acetylation of nucleosomal H2A. Nucleic Acids Res 37, 5993-6007.

Choudhary, C., Kumar, C., Gnad, F., Nielsen, M.L., Rehman, M., Walther, T.C., Olsen, J.V., and Mann, M. (2009). Lysine acetylation targets protein complexes and co-regulates major cellular functions. Science 325, 834-840.

Chow, C.M., Georgiou, A., Szutorisz, H., Maia e Silva, A., Pombo, A., Barahona, I., Dargelos, E., Canzonetta, C., and Dillon, N. (2005). Variant histone H3.3 marks promoters of transcriptionally active genes during mammalian cell division. EMBO Rep 6, 354-360.

Clarkson, M.J., Wells, J.R., Gibson, F., Saint, R., and Tremethick, D.J. (1999). Regions of variant histone His2AvD required for Drosophila development. Nature 399, 694-697.

Conerly, M.L., Teves, S.S., Diolaiti, D., Ulrich, M., Eisenman, R.N., and Henikoff, S. (2010). Changes in H2A.Z occupancy and DNA methylation during B-cell lymphomagenesis. Genome Res 20, 1383-1390.

Corona, D.F., Clapier, C.R., Becker, P.B., and Tamkun, J.W. (2002). Modulation of ISWI function by site-specific histone acetylation. EMBO Rep 3, 242-247.

Creyghton, M.P., Cheng, A.W., Welstead, G.G., Kooistra, T., Carey, B.W., Steine, E.J., Hanna, J., Lodato, M.A., Frampton, G.M., Sharp, P.A., et al. (2010). Histone H3K27ac separates active from poised enhancers and predicts developmental state. Proc Natl Acad Sci U S A 107, 21931-21936.

Creyghton, M.P., Markoulaki, S., Levine, S.S., Hanna, J., Lodato, M.A., Sha, K., Young, R.A., Jaenisch, R., and Boyer, L.A. (2008). H2AZ is enriched at polycomb complex target genes in ES cells and is necessary for lineage commitment. Cell 135, 649-661.

Das, C., Lucia, M.S., Hansen, K.C., and Tyler, J.K. (2009). CBP/p300-mediated acetylation of histone H3 on lysine 56. Nature 459, 113-117.

Davey, C.A., Sargent, D.F., Luger, K., Maeder, A.W., and Richmond, T.J. (2002). Solvent mediated interactions in the structure of the nucleosome core particle at 1.9 a resolution. J Mol Biol 319, 1097-1113.

Dhillon, N., and Kamakaka, R.T. (2000). A histone variant, Htz1p, and a Sir1p-like protein, Esc2p, mediate silencing at HMR. Mol Cell 6, 769-780.

Dhillon, N., Oki, M., Szyjka, S.J., Aparicio, O.M., and Kamakaka, R.T. (2006). H2A.Z functions to regulate progression through the cell cycle. Mol Cell Biol 26, 489-501.

Dion, M.F., Altschuler, S.J., Wu, L.F., and Rando, O.J. (2005). Genomic characterization reveals a simple histone H4 acetylation code. Proc Natl Acad Sci U S A 102, 5501-5506.

Dion, M.F., Kaplan, T., Kim, M., Buratowski, S., Friedman, N., and Rando, O.J. (2007). Dynamics of replication-independent histone turnover in budding yeast. Science 315, 1405-1408.

Dorigo, B., Schalch, T., Kulangara, A., Duda, S., Schroeder, R.R., and Richmond, T.J. (2004). Nucleosome arrays reveal the two-start organization of the chromatin fiber. Science 306, 1571-1573.

Downs, J.A., Lowndes, N.F., and Jackson, S.P. (2000). A role for Saccharomyces cerevisiae histone H2A in DNA repair. Nature 408, 1001-1004.

Doyen, C.M., Montel, F., Gautier, T., Menoni, H., Claudet, C., Delacour-Larose, M., Angelov, D., Hamiche, A., Bednar, J., Faivre-Moskalenko, C., et al. (2006). Dissection of the unusual structural and functional properties of the variant H2A.Bbd nucleosome. EMBO J 25, 4234-4244.

Draker, R., and Cheung, P. (2009). Transcriptional and epigenetic functions of histone variant H2A.Z. Biochem Cell Biol 87, 19-25.

Driscoll, R., Hudson, A., and Jackson, S.P. (2007). Yeast Rtt109 promotes genome stability by acetylating histone H3 on lysine 56. Science 315, 649-652.

Dryhurst, D., Ishibashi, T., Rose, K.L., Eirin-Lopez, J.M., McDonald, D., Silva-Moreno, B., Veldhoen, N., Helbing, C.C., Hendzel, M.J., Shabanowitz, J., et al. (2009). Characterization of the histone H2A.Z-1 and H2A.Z-2 isoforms in vertebrates. BMC Biol 7, 86.

Dryhurst, D., McMullen, B., Fazli, L., Rennie, P.S., and Ausio, J. (2011). Histone H2A.Z prepares the prostate specific antigen (PSA) gene for androgen receptor-mediated transcription and is upregulated in a model of prostate cancer progression. Cancer Lett 315, 38-47.

Dryhurst, D., Thambirajah, A.A., and Ausio, J. (2004). New twists on H2A.Z: a histone variant with a controversial structural and functional past. Biochem Cell Biol 82, 490-497.

Durand-Dubief, M., Will, W.R., Petrini, E., Theodorou, D., Harris, R.R., Crawford, M.R., Paszkiewicz, K., Krueger, F., Correra, R.M., Vetter, A.T., et al. (2012). SWI/SNF-like chromatin remodeling factor Fun30 supports point centromere function in S. cerevisiae. PLoS Genet 8, e1002974.

Edmondson, D.G., Davie, J.K., Zhou, J., Mirnikjoo, B., Tatchell, K., and Dent, S.Y. (2002). Site-specific loss of acetylation upon phosphorylation of histone H3. J Biol Chem 277, 29496-29502.

Egelhofer, T.A., Minoda, A., Klugman, S., Lee, K., Kolasinska-Zwierz, P., Alekseyenko, A.A., Cheung, M.S., Day, D.S., Gadel, S., Gorchakov, A.A., et al. (2011). An assessment of histone-modification antibody quality. Nat Struct Mol Biol 18, 91-93.

Eirin-Lopez, J., and Ausio, J. (2007). H2A.Z-Mediated Genome-Wide Chromatin Specialization. Curr Genomics 8, 59-66.

Eirin-Lopez, J.M., Gonzalez-Romero, R., Dryhurst, D., Ishibashi, T., and Ausio, J. (2009). The evolutionary differentiation of two histone H2A.Z variants in chordates (H2A.Z-1 and H2A.Z-2) is mediated by a stepwise mutation process that affects three amino acid residues. BMC Evol Biol 9, 31.

Faast, R., Thonglairoam, V., Schulz, T.C., Beall, J., Wells, J.R., Taylor, H., Matthaei, K., Rathjen, P.D., Tremethick, D.J., and Lyons, I. (2001). Histone variant H2A.Z is required for early mammalian development. Curr Biol 11, 1183-1187.

Fan, J.Y., Gordon, F., Luger, K., Hansen, J.C., and Tremethick, D.J. (2002). The essential histone variant H2A.Z regulates the equilibrium between different chromatin conformational states. Nat Struct Biol 9, 172-176.

Fan, J.Y., Rangasamy, D., Luger, K., and Tremethick, D.J. (2004). H2A.Z alters the nucleosome surface to promote HP1alpha-mediated chromatin fiber folding. Mol Cell 16, 655-661.

Farris, S.D., Rubio, E.D., Moon, J.J., Gombert, W.M., Nelson, B.H., and Krumm, A. (2005). Transcription-induced chromatin remodeling at the c-myc gene involves the local exchange of histone H2A.Z. J Biol Chem 280, 25298-25303.

Fiedler, D., Braberg, H., Mehta, M., Chechik, G., Cagney, G., Mukherjee, P., Silva, A.C., Shales, M., Collins, S.R., van Wageningen, S., et al. (2009). Functional organization of the S. cerevisiae phosphorylation network. Cell 136, 952-963.

Filippakopoulos, P., Picaud, S., Mangos, M., Keates, T., Lambert, J.P., Barsyte-Lovejoy, D., Felletar, I., Volkmer, R., Muller, S., Pawson, T., et al. (2012). Histone recognition and large-scale structural analysis of the human bromodomain family. Cell 149, 214-231.

Fraga, M.F., Ballestar, E., Villar-Garea, A., Boix-Chornet, M., Espada, J., Schotta, G., Bonaldi, T., Haydon, C., Ropero, S., Petrie, K., et al. (2005). Loss of acetylation at Lys16 and trimethylation at Lys20 of histone H4 is a common hallmark of human cancer. Nat Genet 37, 391-400.

Fuchs, S.M., Krajewski, K., Baker, R.W., Miller, V.L., and Strahl, B.D. (2011). Influence of combinatorial histone modifications on antibody and effector protein recognition. Curr Biol 21, 53-58.

Galbiati, L., Mendoza-Maldonado, R., Gutierrez, M.I., and Giacca, M. (2005). Regulation of E2F-1 after DNA damage by p300-mediated acetylation and ubiquitination. Cell Cycle 4, 930-939.

Gaucher, J., Reynoird, N., Montellier, E., Boussouar, F., Rousseaux, S., and Khochbin, S. (2010). From meiosis to postmeiotic events: the secrets of histone disappearance. FEBS J 277, 599-604.

Gervais, A.L., and Gaudreau, L. (2009). Discriminating nucleosomes containing histone H2A.Z or H2A based on genetic and epigenetic information. BMC Mol Biol 10, 18.

Gevry, N., Chan, H.M., Laflamme, L., Livingston, D.M., and Gaudreau, L. (2007). p21 transcription is regulated by differential localization of histone H2A.Z. Genes Dev 21, 1869-1881.

Gevry, N., Hardy, S., Jacques, P.E., Laflamme, L., Svotelis, A., Robert, F., and Gaudreau, L. (2009). Histone H2A.Z is essential for estrogen receptor signaling. Genes Dev 23, 1522-1533.

Glozak, M.A., Sengupta, N., Zhang, X., and Seto, E. (2005). Acetylation and deacetylation of non-histone proteins. Gene 363, 15-23.

Goecks, J., Nekrutenko, A., and Taylor, J. (2010). Galaxy: a comprehensive approach for supporting accessible, reproducible, and transparent computational research in the life sciences. Genome Biol 11, R86.

Goldberg, A.D., Banaszynski, L.A., Noh, K.M., Lewis, P.W., Elsaesser, S.J., Stadler, S., Dewell, S., Law, M., Guo, X., Li, X., et al. (2010). Distinct factors control histone variant H3.3 localization at specific genomic regions. Cell 140, 678-691.

Greaves, I.K., Rangasamy, D., Devoy, M., Marshall Graves, J.A., and Tremethick, D.J. (2006). The X and Y chromosomes assemble into H2A.Z-containing [corrected] facultative heterochromatin [corrected] following meiosis. Mol Cell Biol 26, 5394-5405.

Greaves, I.K., Rangasamy, D., Ridgway, P., and Tremethick, D.J. (2007). H2A.Z contributes to the unique 3D structure of the centromere. Proc Natl Acad Sci U S A 104, 525-530.

Grunstein, M. (1997). Histone acetylation in chromatin structure and transcription. Nature, 389(6649), 349-352.

Guillemette, B., Bataille, A.R., Gevry, N., Adam, M., Blanchette, M., Robert, F., and Gaudreau, L. (2005). Variant histone H2A.Z is globally localized to the promoters of inactive yeast genes and regulates nucleosome positioning. PLoS Biol 3, e384.

Gunjan, A., and Verreault, A. (2003). A Rad53 kinase-dependent surveillance mechanism that regulates histone protein levels in S. cerevisiae. Cell 115, 537-549.

Halley, J.E., Kaplan, T., Wang, A.Y., Kobor, M.S., and Rine, J. (2010). Roles for H2A.Z and its acetylation in GAL1 transcription and gene induction, but not GAL1-transcriptional memory. PLoS Biol 8, e1000401.

Hammoud, S.S., Nix, D.A., Zhang, H., Purwar, J., Carrell, D.T., and Cairns, B.R. (2009). Distinctive chromatin in human sperm packages genes for embryo development. Nature 460, 473-478.

Han, J., Zhou, H., Horazdovsky, B., Zhang, K., Xu, R.M., and Zhang, Z. (2007). Rtt109 acetylates histone H3 lysine 56 and functions in DNA replication. Science 315, 653-655.

Hansen, D.F., Zhou, Z., Feng, H., Miller Jenkins, L.M., Bai, Y., and Kay, L.E. (2009). Binding kinetics of histone chaperone Chz1 and variant histone H2A.Z-H2B by relaxation dispersion NMR spectroscopy. J Mol Biol 387, 1-9.

Hardy, S., Jacques, P.E., Gevry, N., Forest, A., Fortin, M.E., Laflamme, L., Gaudreau, L., and Robert, F. (2009). The euchromatic and heterochromatic landscapes are shaped by antagonizing effects of transcription on H2A.Z deposition. PLoS Genet 5, e1000687.

Hartley, P.D., and Madhani, H.D. (2009). Mechanisms that specify promoter nucleosome location and identity. Cell 137, 445-458.

Harvey, A.C., Jackson, S.P., and Downs, J.A. (2005). Saccharomyces cerevisiae histone H2A Ser122 facilitates DNA repair. Genetics 170, 543-553.

Heintzman, N.D., Hon, G.C., Hawkins, R.D., Kheradpour, P., Stark, A., Harp, L.F., Ye, Z., Lee, L.K., Stuart, R.K., Ching, C.W., et al. (2009). Histone modifications at human enhancers reflect global cell-type-specific gene expression. Nature 459, 108-112.

Heintzman, N.D., Stuart, R.K., Hon, G., Fu, Y., Ching, C.W., Hawkins, R.D., Barrera, L.O., Van Calcar, S., Qu, C., Ching, K.A., et al. (2007). Distinct and predictive chromatin signatures of transcriptional promoters and enhancers in the human genome. Nat Genet 39, 311-318.

Henikoff, S. (2009). Labile H3.3+H2A.Z nucleosomes mark 'nucleosome-free regions'. Nat Genet 41, 865-866.

Hoch, D.A., Stratton, J.J., and Gloss, L.M. (2007). Protein-protein Forster resonance energy transfer analysis of nucleosome core particles containing H2A and H2A.Z. J Mol Biol 371, 971-988.

Hou, H., Wang, Y., Kallgren, S.P., Thompson, J., Yates, J.R., 3rd, and Jia, S. (2009). Histone variant H2A.Z regulates centromere silencing and chromosome segregation in fission yeast. J Biol Chem 285, 1909-1918.

Hu, G., Cui, K., Northrup, D., Liu, C., Wang, C., Tang, Q., Ge, K., Levens, D., Crane-Robinson, C., and Zhao, K. (2013). H2A.Z facilitates access of active and repressive complexes to chromatin in embryonic stem cell self-renewal and differentiation. Cell Stem Cell 12, 180-192.

Hua, S., Kallen, C.B., Dhar, R., Baquero, M.T., Mason, C.E., Russell, B.A., Shah, P.K., Liu, J., Khramtsov, A., Tretiakova, M.S., et al. (2008). Genomic analysis of estrogen cascade reveals histone variant H2A.Z associated with breast cancer progression. Mol Syst Biol 4, 188.

Iouzalen, N., Moreau, J., and Mechali, M. (1996). H2A.ZI, a new variant histone expressed during Xenopus early development exhibits several distinct features from the core histone H2A. Nucleic Acids Res 24, 3947-3952.

Ishibashi, T., Dryhurst, D., Rose, K.L., Shabanowitz, J., Hunt, D.F., and Ausio, J. (2009). Acetylation of vertebrate H2A.Z and its effect on the structure of the nucleosome. Biochemistry 48, 5007-5017.

Ito, T., Ikehara, T., Nakagawa, T., Kraus, W.L., and Muramatsu, M. (2000). p300-mediated acetylation facilitates the transfer of histone H2A-H2B dimers from nucleosomes to a histone chaperone. Genes Dev 14, 1899-1907.

Ivanovska, I., Khandan, T., Ito, T., and Orr-Weaver, T.L. (2005). A histone code in meiosis: the histone kinase, NHK-1, is required for proper chromosomal architecture in Drosophila oocytes. Genes Dev 19, 2571-2582.

Jackson, J.D., Falciano, V.T., and Gorovsky, M.A. (1996). A likely histone H2A.F/Z variant in Saccharomyces cerevisiae. Trends Biochem Sci 21, 466-467.

Jackson, J.D., and Gorovsky, M.A. (2000). Histone H2A.Z has a conserved function that is distinct from that of the major H2A sequence variants. Nucleic Acids Res 28, 3811-3816.

Jiang, W., Wang, S., Xiao, M., Lin, Y., Zhou, L., Lei, Q., Xiong, Y., Guan, K.L., and Zhao, S. (2011). Acetylation regulates gluconeogenesis by promoting PEPCK1 degradation via recruiting the UBR5 ubiquitin ligase. Mol Cell 43, 33-44.

Jin, C., and Felsenfeld, G. (2007). Nucleosome stability mediated by histone variants H3.3 and H2A.Z. Genes Dev 21, 1519-1529.

Jin, C., Zang, C., Wei, G., Cui, K., Peng, W., Zhao, K., and Felsenfeld, G. (2009). H3.3/H2A.Z double variant-containing nucleosomes mark 'nucleosome-free regions' of active promoters and other regulatory regions. Nat Genet 41, 941-945.

Kalocsay, M., Hiller, N.J., and Jentsch, S. (2009). Chromosome-wide Rad51 spreading and SUMO-H2A.Z-dependent chromosome fixation in response to a persistent DNA double-strand break. Mol Cell 33, 335-343.

Kaluarachchi Duffy, S., Friesen, H., Baryshnikova, A., Lambert, J.P., Chong, Y.T., Figeys, D., and Andrews, B. (2012). Exploring the yeast acetylome using functional genomics. Cell 149, 936-948.

Kawano, A., Hayashi, Y., Noguchi, S., Handa, H., Horikoshi, M., and Yamaguchi, Y. (2011). Global analysis for functional residues of histone variant Htz1 using the comprehensive point mutant library. Genes Cells 16, 590-607.

Kelly, T.K., Miranda, T.B., Liang, G., Berman, B.P., Lin, J.C., Tanay, A., and Jones, P.A. (2010). H2A.Z maintenance during mitosis reveals nucleosome shifting on mitotically silenced genes. Mol Cell 39, 901-911.

Kent, W.J., Sugnet, C.W., Furey, T.S., Roskin, K.M., Pringle, T.H., Zahler, A.M., and Haussler, D. (2002). The human genome browser at UCSC. Genome Res 12, 996-1006.

Keogh, M.C., Mennella, T.A., Sawa, C., Berthelet, S., Krogan, N.J., Wolek, A., Podolny, V., Carpenter, L.R., Greenblatt, J.F., Baetz, K., et al. (2006). The Saccharomyces cerevisiae histone H2A variant Htz1 is acetylated by NuA4. Genes Dev 20, 660-665.

Kim, H.S., Vanoosthuyse, V., Fillingham, J., Roguev, A., Watt, S., Kislinger, T., Treyer, A., Carpenter, L.R., Bennett, C.S., Emili, A., et al. (2009). An acetylated form of histone H2A.Z regulates chromosome architecture in Schizosaccharomyces pombe. Nat Struct Mol Biol 16, 1286-1293.

Kim, J.A., Hsu, J.Y., Smith, M.M., and Allis, C.D. (2012). Mutagenesis of pairwise combinations of histone amino-terminal tails reveals functional redundancy in budding yeast. Proc Natl Acad Sci U S A 109, 5779-5784.

Kimura, A., Matsubara, K., and Horikoshi, M. (2005). A decade of histone acetylation: marking eukaryotic chromosomes with specific codes. J Biochem 138, 647-662.

Kind, J., Vaquerizas, J.M., Gebhardt, P., Gentzel, M., Luscombe, N.M., Bertone, P., and Akhtar, A. (2008). Genome-wide analysis reveals MOF as a key regulator of dosage compensation and gene expression in Drosophila. Cell 133, 813-828.

Kobor, M.S., and Lorincz, M.C. (2009). H2A.Z and DNA methylation: irreconcilable differences. Trends Biochem Sci 34, 158-161.

Kobor, M.S., Venkatasubrahmanyam, S., Meneghini, M.D., Gin, J.W., Jennings, J.L., Link, A.J., Madhani, H.D., and Rine, J. (2004). A protein complex containing the conserved Swi2/Snf2-related ATPase Swr1p deposits histone variant H2A.Z into euchromatin. PLoS Biol 2, E131.

Kourmouli, N., Jeppesen, P., Mahadevhaiah, S., Burgoyne, P., Wu, R., Gilbert, D.M., Bongiorni, S., Prantera, G., Fanti, L., Pimpinelli, S., et al. (2004). Heterochromatin and tri-methylated lysine 20 of histone H4 in animals. J Cell Sci 117, 2491-2501.

Kouzarides, T. (2007). Chromatin modifications and their function. Cell 128, 693-705.

Krishnan, N., Jeong, D.G., Jung, S.K., Ryu, S.E., Xiao, A., Allis, C.D., Kim, S.J., and Tonks, N.K. (2009). Dephosphorylation of the C-terminal tyrosyl residue of the DNA damage-related histone H2A.X is mediated by the protein phosphatase eyes absent. J Biol Chem 284, 16066-16070.

Krogan, N.J., Baetz, K., Keogh, M.C., Datta, N., Sawa, C., Kwok, T.C., Thompson, N.J., Davey, M.G., Pootoolal, J., Hughes, T.R., et al. (2004). Regulation of chromosome stability by the histone H2A variant Htz1, the Swr1 chromatin remodeling complex, and the histone acetyltransferase NuA4. Proc Natl Acad Sci U S A 101, 13513-13518.

Krogan, N.J., Keogh, M.C., Datta, N., Sawa, C., Ryan, O.W., Ding, H., Haw, R.A., Pootoolal, J., Tong, A., Canadien, V., et al. (2003). A Snf2 family ATPase complex required for recruitment of the histone H2A variant Htz1. Mol Cell 12, 1565-1576.

Ku, M., Jaffe, J.D., Koche, R.P., Rheinbay, E., Endoh, M., Koseki, H., Carr, S.A., and Bernstein, B.E. (2012). H2A.Z landscapes and dual modifications in pluripotent and multipotent stem cells underlie complex genome regulatory functions. Genome Biol 13, R85.

Kurdistani, S.K., and Grunstein, M. (2003). Histone acetylation and deacetylation in yeast. Nat Rev Mol Cell Biol 4, 276-284.

Kurdistani, S.K., Tavazoie, S., and Grunstein, M. (2004). Mapping global histone acetylation patterns to gene expression. Cell 117, 721-733.

Kusch, T., Florens, L., Macdonald, W.H., Swanson, S.K., Glaser, R.L., Yates, J.R., 3rd, Abmayr, S.M., Washburn, M.P., and Workman, J.L. (2004). Acetylation by Tip60 is required for selective histone variant exchange at DNA lesions. Science 306, 2084-2087.

Lange, M., Kaynak, B., Forster, U.B., Tonjes, M., Fischer, J.J., Grimm, C., Schlesinger, J., Just, S., Dunkel, I., Krueger, T., et al. (2008). Regulation of muscle development by DPF3, a novel histone acetylation and methylation reader of the BAF chromatin remodeling complex. Genes Dev 22, 2370-2384.

Lantermann, A.B., Straub, T., Stralfors, A., Yuan, G.C., Ekwall, K., and Korber, P. (2010). Schizosaccharomyces pombe genome-wide nucleosome mapping reveals positioning mechanisms distinct from those of Saccharomyces cerevisiae. Nat Struct Mol Biol 17, 251-257.

Larochelle, M., and Gaudreau, L. (2003). H2A.Z has a function reminiscent of an activator required for preferential binding to intergenic DNA. EMBO J 22, 4512-4522.

Latham, J.A., and Dent, S.Y. (2007). Cross-regulation of histone modifications. Nat Struct Mol Biol 14, 1017-1024.

Leach, T.J., Mazzeo, M., Chotkowski, H.L., Madigan, J.P., Wotring, M.G., and Glaser, R.L. (2000). Histone H2A.Z is widely but nonrandomly distributed in chromosomes of Drosophila melanogaster. J Biol Chem 275, 23267-23272.

Leduc, C., Claverie, P., Eymin, B., Col, E., Khochbin, S., Brambilla, E., and Gazzeri, S. (2006). p14ARF promotes RB accumulation through inhibition of its Tip60-dependent acetylation. Oncogene 25, 4147-4154.

Lee, J.S., Smith, E., and Shilatifard, A. (2010). The language of histone crosstalk. Cell 142, 682-685.

Lee, K.K., and Workman, J.L. (2007). Histone acetyltransferase complexes: one size doesn't fit all. Nat Rev Mol Cell Biol 8, 284-295.

Li, B., Carey, M., and Workman, J.L. (2007). The role of chromatin during transcription. Cell 128, 707-719.

Li, B., Pattenden, S.G., Lee, D., Gutierrez, J., Chen, J., Seidel, C., Gerton, J., and Workman, J.L. (2005). Preferential occupancy of histone variant H2AZ at inactive promoters influences local histone modifications and chromatin remodeling. Proc Natl Acad Sci U S A 102, 18385-18390.

Li, Z., Gadue, P., Chen, K., Jiao, Y., Tuteja, G., Schug, J., Li, W., and Kaestner, K.H. (2012). Foxa2 and H2A.Z mediate nucleosome depletion during embryonic stem cell differentiation. Cell 151, 1608-1616.

Lickwar, C.R., Mueller, F., Hanlon, S.E., McNally, J.G., and Lieb, J.D. (2012). Genome-wide protein-DNA binding dynamics suggest a molecular clutch for transcription factor function. Nature 484, 251-255.

Lin, Y.Y., Lu, J.Y., Zhang, J., Walter, W., Dang, W., Wan, J., Tao, S.C., Qian, J., Zhao, Y., Boeke, J.D., et al. (2009). Protein acetylation microarray reveals that NuA4 controls key metabolic target regulating gluconeogenesis. Cell 136, 1073-1084.

Lin, Y.Y., Qi, Y., Lu, J.Y., Pan, X., Yuan, D.S., Zhao, Y., Bader, J.S., and Boeke, J.D. (2008). A comprehensive synthetic genetic interaction network governing yeast histone acetylation and deacetylation. Genes Dev 22, 2062-2074.

Liu, C.L., Kaplan, T., Kim, M., Buratowski, S., Schreiber, S.L., Friedman, N., and Rando, O.J. (2005). Single-nucleosome mapping of histone modifications in S. cerevisiae. PLoS Biol 3, e328.

Liu, X., Li, B., and GorovskyMa (1996). Essential and nonessential histone H2A variants in Tetrahymena thermophila. Mol Cell Biol 16, 4305-4311.

Liu, Y., Lu, C., Yang, Y., Fan, Y., Yang, R., Liu, C.F., Korolev, N., and Nordenskiold, L. (2011). Influence of histone tails and H4 tail acetylations on nucleosome-nucleosome interactions. J Mol Biol 414, 749-764.

Lo, W.S., Trievel, R.C., Rojas, J.R., Duggan, L., Hsu, J.Y., Allis, C.D., Marmorstein, R., and Berger, S.L. (2000). Phosphorylation of serine 10 in histone H3 is functionally linked in vitro and in vivo to Gcn5-mediated acetylation at lysine 14. Mol Cell 5, 917-926.

Longtine, M.S., McKenzie, A., 3rd, Demarini, D.J., Shah, N.G., Wach, A., Brachat, A., Philippsen, P., and Pringle, J.R. (1998). Additional modules for versatile and economical PCR-based gene deletion and modification in Saccharomyces cerevisiae. Yeast 14, 953-961.

Lu, J.Y., Lin, Y.Y., Sheu, J.C., Wu, J.T., Lee, F.J., Chen, Y., Lin, M.I., Chiang, F.T., Tai, T.Y., Berger, S.L., et al. (2011). Acetylation of yeast AMPK controls intrinsic aging independently of caloric restriction. Cell 146, 969-979.

Lu, P.Y., Levesque, N., and Kobor, M.S. (2009). NuA4 and SWR1-C: two chromatin-modifying complexes with overlapping functions and components. Biochem Cell Biol 87, 799-815.

Lu, S., Xie, Y.M., Li, X., Luo, J., Shi, X.Q., Hong, X., Pan, Y.H., and Ma, X. (2009). Mass spectrometry analysis of dynamic post-translational modifications of TH2B during spermatogenesis. Mol Hum Reprod 15, 373-378.

Luger, K., Mader, A.W., Richmond, R.K., Sargent, D.F., and Richmond, T.J. (1997). Crystal structure of the nucleosome core particle at 2.8 A resolution. Nature 389, 251-260.

Luk, E., Ranjan, A., Fitzgerald, P.C., Mizuguchi, G., Huang, Y., Wei, D., and Wu, C. (2010). Stepwise histone replacement by SWR1 requires dual activation with histone H2A.Z and canonical nucleosome. Cell 143, 725-736.

Luk, E., Vu, N.D., Patteson, K., Mizuguchi, G., Wu, W.H., Ranjan, A., Backus, J., Sen, S., Lewis, M., Bai, Y., et al. (2007). Chz1, a nuclear chaperone for histone H2AZ. Mol Cell 25, 357-368.

Malik, H.S., and Henikoff, S. (2003). Phylogenomics of the nucleosome. Nat Struct Biol 10, 882-891.

Manohar, M., Mooney, A.M., North, J.A., Nakkula, R.J., Picking, J.W., Edon, A., Fishel, R., Poirier, M.G., and Ottesen, J.J. (2009). Acetylation of histone H3 at the nucleosome dyad alters DNA-histone binding. J Biol Chem 284, 23312-23321.

March-Diaz, R., Garcia-Dominguez, M., Lozano-Juste, J., Leon, J., Florencio, F.J., and Reyes, J.C. (2008). Histone H2A.Z and homologues of components of the SWR1 complex are required to control immunity in Arabidopsis. Plant J 53, 475-487.

Martinato, F., Cesaroni, M., Amati, B., and Guccione, E. (2008). Analysis of Myc-induced histone modifications on target chromatin. PLoS One 3, e3650.

Maston, G.A., Landt, S.G., Snyder, M., and Green, M.R. (2012). Characterization of enhancer function from genome-wide analyses. Annu Rev Genomics Hum Genet 13, 29-57.

Mateo, F., Vidal-Laliena, M., Canela, N., Busino, L., Martinez-Balbas, M.A., Pagano, M., Agell, N., and Bachs, O. (2009). Degradation of cyclin A is regulated by acetylation. Oncogene 28, 2654-2666.

Matsuda, R., Hori, T., Kitamura, H., Takeuchi, K., Fukagawa, T., and Harata, M. (2010). Identification and characterization of the two isoforms of the vertebrate H2A.Z histone variant. Nucleic Acids Res 38, 4263-4273.

Mavrich, T.N., Jiang, C., Ioshikhes, I.P., Li, X., Venters, B.J., Zanton, S.J., Tomsho, L.P., Qi, J., Glaser, R.L., Schuster, S.C., et al. (2008). Nucleosome organization in the Drosophila genome. Nature 453, 358-362.

Mehta, M., Braberg, H., Wang, S., Lozsa, A., Shales, M., Solache, A., Krogan, N.J., and Keogh, M.C. (2010). Individual lysine acetylations on the N terminus of Saccharomyces cerevisiae H2A.Z are highly but not differentially regulated. J Biol Chem 285, 39855-39865.

Meneghini, M.D., Wu, M., and Madhani, H.D. (2003). Conserved histone variant H2A.Z protects euchromatin from the ectopic spread of silent heterochromatin. Cell 112, 725-736.

Millar, C.B. (2013). Organizing the genome with H2A histone variants. Biochem J 449, 567-579.

Millar, C.B., and Grunstein, M. (2006). Genome-wide patterns of histone modifications in yeast. Nat Rev Mol Cell Biol 7, 657-666.

Millar, C.B., Kurdistani, S.K., and Grunstein, M. (2004). Acetylation of yeast histone H4 lysine 16: a switch for protein interactions in heterochromatin and euchromatin. Cold Spring Harb Symp Quant Biol 69, 193-200.

Millar, C.B., Xu, F., Zhang, K., and Grunstein, M. (2006). Acetylation of H2AZ Lys 14 is associated with genome-wide gene activity in yeast. Genes Dev 20, 711-722.

Mitchell, L., Lambert, J.P., Gerdes, M., Al-Madhoun, A.S., Skerjanc, I.S., Figeys, D., and Baetz, K. (2008). Functional dissection of the NuA4 histone acetyltransferase reveals its role as a genetic hub and that Eaf1 is essential for complex integrity. Mol Cell Biol 28, 2244-2256.

Mitchell, L., Lau, A., Lambert, J.P., Zhou, H., Fong, Y., Couture, J.F., Figeys, D., and Baetz, K. (2011). Regulation of septin dynamics by the Saccharomyces cerevisiae lysine acetyltransferase NuA4. PLoS One 6, e25336.

Mito, Y., Henikoff, J.G., and Henikoff, S. (2005). Genome-scale profiling of histone H3.3 replacement patterns. Nat Genet 37, 1090-1097.

Mizuguchi, G., Shen, X., Landry, J., Wu, W.H., Sen, S., and Wu, C. (2004). ATP-driven exchange of histone H2AZ variant catalyzed by SWR1 chromatin remodeling complex. Science 303, 343-348.

Moran, L., Norris, D., and Osley, M.A. (1990). A yeast H2A-H2B promoter can be regulated by changes in histone gene copy number. Genes Dev 4, 752-763.

Morillo-Huesca, M., Clemente-Ruiz, M., Andujar, E., and Prado, F. (2010). The SWR1 histone replacement complex causes genetic instability and genome-wide transcription misregulation in the absence of H2A.Z. PLoS One 5, e12143.

Morris, S.A., Rao, B., Garcia, B.A., Hake, S.B., Diaz, R.L., Shabanowitz, J., Hunt, D.F., Allis, C.D., Lieb, J.D., and Strahl, B.D. (2007). Identification of histone H3 lysine 36 acetylation as a highly conserved histone modification. J Biol Chem 282, 7632-7640.

Morrison, A.J., and Shen, X. (2009). Chromatin remodelling beyond transcription: the INO80 and SWR1 complexes. Nat Rev Mol Cell Biol 10, 373-384.

Nakamura, T.M., Du, L.L., Redon, C., and Russell, P. (2004). Histone H2A phosphorylation controls Crb2 recruitment at DNA breaks, maintains checkpoint arrest, and influences DNA repair in fission yeast. Mol Cell Biol 24, 6215-6230.

Nakayama, J., Rice, J.C., Strahl, B.D., Allis, C.D., and Grewal, S.I. (2001). Role of histone H3 lysine 9 methylation in epigenetic control of heterochromatin assembly. Science 292, 110-113.

Nekrasov, M., Amrichova, J., Parker, B.J., Soboleva, T.A., Jack, C., Williams, R., Huttley, G.A., and Tremethick, D.J. (2012). Histone H2A.Z inheritance during the cell cycle and its impact on promoter organization and dynamics. Nat Struct Mol Biol 19, 1076-1083.

Nicol, J.W., Helt, G.A., Blanchard, S.G., Jr., Raja, A., and Loraine, A.E. (2009). The Integrated Genome Browser: free software for distribution and exploration of genome-scale datasets. Bioinformatics 25, 2730-2731.

Papamichos-Chronakis, M., Watanabe, S., Rando, O.J., and Peterson, C.L. (2011). Global regulation of H2A.Z localization by the INO80 chromatin-remodeling enzyme is essential for genome integrity. Cell 144, 200-213.

Park, Y.J., Dyer, P.N., Tremethick, D.J., and Luger, K. (2004). A new fluorescence resonance energy transfer approach demonstrates that the histone variant H2AZ stabilizes the histone octamer within the nucleosome. J Biol Chem 279, 24274-24282.

Peach, S.E., Rudomin, E.L., Udeshi, N.D., Carr, S.A., and Jaffe, J.D. (2012). Quantitative assessment of chromatin immunoprecipitation grade antibodies directed against histone

modifications reveals patterns of co-occurring marks on histone protein molecules. Mol Cell Proteomics 11, 128-137.

Pehrson, J.R., and Fried, V.A. (1992). MacroH2A, a core histone containing a large nonhistone region. Science 257, 1398-1400.

Phillips, D.M. (1963). The presence of acetyl groups of histones. Biochem J 87, 258-263.

Pokholok, D.K., Harbison, C.T., Levine, S., Cole, M., Hannett, N.M., Lee, T.I., Bell, G.W., Walker, K., Rolfe, P.A., Herbolsheimer, E., et al. (2005). Genome-wide map of nucleosome acetylation and methylation in yeast. Cell 122, 517-527.

Qian, M.X., Pang, Y., Liu, C.H., Haratake, K., Du, B.Y., Ji, D.Y., Wang, G.F., Zhu, Q.Q., Song, W., Yu, Y., et al. (2013). Acetylation-mediated proteasomal degradation of core histones during DNA repair and spermatogenesis. Cell 153, 1012-1024.

Rada-Iglesias, A., Bajpai, R., Swigut, T., Brugmann, S.A., Flynn, R.A., and Wysocka, J. (2010). A unique chromatin signature uncovers early developmental enhancers in humans. Nature 470, 279-283.

Raisner, R.M., Hartley, P.D., Meneghini, M.D., Bao, M.Z., Liu, C.L., Schreiber, S.L., Rando, O.J., and Madhani, H.D. (2005). Histone variant H2A.Z marks the 5' ends of both active and inactive genes in euchromatin. Cell 123, 233-248.

Ramos, E., Pineiro, D., Soto, M., Abanades, D.R., Martin, M.E., Salinas, M., and Gonzalez, V.M. (2007). A DNA aptamer population specifically detects Leishmania infantum H2A antigen. Lab Invest 87, 409-416.

Rangasamy, D., Berven, L., Ridgway, P., and Tremethick, D.J. (2003). Pericentric heterochromatin becomes enriched with H2A.Z during early mammalian development. EMBO J 22, 1599-1607.

Rangasamy, D., Greaves, I., and Tremethick, D.J. (2004). RNA interference demonstrates a novel role for H2A.Z in chromosome segregation. Nat Struct Mol Biol 11, 650-655.

Ranjan, A., Mizuguchi, G., Fitzgerald, P.C., Wei, D., Wang, F., Huang, Y., Luk, E., Woodcock, C.L., and Wu, C. (2013). Nucleosome-free Region Dominates Histone Acetylation in Targeting SWR1 to Promoters for H2A.Z Replacement. Cell 154, 1232-1245.

Ranjitkar, P., Press, M.O., Yi, X., Baker, R., MacCoss, M.J., and Biggins, S. (2010). An E3 ubiquitin ligase prevents ectopic localization of the centromeric histone H3 variant via the centromere targeting domain. Mol Cell 40, 455-464.

Redon, C., Pilch, D.R., and Bonner, W.M. (2006). Genetic analysis of Saccharomyces cerevisiae H2A serine 129 mutant suggests a functional relationship between H2A and the sister-chromatid cohesion partners Csm3-Tof1 for the repair of topoisomerase I-induced DNA damage. Genetics 172, 67-76.

Ren, Q., and Gorovsky, M.A. (2001). Histone H2A.Z acetylation modulates an essential charge patch. Mol Cell 7, 1329-1335.

Ren, Q., and Gorovsky, M.A. (2003). The nonessential H2A N-terminal tail can function as an essential charge patch on the H2A.Z variant N-terminal tail. Mol Cell Biol 23, 2778-2789.

Rhodes, D.R., Yu, J., Shanker, K., Deshpande, N., Varambally, R., Ghosh, D., Barrette, T., Pandey, A., and Chinnaiyan, A.M. (2004). Large-scale meta-analysis of cancer microarray data identifies common transcriptional profiles of neoplastic transformation and progression. Proc Natl Acad Sci U S A 101, 9309-9314.

Ridgway, P., Rangasamy, D., Berven, L., Svensson, U., and Tremethick, D.J. (2004). Analysis of histone variant H2A.Z localization and expression during early development. Methods Enzymol 375, 239-252.

Robinson, P.J., An, W., Routh, A., Martino, F., Chapman, L., Roeder, R.G., and Rhodes, D. (2008). 30 nm chromatin fibre decompaction requires both H4-K16 acetylation and linker histone eviction. J Mol Biol 381, 816-825.

Roh, T.Y., Cuddapah, S., and Zhao, K. (2005). Active chromatin domains are defined by acetylation islands revealed by genome-wide mapping. Genes Dev 19, 542-552.

Rothbart, S.B., Lin, S., Britton, L.M., Krajewski, K., Keogh, M.C., Garcia, B.A., and Strahl, B.D. (2012). Poly-acetylated chromatin signatures are preferred epitopes for site-specific histone H4 acetyl antibodies. Sci Rep 2, 489.

Ruhl, D.D., Jin, J., Cai, Y., Swanson, S., Florens, L., Washburn, M.P., Conaway, R.C., Conaway, J.W., and Chrivia, J.C. (2006). Purification of a human SRCAP complex that remodels chromatin by incorporating the histone variant H2A.Z into nucleosomes. Biochemistry 45, 5671-5677.

Rusche, L.N., Kirchmaier, A.L., and Rine, J. (2003). The establishment, inheritance, and function of silenced chromatin in Saccharomyces cerevisiae. Annu Rev Biochem 72, 481-516.

Santisteban, M.S., Hang, M., and Smith, M.M. (2011). Histone variant H2A.Z and RNA polymerase II transcription elongation. Mol Cell Biol 31, 1848-1860.

Santisteban, M.S., Kalashnikova, T., and Smith, M.M. (2000). Histone H2A.Z regulats transcription and is partially redundant with nucleosome remodeling complexes. Cell 103, 411-422.

Sarcinella, E., Zuzarte, P.C., Lau, P.N., Draker, R., and Cheung, P. (2007). Monoubiquitylation of H2A.Z distinguishes its association with euchromatin or facultative heterochromatin. Mol Cell Biol 27, 6457-6468.

Sarg, B., Helliger, W., Talasz, H., Koutzamani, E., and Lindner, H.H. (2004). Histone H4 hyperacetylation precludes histone H4 lysine 20 trimethylation. J Biol Chem 279, 53458-53464.

Sarma, K., and Reinberg, D. (2005). Histone variants meet their match. Nat Rev Mol Cell Biol 6, 139-149.

Schones, D.E., Cui, K., Cuddapah, S., Roh, T.Y., Barski, A., Wang, Z., Wei, G., and Zhao, K. (2008). Dynamic regulation of nucleosome positioning in the human genome. Cell 132, 887-898.

Sharma, U., Stefanova, D., and Holmes, S.G. (2013). Histone variant H2A.Z functions in sister chromatid cohesion in Saccharomyces cerevisiae. Mol Cell Biol 33, 3473-3481.

Shia, W.J., Li, B., and Workman, J.L. (2006). SAS-mediated acetylation of histone H4 Lys 16 is required for H2A.Z incorporation at subtelomeric regions in Saccharomyces cerevisiae. Genes Dev 20, 2507-2512.

Shimazu, T., Komatsu, Y., Nakayama, K.I., Fukazawa, H., Horinouchi, S., and Yoshida, M. (2006). Regulation of SV40 large T-antigen stability by reversible acetylation. Oncogene 25, 7391-7400.

Shogren-Knaak, M., Ishii, H., Sun, J.M., Pazin, M.J., Davie, J.R., and Peterson, C.L. (2006). Histone H4-K16 acetylation controls chromatin structure and protein interactions. Science 311, 844-847.

Singh, R.K., Kabbaj, M.H., Paik, J., and Gunjan, A. (2009). Histone levels are regulated by phosphorylation and ubiquitylation-dependent proteolysis. Nat Cell Biol 11, 925-933.

Smith, E.R., Eisen, A., Gu, W., Sattah, M., Pannuti, A., Zhou, J., Cook, R.G., Lucchesi, J.C., and Allis, C.D. (1998). ESA1 is a histone acetyltransferase that is essential for growth in yeast. Proc Natl Acad Sci U S A 95, 3561-3565.

Stargell, L.A., Bowen, J., Dadd, C.A., Dedon, P.C., Davis, M., Cook, R.G., Allis, C.D., and Gorovsky, M.A. (1993). Temporal and spatial association of histone H2A variant hv1 with transcriptionally competent chromatin during nuclear development in Tetrahymena thermophila. Genes Dev 7, 2641-2651.

Strahl, B.D., and Allis, C.D. (2000). The language of covalent histone modifications. Nature 403, 41-45.

Stralfors, A., Walfridsson, J., Bhuiyan, H., and Ekwall, K. (2011). The FUN30 chromatin remodeler, Fft3, protects centromeric and subtelomeric domains from euchromatin formation. PLoS Genet 7, e1001334.

Straube, K., Blackwell, J.S., Jr., and Pemberton, L.F. (2010). Nap1 and Chz1 have separate Htz1 nuclear import and assembly functions. Traffic 11, 185-197.

Stucki, M. (2009). Histone H2A.X Tyr142 phosphorylation: a novel sWItCH for apoptosis? DNA Repair (Amst) 8, 873-876.

Suka, N., Suka, Y., Carmen, A.A., Wu, J., and Grunstein, M. (2001). Highly specific antibodies determine histone acetylation site usage in yeast heterochromatin and euchromatin. Mol Cell 8, 473-479.

Suto, R.K., Clarkson, M.J., Tremethick, D.J., and Luger, K. (2000). Crystal structure of a nucleosome core particle containing the variant histone H2A.Z. Nat Struct Biol 7, 1121-1124.

Svotelis, A., Gevry, N., and Gaudreau, L. (2009). Regulation of gene expression and cellular proliferation by histone H2A.Z. Biochem Cell Biol 87, 179-188.

Svotelis, A., Gevry, N., Grondin, G., and Gaudreau, L. (2010). H2A.Z overexpression promotes cellular proliferation of breast cancer cells. Cell Cycle 9, 364-370.

Swaminathan, J., Baxter, E.M., and Corces, V.G. (2005). The role of histone H2Av variant replacement and histone H4 acetylation in the establishment of Drosophila heterochromatin. Genes Dev 19, 65-76.

Talbert, P.B., and Henikoff, S. (2010). Histone variants--ancient wrap artists of the epigenome. Nat Rev Mol Cell Biol 11, 264-275.

Tamkun, J.W., Deuring, R., Scott, M.P., Kissinger, M., Pattatucci, A.M., Kaufman, T.C., and Kennison, J.A. (1992). brahma: a regulator of Drosophila homeotic genes structurally related to the yeast transcriptional activator SNF2/SWI2. Cell 68, 561-572.

Tan, M., Luo, H., Lee, S., Jin, F., Yang, J.S., Montellier, E., Buchou, T., Cheng, Z., Rousseaux, S., Rajagopal, N., et al. (2011). Identification of 67 histone marks and histone lysine crotonylation as a new type of histone modification. Cell 146, 1016-1028.

Tanabe, M., Kouzmenko, A.P., Ito, S., Sawatsubashi, S., Suzuki, E., Fujiyama, S., Yamagata, K., Zhao, Y., Kimura, S., Ueda, T., et al. (2008). Activation of facultatively silenced Drosophila loci associates with increased acetylation of histone H2AvD. Genes Cells 13, 1279-1288.

Taylor, G., Eskeland, R., Hekimoglu-Balkan, B., Pradeepa, M., and Bickmore, W.A. (2013). H4K16 acetylation marks active genes and enhancers of embryonic stem cells, but does not alter chromatin compaction. Genome Res.

Thakar, A., Gupta, P., Ishibashi, T., Finn, R., Silva-Moreno, B., Uchiyama, S., Fukui, K., Tomschik, M., Ausio, J., and Zlatanova, J. (2009). H2A.Z and H3.3 histone variants affect nucleosome structure: biochemical and biophysical studies. Biochemistry 48, 10852-10857.

Thambirajah, A.A., Dryhurst, D., Ishibashi, T., Li, A., Maffey, A.H., and Ausio, J. (2006). H2A.Z stabilizes chromatin in a way that is dependent on core histone acetylation. J Biol Chem 281, 20036-20044.

Turner, B.M., Birley, A.J., and Lavender, J. (1992). Histone H4 isoforms acetylated at specific lysine residues define individual chromosomes and chromatin domains in Drosophila polytene nuclei. Cell 69, 375-384.

Unnikrishnan, A., Gafken, P.R., and Tsukiyama, T. (2010). Dynamic changes in histone acetylation regulate origins of DNA replication. Nat Struct Mol Biol 17, 430-437.

Utley, R.T., Lacoste, N., Jobin-Robitaille, O., Allard, S., and Cote, J. (2005). Regulation of NuA4 histone acetyltransferase activity in transcription and DNA repair by phosphorylation of histone H4. Mol Cell Biol 25, 8179-8190.

Valdes-Mora, F., Song, J.Z., Statham, A.L., Strbenac, D., Robinson, M.D., Nair, S.S., Patterson, K.I., Tremethick, D.J., Stirzaker, C., and Clark, S.J. (2011). Acetylation of

H2A.Z is a key epigenetic modification associated with gene deregulation and epigenetic remodeling in cancer. Genome Res 22, 307-321.

van Attikum, H., Fritsch, O., Hohn, B., and Gasser, S.M. (2004). Recruitment of the INO80 complex by H2A phosphorylation links ATP-dependent chromatin remodeling with DNA double-strand break repair. Cell 119, 777-788.

van Daal, A., White, E.M., Elgin, S.C., and Gorovsky, M.A. (1990). Conservation of intron position indicates separation of major and variant H2As is an early event in the evolution of eukaryotes. J Mol Evol 30, 449-455.

Viens, A., Mechold, U., Brouillard, F., Gilbert, C., Leclerc, P., and Ogryzko, V. (2006). Analysis of human histone H2AZ deposition in vivo argues against its direct role in epigenetic templating mechanisms. Mol Cell Biol 26, 5325-5335.

Wan, Y., Saleem, R.A., Ratushny, A.V., Roda, O., Smith, J.J., Lin, C.H., Chiang, J.H., and Aitchison, J.D. (2009). Role of the histone variant H2A.Z/Htz1p in TBP recruitment, chromatin dynamics, and regulated expression of oleate-responsive genes. Mol Cell Biol 29, 2346-2358.

Wang, A.Y., Aristizabal, M.J., Ryan, C., Krogan, N.J., and Kobor, M.S. (2011). Key functional regions in the histone variant H2A.Z C-terminal docking domain. Mol Cell Biol 31, 3871-3884.

Wang, Z., Zang, C., Cui, K., Schones, D.E., Barski, A., Peng, W., and Zhao, K. (2009). Genome-wide mapping of HATs and HDACs reveals distinct functions in active and inactive genes. Cell 138, 1019-1031.

Wang, Z., Zang, C., Rosenfeld, J.A., Schones, D.E., Barski, A., Cuddapah, S., Cui, K., Roh, T.Y., Peng, W., Zhang, M.Q., et al. (2008). Combinatorial patterns of histone acetylations and methylations in the human genome. Nat Genet 40, 897-903.

Watanabe, S., Radman-Livaja, M., Rando, O.J., and Peterson, C.L. (2013). A histone acetylation switch regulates H2A.Z deposition by the SWR-C remodeling enzyme. Science 340, 195-199.

Weber, C.M., Henikoff, J.G., and Henikoff, S. (2010). H2A.Z nucleosomes enriched over active genes are homotypic. Nat Struct Mol Biol 17, 1500-1507.

West, M.H., and Bonner, W.M. (1980). Histone 2A, a heteromorphous family of eight protein species. Biochemistry 19, 3238-3245.

Whittle, C.M., McClinic, K.N., Ercan, S., Zhang, X., Green, R.D., Kelly, W.G., and Lieb, J.D. (2008). The genomic distribution and function of histone variant HTZ-1 during C. elegans embryogenesis. PLoS Genet 4, e1000187.

Williams, B.A., Lin, L., Lindsay, S.M., and Chaput, J.C. (2009). Evolution of a histone H4-K16 acetyl-specific DNA aptamer. J Am Chem Soc 131, 6330-6331.

Wong, L.H., Ren, H., Williams, E., McGhie, J., Ahn, S., Sim, M., Tam, A., Earle, E., Anderson, M.A., Mann, J., et al. (2009). Histone H3.3 incorporation provides a unique and functionally essential telomeric chromatin in embryonic stem cells. Genome Res 19, 404-414.

Wong, M.M., Cox, L.K., and Chrivia, J.C. (2007). The chromatin remodeling protein, SRCAP, is critical for deposition of the histone variant H2A.Z at promoters. J Biol Chem 282, 26132-26139.

Wratting, D., Thistlethwaite, A., Harris, M., Zeef, L.A., and Millar, C.B. (2012). A conserved function for the H2A.Z C terminus. J Biol Chem 287, 19148-19157.

Wu, W.H., Alami, S., Luk, E., Wu, C.H., Sen, S., Mizuguchi, G., Wei, D., and Wu, C. (2005). Swc2 is a widely conserved H2AZ-binding module essential for ATP-dependent histone exchange. Nat Struct Mol Biol 12, 1064-1071.

Xu, F., Zhang, K., and Grunstein, M. (2005). Acetylation in histone H3 globular domain regulates gene expression in yeast. Cell 121, 375-385.

Xu, Y., and Price, B.D. (2011). Chromatin dynamics and the repair of DNA double strand breaks. Cell Cycle 10, 261-267.

Xu, Z., Wei, W., Gagneur, J., Perocchi, F., Clauder-Munster, S., Camblong, J., Guffanti, E., Stutz, F., Huber, W., and Steinmetz, L.M. (2009). Bidirectional promoters generate pervasive transcription in yeast. Nature 457, 1033-1037.

Yang, X., Zaurin, R., Beato, M., and Peterson, C.L. (2007). Swi3p controls SWI/SNF assembly and ATP-dependent H2A-H2B displacement. Nat Struct Mol Biol 14, 540-547.

Yang, X.J., and Seto, E. (2008). Lysine acetylation: codified crosstalk with other posttranslational modifications. Mol Cell 31, 449-461.

Ye, T., Krebs, A.R., Choukrallah, M.A., Keime, C., Plewniak, F., Davidson, I., and Tora, L. (2010). seqMINER: an integrated ChIP-seq data interpretation platform. Nucleic Acids Res 39, e35.

Yi, H., Sardesai, N., Fujinuma, T., Chan, C.W., Veena, and Gelvin, S.B. (2006). Constitutive expression exposes functional redundancy between the Arabidopsis histone H2A gene HTA1 and other H2A gene family members. Plant Cell 18, 1575-1589.

Zemach, A., McDaniel, I.E., Silva, P., and Zilberman, D. (2010). Genome-wide evolutionary analysis of eukaryotic DNA methylation. Science 328, 916-919.

Zeng, L., Zhang, Q., Li, S., Plotnikov, A.N., Walsh, M.J., and Zhou, M.M. (2010). Mechanism and regulation of acetylated histone binding by the tandem PHD finger of DPF3b. Nature 466, 258-262.

Zeng, L., and Zhou, M.M. (2002). Bromodomain: an acetyl-lysine binding domain. FEBS Lett 513, 124-128.

Zentner, G.E., and Henikoff, S. (2013). Regulation of nucleosome dynamics by histone modifications. Nat Struct Mol Biol 20, 259-266.

Zhang, H., Richardson, D.O., Roberts, D.N., Utley, R., Erdjument-Bromage, H., Tempst, P., Cote, J., and Cairns, B.R. (2004). The Yaf9 component of the SWR1 and NuA4 complexes is required for proper gene expression, histone H4 acetylation, and Htz1 replacement near telomeres. Mol Cell Biol 24, 9424-9436.

Zhang, H., Roberts, D.N., and Cairns, B.R. (2005). Genome-wide dynamics of Htz1, a histone H2A variant that poises repressed/basal promoters for activation through histone loss. Cell 123, 219-231.

Zhang, X.Y., Pfeiffer, H.K., Thorne, A.W., and McMahon, S.B. (2008). USP22, an hSAGA subunit and potential cancer stem cell marker, reverses the polycomb-catalyzed ubiquitylation of histone H2A. Cell Cycle 7, 1522-1524.

Zhang, Y., Griffin, K., Mondal, N., and Parvin, J.D. (2004). Phosphorylation of histone H2A inhibits transcription on chromatin templates. J Biol Chem 279, 21866-21872.

Zhao, S., Xu, W., Jiang, W., Yu, W., Lin, Y., Zhang, T., Yao, J., Zhou, L., Zeng, Y., Li, H., et al. (2010). Regulation of cellular metabolism by protein lysine acetylation. Science 327, 1000-1004.

Zheng, Y., Thomas, P.M., and Kelleher, N.L. (2013). Measurement of acetylation turnover at distinct lysines in human histones identifies long-lived acetylation sites. Nat Commun 4, 2203.

Zhou, Z., Feng, H., Hansen, D.F., Kato, H., Luk, E., Freedberg, D.I., Kay, L.E., Wu, C., and Bai, Y. (2008). NMR structure of chaperone Chz1 complexed with histones H2A.Z-H2B. Nat Struct Mol Biol 15, 868-869.

Zilberman, D., Coleman-Derr, D., Ballinger, T., and Henikoff, S. (2008). Histone H2A.Z and DNA methylation are mutually antagonistic chromatin marks. Nature 456, 125-129.

Zippo, A., Serafini, R., Rocchigiani, M., Pennacchini, S., Krepelova, A., and Oliviero, S. (2009). Histone crosstalk between H3S10ph and H4K16ac generates a histone code that mediates transcription elongation. Cell 138, 1122-1136.

Zlatanova, J., and Thakar, A. (2008). H2A.Z: view from the top. Structure 16, 166-179.

Zofall, M., Fischer, T., Zhang, K., Zhou, M., Cui, B., Veenstra, T.D., and Grewal, S.I. (2009). Histone H2A.Z cooperates with RNAi and heterochromatin factors to suppress antisense RNAs. Nature 461, 419-422.

Zucchi, I., Mento, E., Kuznetsov, V.A., Scotti, M., Valsecchi, V., Simionati, B., Vicinanza, E., Valle, G., Pilotti, S., Reinbold, R., et al. (2004). Gene expression profiles of epithelial cells microscopically isolated from a breast-invasive ductal carcinoma and a nodal metastasis. Proc Natl Acad Sci U S A 101, 18147-18152.

APPENDIX A

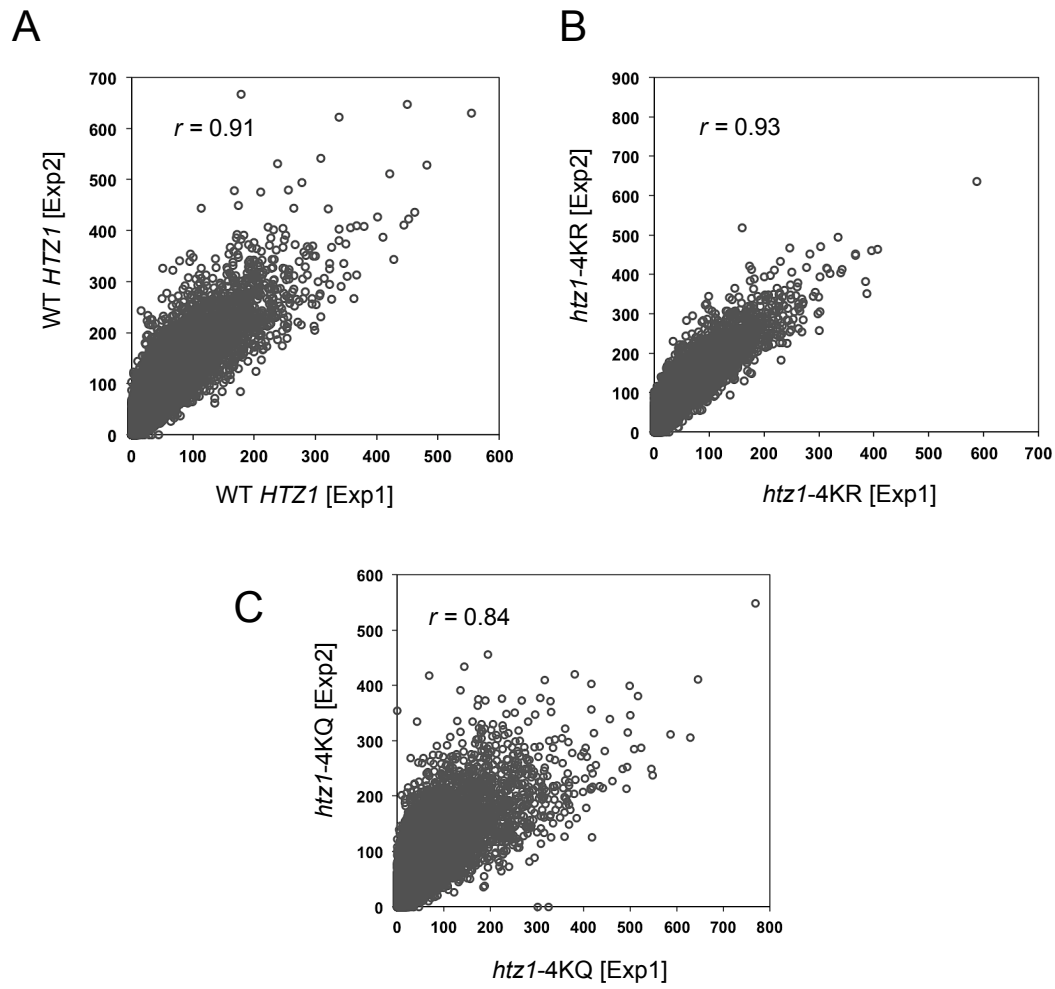

Quantification of ChIP-Seq datasets reveals highly correlated patterns between two independent experiments

Dot plots compare signal intensities between two ChIP-Seq replicates after they have been normalised to input. Data from WT HTZ1 (A), *htz1*-4KR (B) and *htz1*-4KQ (C) are shown. Enrichments of Htz1 from indicated yeast strains were calculated within a window of 150-bp bins across the yeast genome. Each gray dot represents the normalised ChIP signals within 150-bp bins (*r* = Pearson correlation coefficient)

APPENDIX B

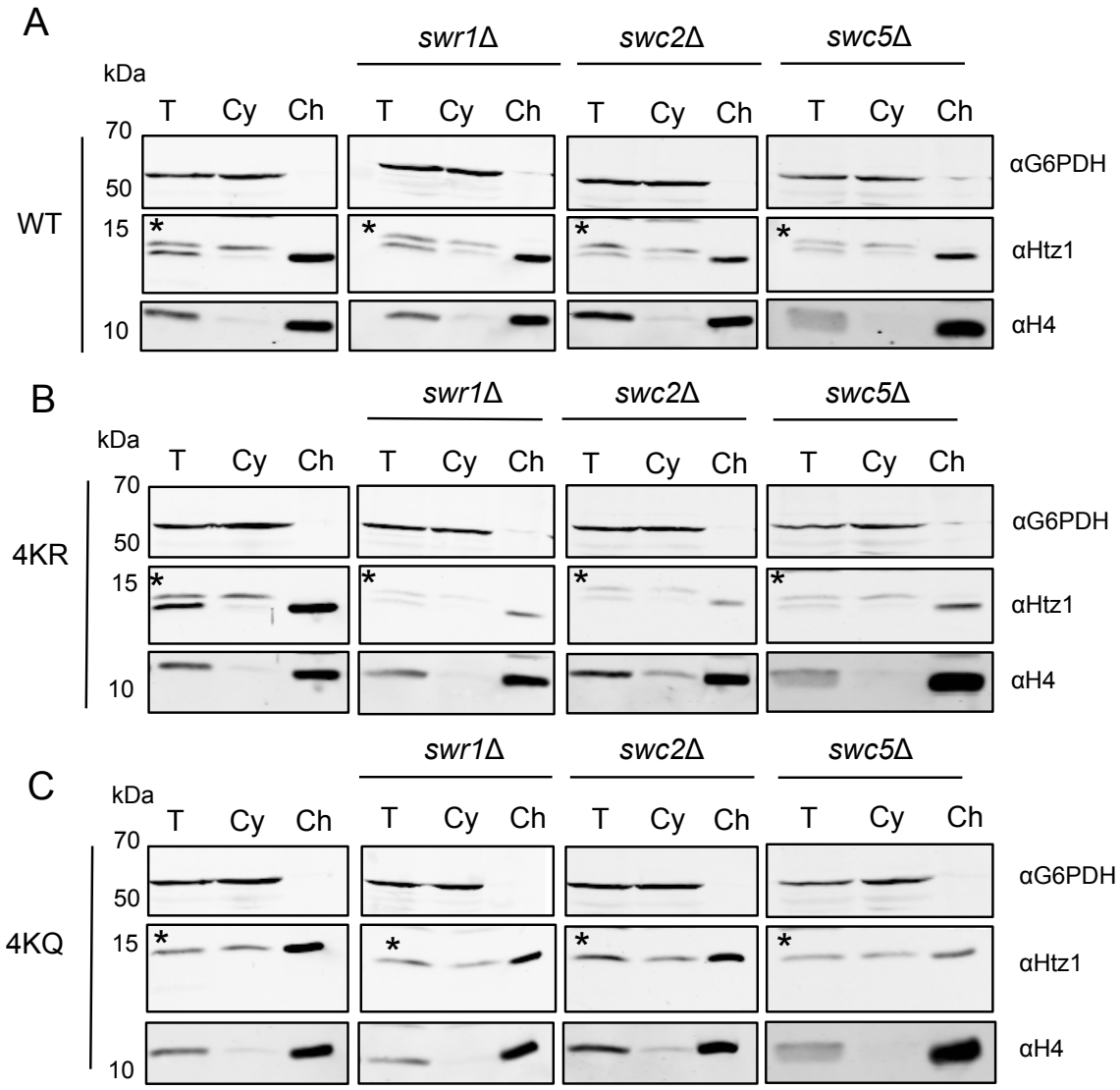

Comparison of sub-cellular localisation of WT, 4KR and 4KQ in the mutants of SWR-C remodelling enzyme (*swr1*Δ, *swc2*Δ and *swc5*Δ)

Cell fractionation experiments were carried out in yeast strains with indicated genotypes WT HTZ1 (A), htz1-4KR (B) and htz1-4KQ (C).

Total lysate (T), Cytoplasmic fraction (Cy) and Chromatin fraction (Ch) samples were analysed by western blotting with anti-Htz1 antibody. Anti-G6PDH and anti-H4 antibodies were used as sub-cellular compartments control. Asterisks indicate cross-reactivity of anti-Htz1 with cytoplasmic proteins in which are not present in the chromatin fraction. Representative data from two independent experiments are shown (*n*=2). Lysine-to-glutamine mutations affect the migration of *htz1*-4KQ in panel C in SDS-PAGE; consequently the bands shift to the same molecular weight as cross-reactivity protein bands.

APPENDIX B (Continued)

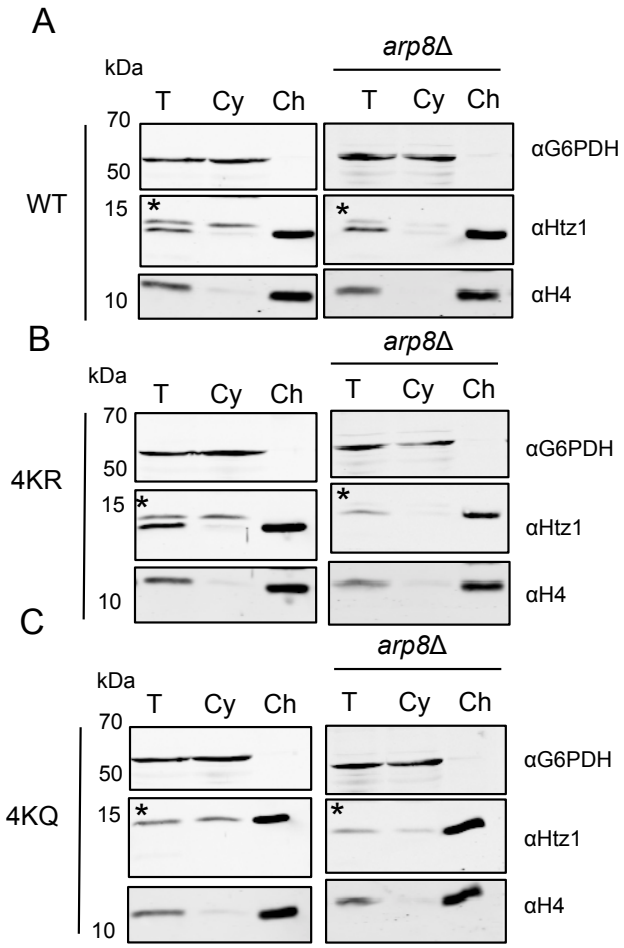

Comparison of sub-cellular localisation of WT, 4KR and 4KQ in the mutants of INO80 remodelling enzyme (*arp8*Δ)
Cell fractionation experiments were performed as previously described in yeast strains with indicated genotypes WT HTZ1 (A), htz1-4KR (B) and htz1-4KQ (C).